

**PRODUCTION AND BIOLOGICAL ACTIVITY OF  
CHITO-OLIGOSACCHARIDE GENERATED  
BY ENZYME TECHNOLOGY**



**Phornsiri Pechsrichuang**

**A Thesis Submitted in Partial Fulfillment of the Requirements for the  
Degree of Doctor of Philosophy in Biotechnology  
Suranaree University of Technology  
Academic Year 2017**

การผลิตและฤทธิ์ทางชีวภาพของโคโตโอลิโกแซคคาไรด์ (คอซ)

ที่ถูกสร้างขึ้นด้วยเทคโนโลยีเอนไซม์



วิทยานิพนธ์นี้เป็นส่วนหนึ่งของการศึกษาตามหลักสูตรปริญญาวิทยาศาสตรดุษฎีบัณฑิต

สาขาวิชาเทคโนโลยีชีวภาพ

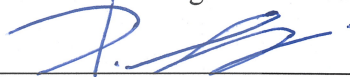
มหาวิทยาลัยเทคโนโลยีสุรนารี

ปีการศึกษา 2560

**PRODUCTION AND BIOLOGICAL ACTIVITY OF  
CHITO-OLIGOSACCHARIDE GENERATED  
BY ENZYME TECHNOLOGY**

Suranaree University of Technology has approved this thesis submitted in partial fulfillment of the requirements for the Degree of Doctor of Philosophy.

Thesis Examining Committee

  
\_\_\_\_\_  
(Asst. Prof. Dr. Parinya Noisa)

Chairperson

  
\_\_\_\_\_  
(Prof. Dr. Montarop Yamabhai)

Member (Thesis Advisor)

  
\_\_\_\_\_  
(Prof. Dr. Vincent Eijsink)

Member

  
\_\_\_\_\_  
(Dr. Berit Bjugan Aam)

Member

  
\_\_\_\_\_  
(Dr. Chomphunuch Songsiriritthigul)

Member



\_\_\_\_\_  
(Prof. Dr. Santi Maensiri)

Vice Rector for Academic Affairs  
and Internationalization



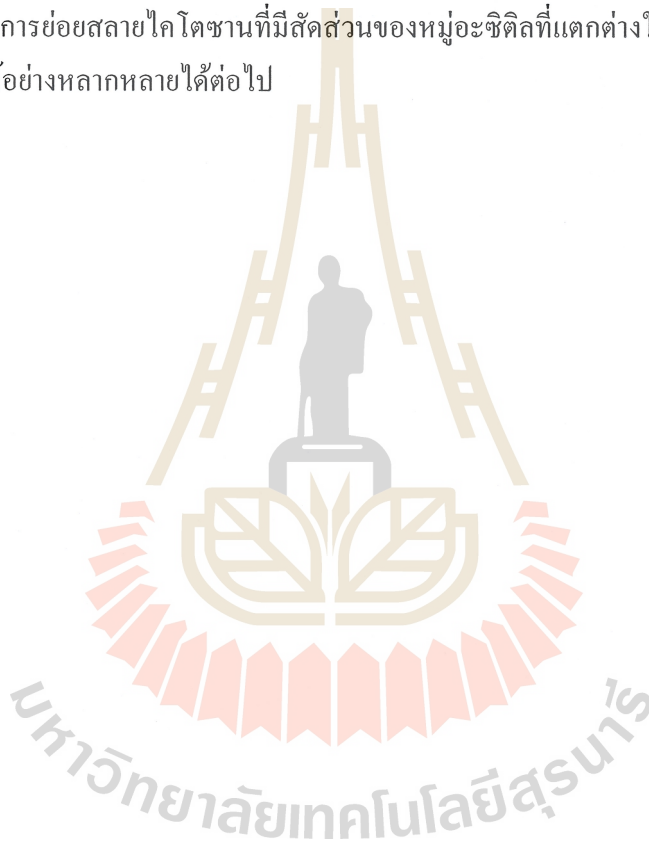
\_\_\_\_\_  
(Prof. Dr. Neung Teaumroong)

Dean of Institute of Agricultural Technology

พรศิริ เพชรศรีช่วง : การผลิตและฤทธิ์ทางชีวภาพของไคโตโอลิโกแซคคาไรด์ (คอช) ที่ถูกสร้าง  
ขึ้นด้วยเทคโนโลยีเอนไซม์ (PRODUCTION AND BIOLOGICAL ACTIVITY OF CHITO-  
OLIGOSACCHARIDE GENERATED BY ENZYME TECHNOLOGY) อาจารย์ที่ปรึกษา :  
ศาสตราจารย์ ดร.มณฑารพ ยมาภย์, 126 หน้า.

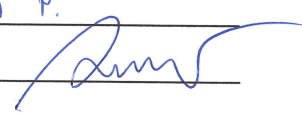
ไคตินและไคโตซานเป็นโพลีเมอร์ที่มีฤทธิ์ทางชีวภาพ พบในโครงสร้างของสัตว์ขาปล้อง  
ปลาหมึก และผนังเซลล์ของรา แหล่งวัตถุดิบหลักทางอุตสาหกรรมที่ใช้ในการผลิตไคตินและไคโตซาน มา  
จากกากของเสียจากอุตสาหกรรมแปรรูปอาหารทะเล เนื่องจากไคตินและไคโตซานไม่สามารถละลายใน  
น้ำได้ ดังนั้นไคโตโอลิโกแซคคาไรด์หรือ คอช ซึ่งเป็นน้ำตาลสายสั้น ที่ผลิตจากไคตินและไคโตซานจึง  
เป็นที่น่าสนใจในการนำมาประยุกต์ใช้มากกว่าไคตินและไคโตซาน เพราะ คอช มีคุณสมบัติในการละลาย  
น้ำได้ดี ไม่เป็นพิษต่อเซลล์ และสามารถเข้ากันได้กับสถานะชีวภาพ ไคโตซานเนสเป็นเอนไซม์ที่สามารถ  
นำไปใช้ในการผลิตคอชที่ประกอบด้วยหมู่อะซิติกบางส่วน ซึ่งอาจนำมาใช้ประโยชน์ในด้านต่างๆอย่าง  
หลากหลาย งานวิจัยก่อนหน้าได้แสดงให้เห็นว่าเอนไซม์ไคโตซานเนส ตระกูล 46 จาก *บาชิลลัส สับติ-*  
*ลิส (BsCsn46A)* เป็นเอนไซม์ที่มีศักยภาพสูงสำหรับการใช้งานในทางอุตสาหกรรม โดยได้ทำการสร้าง  
เอนไซม์ *BsCsn46A* จาก *บาชิลลัส สับติลิส* สองรูปแบบ ได้แก่ ไคโตซานเนสที่มีเปปไทด์นำทางของ  
*บาชิลลัส* และไคโตซานเนสที่มีเปปไทด์นำทางของแบคทีเรีย *เอสเชอริเชีย โคลิ (อี. โคลิ)* ชื่อว่า *OmpA*  
จากนั้นเอนไซม์ทั้งสองรูปแบบได้ถูกทำให้แสดงออกเป็นจำนวนมากใน *อี. โคลิ* เพื่อประเมิน  
ประสิทธิภาพการหลั่ง ผลการทดลองพบว่า ไคโตซานเนสที่มีเปปไทด์นำทางดั้งเดิมเมื่อหลั่งออกมา จะถูก  
ตัดออกเป็นเอนไซม์สมบูรณ์แบบที่มีโครงสร้างเหมือนกันหมด และมีลำดับของกรดอะมิโนที่ปลายเอ็น  
เช่นเดียวกับแบคทีเรียชนิดดั้งเดิม ขณะที่ *BsCsn46A* ที่มีเปปไทด์ส่งสัญญาณ *OmpA* นั้นเมื่อถูกตัดออก จะมี  
ลำดับของกรดอะมิโนที่ปลายเอ็นที่แตกต่างกัน อย่างไรก็ตาม จากการทดสอบกิจกรรมของเอนไซม์พบว่า  
*BsCsn46A* ที่มีเปปไทด์ส่งสัญญาณ *อี. โคลิ OmpA* มีระดับการแสดงออกที่สูงกว่ามีเปปไทด์ส่งสัญญาณ  
*บาชิลลัส* ดังนั้น *BsCsn46A* ที่ประกอบด้วยสัญญาณเปปไทด์ *OmpA* จึงถูกนำมาใช้สำหรับการทดลองขั้น  
ต่อไป คือการศึกษาคุณสมบัติเชิงลึกในการทำปฏิกิริยาของ *BsCsn46A* และความสามารถในการย่อย  
สลายไคโตซานที่มีสัดส่วนของหมู่อะซิติก ( $F_A$ ) ที่แตกต่างกัน โดยใช้เทคนิคโครมาโตกราฟีแบบแยก  
โดยขนาด (SEC), โปรตอนนิวเคลียร์แมกติกเรโซแนนซ์ ( $^1\text{H-NMR}$ ) และ แมสสเปกโตรเมตรี (MS)  
ผลการศึกษารูปแบบการจับของเอนไซม์แสดงให้เห็นว่า *BsCsn46A* ชอบจับตำแหน่ง D ที่ตำแหน่ง-1  
อย่างไรก็ตามเอนไซม์นี้สามารถสลายพันธะไกลโคสิติกที่ตำแหน่ง A ได้เช่นเดียวกัน โดย *BsCsn46A* จะ  
สลายพันธะจากด้านในแบบไม่จับยึดแน่น จึงทำให้สามารถย่อยสลายไคโตซานที่มีจำนวนหมู่อะซิติกที่  
แตกต่างกันให้เป็นคอชที่มีความยาว และองค์ประกอบหลากหลายได้อย่างมีประสิทธิภาพ ทั้งนี้ขึ้นอยู่กับ  
คุณสมบัติของสารตั้งต้นและสถานะที่ใช้ในการทำปฏิกิริยา สิ่งที่โดดเด่นของงานวิจัยนี้คือ *BsCsn46A*  
น่าจะเป็นหนึ่งในไคโตซานเนสที่ทำปฏิกิริยาได้เร็วมากที่สุด โดยพบว่าการกิจกรรมจำเพาะในช่วงเริ่มต้น  
ปฏิกิริยามีค่า  $5.5 \times 10^3$  และ  $8.4 \times 10^3$  ต่อนาที เมื่อใช้ไคโตซานที่มีค่า  $F_A$  0.15 และ  $F_A$  0.3 ตามลำดับ ขึ้นตอน

สุดท้ายของงานวิจัยนี้ คือ การเตรียมคอกซ์ที่มีค่า  $F_A$  ที่แตกต่างกันสามชนิด โดยใช้ *BsCsn46A* ในการย่อยสลายไคโตซานที่มีค่า  $F_A$  0.15 และ  $F_A$  0.3 และ เอนไซม์ไคตินเนสจาก*บาซิลลัส ไคเคนนิฟอร์มิส* ที่ถูกปรับปรุงโดยการทำให้กลายพันธุ์ (*BIChiA3*) เพื่อย่อยสลายไคโตซานที่มีหมู่อะซิติลสูง ( $F_A$  0.6) จากนั้นจึงทำการทดสอบฤทธิ์ทางชีวภาพของคอกซ์ที่มีระดับของหมู่อะซิติลที่แตกต่างกัน ( $F_A$  0.15, 0.3 และ 0.6) ผลการศึกษาพบว่าคอกซ์มีฤทธิ์ปกป้อง SH-SY5Y เซลล์จากสารก่อพิษในระบบประสาทได้อย่างมีประสิทธิภาพ จากการทดลองศึกษาผลของ คอกซ์ ต่อกระบวนการเกิด autophagy ในเซลล์ SH-SY5Y พบว่าคอกซ์ที่มีสัดส่วนของหมู่อะซิติลที่แตกต่างกันนั้นมีกิจกรรมทางชีวภาพที่แตกต่างกัน รวมถึงยังมีฤทธิ์ในการปกป้องเซลล์ประสาทด้วย จากผลการทดลองทั้งหมดสรุปได้ว่า *BsCsn46A* เป็นเอนไซม์ที่มีประสิทธิภาพในการย่อยสลายไคโตซานที่มีสัดส่วนของหมู่อะซิติลที่แตกต่างกันให้เป็นคอกซ์ที่มีมูลค่าเพิ่มขึ้นเพื่อใช้ประโยชน์อย่างหลากหลายได้ต่อไป



สาขาวิชาเทคโนโลยีชีวภาพ  
ปีการศึกษา 2560

ลายมือชื่อนักศึกษา Phornsiri P.

ลายมือชื่ออาจารย์ที่ปรึกษา 

PHORNSIRI PECHSRICHUANG : PRODUCTION AND BIOLOGICAL  
ACTIVITY OF CHITO-OLIGOSACCHARIDE PRODUCED BY ENZYME  
TECHNOLOGY. THESIS ADVISOR : PROF. MONTAROP YAMABHAI,  
Ph.D., 126 PP.

CHITIN/CHITOSAN/CHITOSANASE/CHITO-OLIGOSACCHARIDE/CHOS/  
BACILLIS/ANTIOXIDANT/AUTOPHAGY

Chitin and chitosan are bioactive polymers found in the exoskeleton of arthropods, cephalopods, and cell walls of fungi. The main industrial sources of chitin and chitosan are wastes from seafood processing industries. Since chitin and chitosan have poor solubility in water. Chito-oligosaccharides (CHOS), oligomers of chitin and chitosan, are more interesting for a wide variety of applications because they are water soluble, non-toxic, and biocompatible. Chitosanase can be used to produce partially acetylated CHOS for several applications. Previously, the family 46 chitosanase from *Bacillus subtilis* (*BsCsn46A*) has been shown to possess high potential for industrial applications. In this, two forms of recombinant *BsCsn46A* from *B. subtilis* containing the native *Bacillus* or *Escherichia coli* OmpA signal peptide were constructed and overexpressed in *E. coli* to evaluate their secretion efficiency. The results showed that only the construct with the native signal peptide could be cleaved homogeneously, generating the same *N*-terminal sequence as in the wild type bacteria, whereas, secreted *BsCsn46A* from the construct containing the OmpA signal peptide was heterogeneous. However, the expression level of *BsCsn46A* generated from the construct containing the *E. coli* OmpA signal peptide was much higher compared to the native *Bacillus* signal peptide. Therefore, the construct *BsCsn46A* with OmpA signal peptide was used for the subsequent experiments. In-depth characterization of the mode of action of *BsCsn46A* and

its ability to degrade chitosans with various fractions of *N*-acetylation ( $F_A$ ) were performed, using size exclusion chromatography,  $^1\text{H-NMR}$ , and mass spectrometry (MS) methods. The results showed that *BsCsn46A* has subsite binding preference for D-units in the -1 subsite, although the enzyme can also hydrolyze glycosidic linkages following an A-unit. Utilizing the non-processive endo-mode fashion, *BsCsn46A* can efficiently convert chitosans with different degrees of acetylation into mixtures of CHOS with varying chain lengths and compositions, depending on the substrate and the reaction conditions. Notably, this enzyme seems to be one of the fastest chitosanases so far. The initial specific activities of chitosan degradation were  $5.5 \times 10^3$  and  $8.4 \times 10^3 \text{ min}^{-1}$  for chitosans with  $F_A$  0.15 and  $F_A$  0.3, respectively. Finally, CHOS with various  $F_A$  were produced by enzymatic hydrolysis using *BsCsn46A* for chitosan with  $F_A$  0.15 and  $F_A$  0.3, or a mutant of *B. licheniformis* chitinase (*BIChiA3*) with improved properties for highly acetylated chitosan ( $F_A$  0.6). Then, the biological activities of various degrees of acetylation of CHOS with  $F_A$  0.15, 0.3 and 0.6 on a model cell line for neuronal function and differentiation were studied. The results suggested that CHOS effectively protect the SH-SY5Y cells from a neurotoxic agent. Interestingly, CHOS could enhance autophagy activity in SH-SY5Y cells. CHOS with different degrees of acetylation showed different biological activities including neuroprotective effects. In conclusion, *BsCsn46A* is a suitable enzyme for the bioconversion of chitosans with various degrees of acetylation into value-added CHOS for different applications.

School of Biotechnology

Academic Year 2017

Student's Signature Phornsiri P.

Advisor's Signature 

## ACKNOWLEDGEMENT

Firstly, I would like to express my sincere gratitude to thesis advisor Prof. Dr. Montarop Yamabhai, the continuous support of my Ph.D study and related research, for her patience, motivation, and immense knowledge. I appreciate her contributions of time, ideas, and funding to make my Ph.D. experience productive and stimulating.

I would like to express my gratitude to Prof. Vincent Eijsink who provided me an opportunity to work as intern at NMBU for a year. He guided me, giving a good help by sharing his expertise in the field.

I am also greatly thankful for Dr.Parinya Noisa for his guidance on biological activity assay.

I would like to thanks all committees Prof. Vincent Eijsink, Dr. Berit Bjugan Aam, Dr. Parinya Noisa and Dr. Chomphunuch Songsiriritthigul for their valuable time and patience to read my thesis.

I would also like to thanks Suranaree University of Technology for their financial support (SUT-Ph.D. scholarship) for my study and research experience at Faculty of Chemistry, Biotechnology, Biotechnology and Food Science, Norwegian University of Life Science, Norway for 1 year.

I would also like to thanks Dr.Mattaka Kongkaw for giving me opportunity to collaborate with her team at nanocosmetics laboratory, NANOTEC, Thai Science Park.

I would like to thanks MY lab members; P' Kun, Bee, P'Pang, N'Pang, Otto, Kik, N'Kik, P' Tae Tae, Chainoy and N'Nan. I am grateful for their good help and friendship.

I would like to thanks the member from protein engineering and proteomics group (PEP) at NMBU especially Tina, Silje, Berit, Anna Grethe, Christine, Sofi, Madhu, Simen and Rianne

that have contributed immensely to my personal and professional time at NMBU, Norway. The group has been a source of friendships as well as good advice and collaboration.

Special thanks to Dr.Thongchai Koobkokkrud for his love, encouragement and supporting.

Finally, I express my very profound gratitude to my parents, my sister, my aunt to for providing me with unfailing support and continuous encouragement throughout my years of study. This accomplishment would not have been possible without them.

Phornsiri Pechsrichuang



# CONTENTS

	<b>Page</b>
ABSTRACT IN THAI.....	I
ABSTRACT IN ENGLISH.....	III
ACKNOWLEDGEMENTS.....	V
CONTENTS.....	VII
LIST OF TABLES.....	XII
LIST OF FIGURES.....	XIII
LIST OF ABBREVIATIONS.....	XV
<b>CHAPTER</b>	
<b>I INTRODUCTION.....</b>	<b>1</b>
1.1 Significant of this study.....	1
1.2 Research objectives.....	3
1.3 Scope of the study.....	3
1.4 References.....	4
<b>II BIOCONVERSION OF CHITIN AND CHITOSAN.....</b>	<b>6</b>
2.1 Abstract.....	6
2.2 Chitin, chitosan and CHOS.....	7
2.3 Production of chitin and chitosan from crustacean shells using microbial fermentation.....	10
2.4 Conversion of chitin into chitosan by chitin deacetylase.....	12
2.5 Production of CHOS by enzymatic method.....	14
2.5.1 Hydrolysis activity by chitinase and chitosanase.....	14

## CONTENTS (Continued)

	<b>Page</b>
2.5.2 Transglycosylation activity.....	16
2.5.3 Auxiliary activity.....	18
2.6 Conclusion.....	20
2.7 References.....	21
 <b>III EXPRESSION OF RECOMBINANT <i>BACILLUS SUBTILIS</i></b>	
<b>CHITOSANASE IN <i>E. COLI</i> EXPRESSION SYSTEM.....</b>	
<b>33</b>	
3.1 Abstract.....	33
3.2 Introduction.....	34
3.3 Materials and Methods.....	35
3.3.1 Bacterial strains and plasmids.....	35
3.3.2 Substrate.....	35
3.3.3 Molecular cloning.....	36
3.3.4 Expression and preparation of recombinant chitosanases from various compartments.....	37
3.3.5 SDS-PAGE.....	37
3.3.6 Chitosanase activity assay on chitosan agar plate.....	38
3.3.7 Chitosanase activity assay.....	38
3.3.8 Purification of recombinant chitosanase.....	38
3.3.9 N-terminal sequencing.....	38
3.3.10 MALDI-TOF MS.....	39
3.4 Results.....	40
3.4.1 Cloning and secretion of recombinant Csn containing two different signal peptides on agar plates.....	40

## CONTENTS (Continued)

	<b>Page</b>
3.4.2 Effect of signal peptides on yield and secretion efficiency.....	43
3.4.3 N-terminal sequencing of secreted recombinant Csn.....	46
3.4.4 MALDI-TOF mass spectrometry of secreted recombinant Csn.....	49
3.5 Discussion.....	50
3.6 Conclusion.....	53
3.7 References.....	54
 <b>IV IN-DEPTH CHARACTERIZATION OF FAMILY 46</b>	
<b>CHITOSANASE FROM <i>BACILLUS SUBTILIS</i> (BSCSN46A).....</b>	<b>58</b>
4.1 Abstract.....	58
4.2 Introduction.....	59
4.3 Material and Methods.....	61
4.3.1 Chitosans.....	61
4.3.2 Expression of recombinant <i>BsCsn46A</i> gene in <i>E. coli</i> .....	61
4.3.3 Enzymatic degradation of chitosan.....	62
4.3.4 Size-exclusion chromatography.....	63
4.3.5 NMR spectroscopy.....	63
4.3.6 Analysis of CHOS by mass spectrometry (MS).....	64
4.3.7 CHOS sequencing.....	64
4.3.8 Hydrolysis of (GlcN) <sub>5</sub> and (GlcN) <sub>6</sub> in H <sub>2</sub> <sup>18</sup> O for Subsite mapping.....	65
4.4 Results and discussion.....	66

## CONTENTS (Continued)

	<b>Page</b>
4.4.1 Hydrolysis of chitosan.....	66
4.4.2 Size distribution of CHOS obtained after degradation of chitosans with varying degrees of acetylation.....	71
4.4.3 Chemical composition of CHOS fractions obtained after degradation of chitosans with varying F <sub>A</sub> .....	73
4.4.4 CHOS sequences.....	74
4.4.5 Substrate positioning in the active site of <i>BsCsn46A</i> .....	82
4.5 Conclusions.....	84
4.6 References.....	86
<b>V BIOLOGICAL ACTIVITY OF CHITO-OLIGOSACCHARIDES (CHOS)</b> .....	<b>90</b>
5.1 Abstract.....	90
5.2 Introduction.....	92
5.3 Material and Method.....	94
5.3.1 Chitosan.....	94
5.3.2 Chitooligosaccharide production and analysis.....	94
5.3.3 Size exclusion chromatography (SEC).....	95
5.3.4 NMR spectroscopy.....	96
5.3.5 Analysis of CHOS by Mass spectrometry.....	96
5.3.6 Cell culture.....	96
5.3.7 Measurement of cell viability by (MTT) assay.....	97
5.3.8 Apoptosis detection using AnnexinV and 7-AAd staining.....	97
5.3.9 Real-time quantitative reverse transcription PCR (qPCR).....	98

**CONTENTS (Continued)**

	<b>Page</b>
5.3.10 Measurement of intracellular reactive oxidation species (ROS) by DCF assay.....	99
5.3.11 Detection of microtubule-associated protein 1A/1B-light chain 3 ( <i>LC3 I/II</i> ) by immunofluorescence staining.....	100
5.3.12 Detection of autophagosome using monodansylcadaverine (MDC) staining.....	101
5.3.13 Western blot analysis.....	101
5.4 Results.....	102
5.4.1 Production and characterization of CHOS.....	102
5.4.2 Cytotoxicity of CHOS.....	106
5.4.3 CHOS reduced paraquat-induced intracellular ROS and apoptosis in SH-SY5Y cells.....	107
5.4.4 Effect of CHOS on apoptosis related gene expression exposed to paraquat and antioxidant gene expression in SH-SY5Y.....	108
5.4.5 CHOS induced autophagy in SH-SY5Y cells.....	110
5.5 Discussion and conclusion.....	115
5.6 References.....	117
<b>VI CONCLUSION.....</b>	<b>124</b>
<b>BIOGRAPHY.....</b>	<b>125</b>

## LIST OF TABLES

Table	Page
2.1 Bioconversion of chitin and chitosan from crustacean shells using microbial fermentation.....	12
2.2 Bioconversion of chitin or chitin oligomer into chitosan or chito-oligosaccharide by chitin deacetylase.....	13
2.3 Enzymatic hydrolysis of chitin and chitosan into CHOS by chitinase and chitosanase.....	16
2.4 Bioconversion of chitin and chitosan into CHOS by transglycosylation activity of chitinolytic enzyme.....	18
2.5 Bioconversion of chitin and chitosan into CHOS by recombinant Lytic Polysaccharide Monooxygenase (LPMO).....	20
3.1 Enzyme activity and secretion efficiency.....	44
3.2 Purification of Nat-Csn/pMY202 and OmpA-Csn/pMY202 from culture broth or cell lysate.....	46
4.1 Chemical composition of CHOS fractions .....	74
4.2 Sequences of isolated CHOS.....	81
4.3 Properties of three well-characterized chitosanases.....	85
5.1 qPCR primers of autophagy, antioxidant and apoptosis gene.....	99
5.2 Chemical composition of CHOS fractions.....	106

## LIST OF FIGURES

Figure	Page
2.1	Chemical structure of chitin.....8
2.2	Chemical structure of chitosan.....9
3.1	Map of constructs used in this study.....42
3.2	Secretion of recombinant Csn.....43
3.3	Expression and purification of secreted Nat-Csn and OmpA-Csn from culture supernatant and cell lysate.....47
3.4	Signal peptide cleavage sites. N-terminal sequencing of Nat-Csn and OmpA-Csn.....48
3.5	MALDI-TOF MS analysis of the recombinant OmpA-Csn.....50
4.1	Product formation over time during degradation of chitosans with $F_A$ 0.15 or $F_A$ 0.3 with <i>BsCsn46A</i> , analyzed by $^1\text{H-NMR}$ .....68
4.2	Time-course for the increase in $\alpha$ during degradation of chitosans with $F_A$ 0.15 or $F_A$ 0.3 with <i>BsCsn46A</i> .....69
4.3	Time-course analysis of the initial phase of degradation.....71
4.4	Product analysis by size exclusion chromatography (SEC).....72
4.5	Size distribution of CHOS for sequence analysis.....75
4.6	MS1 spectra of AMAC labeled products of Chitosan with $F_A$ 0.3 degraded to $\alpha = 0.14$ .....77
4.7	MS2 spectra of AMAC labeled mono-acetylated products of chitosan with $F_A$ 0.3 degraded to $\alpha = 0.14$ .....78

## LIST OF FIGURES (Continued)

Figure	Page
4.8	MS1 spectra of AMAC labeled products of chitosan with F <sub>A</sub> 0.3 degraded to $\alpha = 0.26$ .....79
4.9	MS2 spectra of AMAC labeled mono-acetylated products of chitosan with F <sub>A</sub> 0.3 degraded to $\alpha = 0.26$ .....80
4.10	MALDI-TOF-MS analysis of (GlcN) <sub>5</sub> and (GlcN) <sub>6</sub> degradation.....83
4.11	Productive binding modes of <i>BsCsn46A</i> .....84
5.1	Time-course for the increase in $\alpha$ during degradation of chitosans with F <sub>A</sub> 0.15 or F <sub>A</sub> 0.3 with <i>BsCsn46A</i> .....103
5.2	<sup>1</sup> H NMR analysis of CHOS preparation.....104
5.3	Product analysis by size exclusion chromatography (SEC).....105
5.4	Protective effect of CHOS on paraquat-induced neuronal cell death in SH-SY5Y cell.....107
5.5	Protective effect of CHOS on paraquat-induced neuronal cell death in SH-SY5Y cell.....109
5.6	Analysis of antioxidant gene expression by qPCR.....110
5.7	Analysis of autophagy gene expression by qPCR.....111
5.8	Effect of CHOS on <i>LC3 I/II</i> protein expression.....112
5.9	MDC-labeled autophagosome.....113
5.10	Expression level of <i>LC3 I/II</i> and <i>P62</i> determined by western blotting.....115
5.11	Mycoplasma detection by PCR-based technique.....123

## LIST OF ABBREVIATIONS

$\alpha$	=	Degree of scission
A-unit	=	<i>N</i> -acetyl-D-glucosamine or GlcNAc
AMAC	=	2-aminoacridone
BSA	=	Bovine serum albumin
<i>BsCsn46A</i>	=	GH family 46 chitosanase from <i>Bacillus subtilis</i>
<i>BlChiA3</i>	=	Improved chitinase from <i>Bacillus licheniformis</i>
CAZy	=	Carbohydrate-active enZYmes
CHOS	=	Chito-oligosaccharides
CQ	=	Chloroquine
Csn	=	Chitosanase
D-unit	=	D-glucosamine or GlcN
DCFH-DA	=	Dichloro-dihydro-fluorescein diacetate
DHB	=	2,5dihydroxybenzoic acid
DMEM	=	Dulbecco's Modified Eagle Medium
DP <sub>n</sub>	=	Average degree of polymerization
DNA	=	Deoxyribonucleic acid
DP	=	Degree of polymerization
F <sub>A</sub>	=	Fraction of acetylation
GH	=	Glycosyl hydrolase
IMAC	=	Immobilized metal affinity chromatography
LB	=	Luria-Bertani
MDC	=	Monodansylcadavarine

**LIST OF ABBREVIATIONS (Continued)**

MW <sub>n</sub>	=	Average molecular weight
NMR	=	Nuclear magnetic resonance
OD	=	Optical density
OmpA	=	Outer membrane proteinA
P <sub>A</sub>	=	Pattern of acetylation
PAGE	=	Polyacrylamide gel electrophoresis
pH	=	log of the hydrogen ion concentration
qPCR	=	Real-time quantitative reverse transcription PCR
PQ	=	Paraquat
RI	=	Refractive index
RNA	=	Ribonucleic acid
ROS	=	Reactive oxidation species
SDS	=	Sodium dodecyl sulphate
SEC	=	Size exclusion chromatography

**LIST OF ABBREVIATIONS (Continued)**

$\mu\text{g}$	=	microgram
kDa	=	(kilo) Dalton
$\mu\text{l}$	=	microlitre
$^{\circ}\text{C}$	=	degrees Celsius
g	=	grams
h	=	hours
kg	=	kilogram
L	=	litre
M	=	molar
mg	=	milligram
min	=	minute
ml	=	milliliter
ppm	=	Parts per million
rpm	=	Revolution
v/v	=	volume per unit volume
w/v	=	weight per unit volume

# CHAPTER I

## INTRODUCTION

### 1.1 Significant of this study

Chitin, a  $\beta$ -(1,4)-linked polymer of *N*-acetyl D-Glucosamine (GlcNAc; A), is the second most abundant biopolymer on earth after cellulose (Khoushab and Yamabhai). Exoskeleton of insects, cell walls of various fungi, crab and shrimp wastes are the main sources of chitin (Ravi Kumar 2000). Chitosan, a D-glucosamine polymer (GlcN; D), is a completely or partially deacetylated derivative of chitin (Wang et al. 2006). It is usually obtained by the artificial deacetylation of chitin under strongly alkaline conditions. Although chitosan is known to have important biological activities, poor solubility makes them difficult to be used in food and biomedical applications (Kim and Rajapakse 2005). Unlike chitosan, chito-oligosaccharides are readily soluble in water due to their shorter chain lengths and free amino groups in D-glucosamine units. The low viscosity and greater solubility of CHOS at neutral pH have attracted the interest of many researchers to utilize chitosan in its oligosaccharide form (Jeon and Kim 2000).

The biodegradation of chitin in crustacean shell waste is very slow, so the accumulation of large quantities of discards seafood processing industry has become a major environmental concern. The amount of worldwide shrimp and prawn production was 6,091,869 tons in 2005 (FAO 2008). In developing countries, waste shells are often just dumped in landfill or the sea. Disposal of shellfish processing discards has been a challenge for most of the shellfish-producing countries. Out of the different species

of crustaceans, shrimp and crab shell wastes have been widely used as sources for the isolation of chitin. The production of value-added products such as chitin and their derivatives and application in different fields are therefore of utmost interest (Khoushab and Yamabhai). The oligosaccharide of chitin and chitosan have various potential application in the field of food (Fernandes et al. 2008), agricultural (Hadwiger et al. 1984), and pharmaceutical (Dou et al. 2009) industries. Today, commercial interest in the conversion of chitin or chitosan into bioactive CHOS, using enzymatic reaction, mainly chitosanase, has been increased. The substrate specific activity of chitosanase depends on the degree of deacetylation (DDA), fraction of *N*-acetylated residues ( $F_A$ ), degree of polymerization (DP) or molecular weight ( $M_w$ ), molecular weight distribution (PD), and pattern of *N*-acetylation ( $P_A$ ) (Aam et al. 2010). Since the various biological activities of CHOS are dependent on the degree of polymerization and deacetylation, it is essential to produce a well-defined CHOS mixtures for better understanding of the structure-function relationship, so that more appropriate uses of different products can be reached.

Until now, most of the research on molecular mechanism of CHOS has been done with CHOS mixtures with various  $F_A$ ,  $M_w$ , PD and  $P_A$ . Consequently, when using complex mixtures of CHOS in biological activity assays, it is difficult to know which molecule/molecules are causing the effects. Therefore, in this Ph.D.thesis, I will purify/separate CHOS to test the biological activity. In addition, a method for bioconversion of chitosan into CHOS will be invent and the products will be tested for their biological activities.

This thesis is divided into 6 Chapters. Chapter I is an introduction, including significance of this study, research objective and scope of the study. Chapter II is a

literature review involving the bioconversion of chitin and chitosan (manuscript preparation). Chapter III involves expression of recombinant *Bacillus subtilis* chitosanase in *E. Coli* expression system and the effect of signal peptide on the secretion efficiency (Pechsrichuang et al. 2016). Chapter IV is an in-depth characterization of family 46 chitosanase from *Bacillus Subtilis* (*BsCsn46A*) (Pechsrichuang et al. 2018). Chapter V is the study of the biological activity of CHOSs on neuroprotection and autophagy modulation of human neuroblastoma cells (manuscript preparation). Finally, the conclusion is written in Chapter VI.

## 1.2 Research objectives

The key objectives of this study are:

1. To study the recombinant *BsCsn46A* that is over-express and secreted from *E. coli* expression system.
2. To optimize the condition for efficient bioconversion of chitosan into CHOS.
3. To analyzed different hydrolytic products obtained from various bioconversion procession reaction.
4. To elucidate biological activities of different well-defined CHOS products.

## 1.3 Scope of the study

Chitosan from Kitoflokk™ (F<sub>A</sub> 0.15), Hepepe Medical chitosan GmbH (F<sub>A</sub> 0.3), and highly acetylated chitosan with F<sub>A</sub> 0.6 (prepared by homogenous de-*N*-acetylation of chitin from shrimp shells) were used as a substrate of recombinant chitosanase to produce chito-oligosaccharide. The biological assay was done *in vitro*.

## 1.4 References

- Aam, B. B., Heggset, E. B., Norberg, A. L., Sørli, M., Vårum, K. M. and Eijsink, V. G. H. (2010). Production of chitooligosaccharides and their potential applications in medicine. **Marine Drugs** 8(5): 1482-1517.
- Dou, J., Xu, Q., Tan, C., Wang, W., Du, Y., Bai, X. and Ma, X. (2009). Effects of chitosan oligosaccharides on neutrophils from glycogen-induced peritonitis mice model. **Carbohydrate Polymers** 75(1): 119-124.
- FAO (2008). Food and agricultural organisation; FAOSTAT data base.  
<http://faostat.fao.org/faostat/collections?subset=fisheries>.
- Fernandes, J. C., Tavora, F. K., Soares, J. C., Ramos, S., João Monteiro, M., Pintado, M. E. and Xavier Malcata, F. (2008). Antimicrobial effects of chitosans and chitooligosaccharides, upon *Staphylococcus aureus* and *Escherichia coli*, in food model systems. **Food Microbiology** 25(7): 922-928.
- Hadwiger, L. A., Fristensky, B. and Riggleman, R. C. (1984). Chitosan, a natural regulator in plant pathogen interaction increase crop yield. **Chitin, Chitosan and Related Enzyme**: 291-302.
- Jeon, Y.-J. and Kim, S.-K. (2000). Production of chitooligosaccharides using an ultrafiltration membrane reactor and their antibacterial activity. **Carbohydrate Polymers** 41(2): 133-141.
- Khoushab, F. and Yamabhai, M. Chitin Research Revisited. **Marine Drugs** 8(7): 1988-2012.
- Kim, S.-K. and Rajapakse, N. (2005). Enzymatic production and biological activities of chitosan oligosaccharides (COS): A review. **Carbohydrate Polymers** 62(4): 357-368.

- Pechsrichuang, P., Lorentzen, S. B., Aam, B. B., Tuveng, T. R., Hamre, A. G., Eijsink, V. G. H. and Yamabhai, M. (2018). Bioconversion of chitosan into chito-oligosaccharides (CHOS) using family 46 chitosanase from *Bacillus subtilis* (BsCsn46A). **Carbohydrate Polymers** 186: 420-428.
- Pechsrichuang, P., Songsiriritthigul, C., Haltrich, D., Roytrakul, S., Namvijitr, P., Bonaparte, N. and Yamabhai, M. (2016). OmpA signal peptide leads to heterogenous secretion of *B. subtilis* chitosanase enzyme from *E. coli* expression system. **SpringerPlus** 5(1): 1200.
- Ravi Kumar, M. N. V. (2000). A review of chitin and chitosan applications. **Reactive and Functional Polymers** 46(1): 1-27.
- Wang, S.-L., Lin, T.-Y., Yen, Y.-H., Liao, H.-F. and Chen, Y.-J. (2006). Bioconversion of shellfish chitin wastes for the production of *Bacillus subtilis* W-118 chitinase. **Carbohydrate Research** 341(15): 2507-2515.

## **CHAPTER II**

### **BIOCONVERSION OF CHITIN AND CHITOSAN**

#### **2.1 Abstract**

Chitin and chitosan are biopolymers from exoskeleton of arthropods. The main industrial sources of chitin and chitosan are crab, lobster and shrimp wastes from seafood processing industries. Degradation of crustacean shell waste in nature is very slow, so that accumulation of large quantity of discards seafood processing industry has become a major environmental concern. Chitin and chitosan can be prepared by using chemical, enzymatic or microbiological methods. Nowadays, demand of green products to replace pollution-generating products is increasing. Thus, bioconversion processes using enzymatic or microbiological method are more attractive. Preparation of chitin and chitosan from shell waste can be performed by using microbial fermentation for deproteinization and demineralization processes. However, chitin and chitosan have poor solubility in water, making them difficult to use in biological application. Therefore, chito-oligosaccharide, an oligomer of chitin and chitosan, is more interesting due to its water solubility at neutral pH, non-toxicity, biocompatibility and broad variety of applications including agriculture, food, medical and pharmaceutical. Bioconversion of chitin and chitosan into CHOS can be performed by enzymatic method using glycoside hydrolases (GH) namely chitinases and chitosanases. In the past decade, various chitinolytic GHs have been intensively studied and the recombinant GHs have been expressed and engineered to increase the enzyme activity or increase

transglycosylation activity for the production of long chain CHOS. Recently, lytic polysaccharide monoxygenase (LPMO), a new discovered group of carbohydrate active enzymes, classified as auxiliary activities (AA) has been shown to be active on the crystalline structure of  $\alpha$ - and  $\beta$ -chitin. LPMO has been shown to work in synergy with chitinase to degrade  $\alpha$ -chitin, increasing the solubility of chitin. Chitin deacetylase is another chitin-active enzyme which is important for conversion of chitin into chitosan by the hydrolysis of the *N*-acetamido groups of *N*-acetyl-D-glucosamine residues of the chitin polymer. This review summarizes various strategy for the bioconversion marine shell wastes into chitin, chitosan and CHOS via microbial fermentation and enzyme technology. While microbial fermentation is efficient and cost effective, enzymatic hydrolysis is more precise and the property of the hydrolytic products can be tightly controlled and better defined.

**Keywords:** Bioconversion; chitin; chitosan; microbial fermentation; chitinase; chitosanase; enzymatic hydrolysis, transglycosylation; lytic polysaccharide monoxygenase; chitin deacetylase

## 2.2 Chitin, chitosan and CHOS

Chitin is a  $\beta$ -(1,4)-linked polymer of 2-acetamido-2-deoxy- $\beta$ -D-glucopyranose (*N*-acetyl D-Glucosamine; GlcNAc; A) chains, an acetamide group exist at the C2 position (Figure 2.1). Its main source is the exoskeleton of crabs and shrimps, whose availability in nature makes chitin a renewable source of chitosan. Chitin is non-water soluble and arranged in three different microcrystalline structures; antiparallel ( $\uparrow\downarrow\uparrow$ ) sheets ( $\alpha$ -chitin), parallele ( $\uparrow\uparrow\uparrow$ ) sheets ( $\beta$ -chitin) and a combination of both ( $\gamma$ -chitin),

consist of two parallel strands which alternate with a single parallel strand ( $\uparrow\downarrow$ ) (Rudall 1963). The  $\alpha$ -chitin is found in exoskeleton of arthropod, insects and fungal and yeast cell walls, while the  $\beta$ -form mainly obtained from squid pen. The molecular arrangement of  $\alpha$ -chitin is strongly packed with both inter- and intra molecular hydrogen bonding, and it is the most stable form of the three crystalline variations, while  $\beta$ -chitin has weak intramolecular hydrogen bonding (Carlström 1957, Hackman and Goldberg 1965).

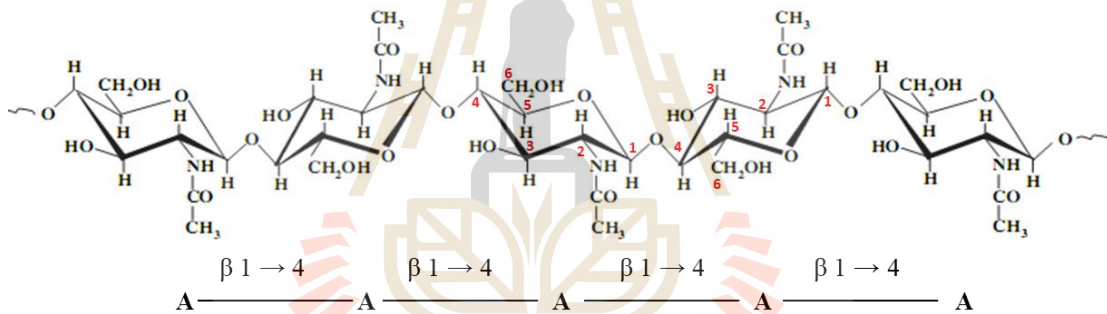


**Figure 2.1** Chemical structure of Chitin (Prashanth and Tharanathan 2007)

Chitosan, a heteropolymer of D-glucosamine polymer (GlcN; D) and *N*-acetyl-D-glucosamine polymer, is a completely or partially deacetylated derivative of chitin (Figure 2.2). It is usually obtained by the artificial deacetylation of chitin in the presence of alkaline. Chitosan can be classified according to degree of *N*-acetylation ( $DA$ ) or fraction of *N*-acetylated residues ( $F_A$ ), the degree of polymerization ( $DP$ ) or molecular weight ( $M_w$ ), the molecular weight distribution ( $PD$ ) and the pattern of *N*-acetylation ( $P_A$ ) (Aam et al. 2010).

Chitosan has a  $pK_a$  value of about 6.5; hence, chitosan is positively charged and is soluble in weakly acidic solutions with a charge density that is dependent on the  $pH$

and the degree of deacetylation. Although chitosan is known to have important biological activities, but it is poor solubility in water that makes them difficult to use in biological application. Unlike CHOS, which are readily soluble in water due to their shorter chain lengths and free amino groups in D-glucosamine units. The low viscosity and greater solubility of CHOS at neutral pH have attracted the interest of many researchers to utilize chitosan in its oligosaccharide form (Jeon and Kim 2000).

Chitin, chitosan and CHOS can be distinguished by  $F_A$  and DP values. The  $F_A$  needs to be below 0.7 for the chitosan to be soluble in weak acid, while  $F_A$  of chitin is above 0.7 and insoluble in water. The DP of Chitin and chitosan polymers are more than DP 100, while DP of CHOS is less than 100.

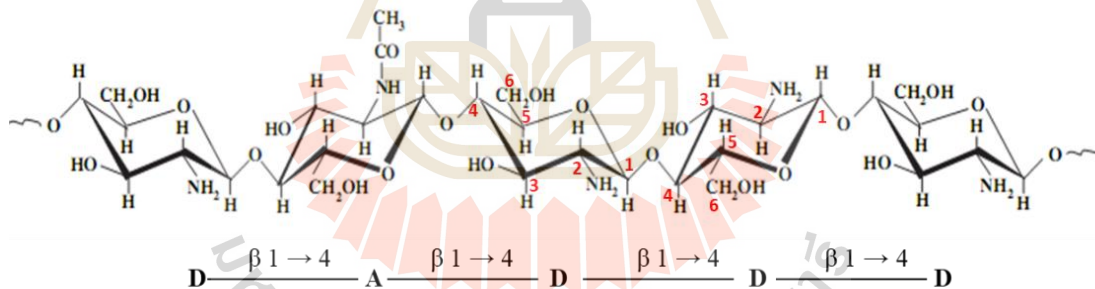


**Figure 2.2** Chemical structure of Chitosan (Prashanth and Tharanathan 2007)

The crustacean shells have three main components including chitin, minerals (mainly calcium carbonate) and proteins (Ferrer et al. 1996). Therefore, the industrial techniques to extract chitin and chitosan from crab and shrimp shell wastes mainly employs stepwise chemical method consisting of three steps: demineralization, deproteinization and bleaching which involves hazardous chemical. Demineralization can be achieved using diluted HCl (1-8%) or using other acid such as acetic and sulfuric acid and NaOH for the deproteinization step. For decolourization step, NaOCl or H<sub>2</sub>O<sub>2</sub>

solutions are being used as a bleaching agent. Chitin deacetylation forming chitosan may follow chitin extraction by using very strong NaOH (40-50%) solution to deacetylate the *N*-acetyl linkages (Hayes et al. 2008). However, the chemical process has many disadvantages including high cost, inconsistent of molecular weight (MW) and degree of acetylation (DA) and a disposal problem to the environment (Kaur and Dhillon 2015). Therefore, the environmentally friendly processes, i.e., deproteinization and demineralization by microbial fermentation using protease producing bacteria and lactic acid bacteria and deacetylation by chitin deacetylase are in demanded.

Because of the abundant of shellfish wastes, the production of value-added products such as chitin and their derivatives and application in different fields are highly interesting. The oligosaccharide of chitin and chitosan have various potential application in the field of food (Lee et al. 2002), agricultural (Yin et al. 2010), and pharmaceutical industries (Muanprasat and Chatsudthipong 2017). Because of the interest in green technology nowadays, commercial interest in the conversion of chitin or chitosan to generate bioactive CHOS, using microbial or enzymatic method has been gradually increased.

### **2.3 Production of chitin and chitosan from crustacean shells using microbial fermentation**

Chitin and chitosan from crustacean shell is generally prepared using inorganic acid for demineralization and strong alkali for deproteinization (Aye and Stevens 2004). The chemical chitin and chitosan extraction processes have many disadvantages, including environmental pollution, abundant of toxic waste, and is harmful to human health. Therefore, the alternative method for chitin and chitosan extraction which is

more environmentally approach using microbial fermentation has been developed to replace the toxic chemical method. Chitin from crustacean shell has been produced using microbiological method, in which deproteination takes place by function of proteases obtained from microorganisms and demineralization by acid produced from microorganism during fermentation. These include *Serratia marcescens* B742, *Pseudomonas aeruginosa*, *Bacillus pumilus* A1, *Pseudomonas aeruginosa* F722, *Lactobacillus plantarum* ATCC 8014, *Lactobacillus paracasei* subsp. *tolerans* KCTC-3074 and *Serratia marcescens* FS-3 (Table 2.1). These microorganism have been shown to produce organic acid to dissolve calcium carbonate and protease to hydrolyze proteins in the crustacean shell. The efficiency of fermentation is depending on raw material, fermentation type (fermentation in single step and co-fermentation) and incubation condition as summarized in Table 2.1. However, the extraction of chitin by microbial fermentation is not highly efficient when compared to the chemical method and requires complicated downstream processing for isolated of CHOS.

**Table 2.1** Bioconversion of chitin and chitosan from crustacean shells using microbial fermentation

Raw materials	Microorganism	Condition	% Yield	%DP <sup>1)</sup> and %DM <sup>2)</sup>	References
Shrimp shell powders (SSPs)	- <i>Serratia marcescens</i> B742 (deproteinization) - <i>Lactobacillus plantarum</i> ATCC 8014 (Demineralization) - <i>Rhizopus japonicus</i> M193 (Deacetylation)	- 35 °C, 11 days - Submerged fermentation	21.35% chitin and 13.11% chitosan	94.5 and 93.0%	(Zhang et al. 2017)
Shrimp waste <i>Penaeus merguensis</i>	<i>Pseudomonas aeruginosa</i> , protease-producing bacterium	20% glucose, 20% inoculation and 6 days at 50 °C	47% chitin	92% and 82%	(Sedaghat et al. 2017)
Shrimp shells, <i>Metapeneaus monoceros</i>	<i>Bacillus pumilus</i> A1	pH 5.0 at 35 °C and 150 rpm for 6 days	27% chitin	94% and 88%	(Ghorbel-Bellaaj et al. 2013)
Crab shell waste	<i>Pseudomonas aeruginosa</i> F722	7 days at 30 °C.	-	63% and 92%	(Oh et al. 2007)
Red crab ( <i>Chionoecetes japonicus</i> )	Cofermentation with <i>Lactobacillus paracasei</i> subsp. <i>tolerans</i> KCTC-3074 and <i>Serratia marcescens</i> FS-3	30 °C, 180 rpm for 7 days	-	52.6% and 97.2%	(Jung et al. 2006)

<sup>1)</sup>%DP is deproteinization rate and <sup>2)</sup>%DM is demineralization rate. %DP and %DM were calculated as previously described in (Sedaghat et al. 2017).

## 2.4 Conversion of chitin into chitosan by chitin deacetylase

Traditional method for conversion of chitin into chitosan is typically achieved by using strong alkaline solution, which generates the environmental problem and unregular deacetylation pattern, making it difficult to control and predict their biological activities. (Chang et al. 1997). Enzymatic method by chitin deacetylase (CDA, EC 3.5.1.41) is an alternative method to deacetylate chitin. Chitin deacetylases belong to the family 4 of carbohydrate esterases (CE4), according to the CAZy classification system (Lombard et al. 2014). Chitin deacetylase had been isolated and partial characterized from many fungi including CDA from *Mucor rouxii* (Kafetzopoulos et al. 1993, Tsigos et al. 1999), *Aspergillus nidulans* (Alfonso et al. 1995), *Colletotrichum*

*lindemuthianum* (Hekmat et al. 2003, Blair et al. 2006), *Vibrio parahaemolyticus* (Hirano et al. 2015) and *Vibrio cholerae* (Andrés et al. 2014). The enzyme chitin deacetylases catalyze the hydrolysis of the acetamido group in GlcNAc units of chitin, chitosan and CHOS, consequently generating glucosamine units and acetic acid (Zhao et al. 2010). This method is controllable, non-degradable process, resulting in the production of well-defined chitosan (Tsigos et al. 2000). So far, several chitin deacetylases have been cloned, purified and in-depth characterized, as shown in Table 2.2. In addition, it has been recently shown that the activity of chitin deacetylase from *Aspergillus nidulans* FGSC A4 on insoluble chitin can be improved by co-administration of CBP21, a chitin-active lytic polysaccharide monoxygenase (LPMO) from *Serratia marcescens* (Liu et al. 2017).

**Table 2.2** Bioconversion of chitin or chitin oligomer into chitosan or chito-oligosaccharide by chitin deacetylase.

Enzyme	Enzyme source	Substrate	Condition	End products	Reference
Chitin deacetylase, PaCDA	<i>Podospora anserine</i> (Yeast system; <i>Hansenula polymorpha</i> )	Colloidal chitin	37 °C, 120h	$\Delta$ DA =15%	(Hoßbach et al. 2018)
Chitin deacetylase, AnCDA, Carbohydrate esterase family4	<i>Aspergillus nidulans</i> FGSC A4 ( <i>E. coli</i> system)	(GlcNAc) <sub>6</sub>	37 °C, 24 h	(GlcNAc) <sub>6</sub> , (GlcNAc) <sub>5</sub> (GlcNAc) <sub>6</sub> , (GlcNAc) <sub>4</sub> (GlcNAc)	(Liu et al. 2017)
Chitin deacetylase, PgtCDA	<i>Puccinia graminis</i> f. sp. <i>tritici</i> ( <i>E. coli</i> system)	- (GlcNAc) <sub>4</sub> - (GlcNAc) <sub>5</sub> - (GlcNAc) <sub>6</sub>	37 °C, 48 h	- A-A-D-D - A-A-D-D-D - A-A-D-D-D-D	(Naqvi et al. 2016)
Chitin deacetylase	<i>Scopulariopsis brevicaulis</i> (fungus)	Chitin from <i>Aspergillus niger</i> mycelium	55 °C, 55 min	37% Deacetylation	(Cai et al. 2006)

## 2.5 Production of CHOS by enzymatic method

### 2.5.1 Hydrolysis activity by chitinase and chitosanase

Bioconversion of chitin and chitosan into CHOS can be performed by enzymatic method using enzyme in the family of glycoside hydrolase (GH), namely chitinases and chitosanases. They are capable of converting chitin and chitosan into CHOS by hydrolyzing the  $\beta$ -1,4 glycosidic linkages between the sugar units. The enzymes responsible for chitin degradation are chitinases (EC3.2.1.14). Chitinases occur in glycoside hydrolase families 18 and GH19, which are found in a variety of organisms such as bacteria, fungi, insects, plants, and animals (Tanaka et al. 2004). Chitinases have the ability to hydrolyzed A-A linkage, but not D-D linkage. Moreover, chitinases also hydrolyze highly acetylated chitosan, varying of CHOS mixture could be produced depending on the degree of acetylation of chitosan (Horn et al. 2006). However, chitinase could not get access to the compact structure of insoluble chitin. Our laboratory has previously studied on the hydrolytic activity of ChiA1 from *Bacillus licheniformis* against colloidal chitin. The result showed that only (GlcNAc)<sub>2</sub> was released (Songsiriritthigul et al. 2010). After that, the activity of the enzyme has been improved 2.7-fold and 2.3-fold at pH 3 and 6.0 by directed evolution, using DNA shuffling technique (Songsiriritthigul et al. 2009).

Chitosanase or chitosan *N*-acetylglucosaminohydrolase (EC 3.2.1.132) catalyzes the hydrolysis of glycosidic bond of chitosan into CHOS (Falcón-Rodríguez et al.). Chitosanases are members of glycosyl hydrolase (GH) families GH5, GH7, GH8, GH46, GH75, and GH80, according to the CAZy database. Among these families, GH46 have been studied extensively in terms of their catalytic features, enzymatic mechanisms and protein structures (Marcotte et al. 1996, Lacombe-Harvey et al. 2009). Chitosanases can be classified into three classes depending on their cleavage specificity.

Class I cleaves GlcNAc–GlcN and GlcN–GlcN bonds, class II cleaves only the GlcN–GlcN bonds and class III chitosanases cleaves GlcN–GlcNAc and GlcN–GlcN bonds (Tanabe et al. 2003). The enzymes have been found in a variety of microorganisms such as bacteria, fungi and a few in plants (Jo et al. 2003). Many of them are derived from the genus *Bacillus* that belong to GH families 8 and 46. Recently, in-depth characterization of endo chitosanase from *Bacillus subtilis* 168 (*BsCsn46A*), which is one of the fastest chitosanases described so far, has been reported (Pechsrichuang et al. 2018). A summary of reports on the bioconversion of chitin and chitosan and the analysis of the hydrolytic products of chitinases and chitosanases from various microorganisms is shown in Table 2.3.

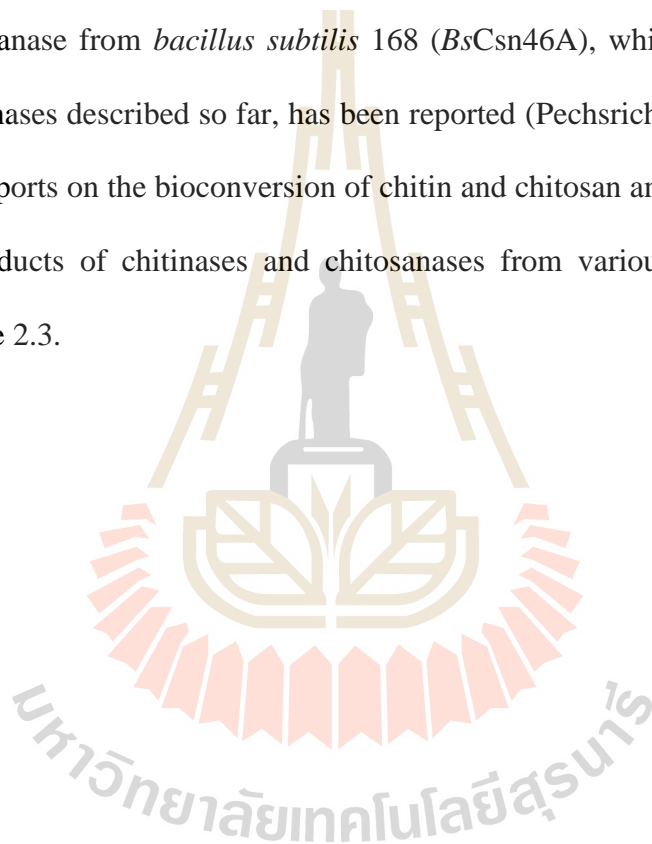


**Table 2.3** Enzymatic hydrolysis of chitin and chitosan into CHOS by chitinase and chitosanase.

Enzyme	Enzyme source	Substrate	Condition	DP of end products	Reference
Chitinase B GH Family 18	<i>Serratia marcescens</i> ( <i>E. coli</i> system)	chitosan F <sub>A</sub> 0.65 (homogeneous de- <i>N</i> - acetylation of chitin)	37°C, 1 week ( $\alpha=0.37$ )	1-4	(Sørbotten et al. 2005)
Chitinase G GH Family 19	<i>Streptomyces coelicolor</i> A3(2) ( <i>E. coli</i> system)	chitosan F <sub>A</sub> 0.64 (homogeneous de- <i>N</i> - acetylation of chitin)	37 °C, 1 week	1-3	(Heggset et al. 2009)
Chitinase (Hsiao et al.) GH family 18	<i>Bacillus licheniformis</i> ( <i>E. coli</i> system)	Colloidal chitin	37 °C, 60 min	2	(Songsiriritt higul et al. 2010)
ScCsn46A GH family 46	<i>Streptomyces coelicolor</i> A3(2) ( <i>E. coli</i> system)	Chitosan F <sub>A</sub> 0.32	37 °C, 7 days	1-3	(Heggset et al. 2010)
Chitosanase	<i>Aspergillus fumigatus</i> ( <i>Pichia pastoris</i> )	Chitosan	60 °C, 24 h	3-6	(Chen et al. 2012)
SaCsn75A GH family 75	<i>Streptomyces</i> <i>avermitilis</i>	Chitosan F <sub>A</sub> 0.31	37 °C, 7 days	2-4	(Heggset et al. 2012)
Chitosanase GH family 8	<i>Bacillus</i> sp. ( <i>E. coli</i> system)	Chiosan (DDA $\geq$ 95%)	50 °C, 2h	3-6	(Zhou et al. 2015)
Chitosanase	<i>Bacillus subtilis</i> ATCC 23857 ( <i>Lactobacillus plantarum</i> WCFS1)	Chitosan	37 °C, 5 min	2-6	(Nguyen et al. 2016)
Chitinase Chi1	<i>Myceliophthora</i> <i>thermophila</i> C1 ( <i>Myceliophthora</i> <i>thermophila</i> C1)	-Swollen chitin - Chitosan 90DDA/100	50 °C, 6h	- 2 - 2-12	(Krolicka et al. 2018)
BsCsn46A GH family 46	<i>Bacillus subtilis</i> strain 168 ( <i>E. coli</i> system)	Chitosan F <sub>A</sub> 0.30	37 °C, 48 h	2-3	(Pechrichu ang et al. 2018)
Chitosanase (GsCsn46A) GH family 46	<i>Rhizobacterium</i> <i>Gynuella sunshinyii</i> ( <i>E. coli</i> system)	Chitosan (DDA $\geq$ 95%)	30 °C for 6 h	2-3	(Qin et al. 2018)

### 2.5.2 Transglycosylation activity

Biosynthesis of CHOS with specific composition and length is becoming more important for many industrial applications such as therapeutic agents (Wu et al. 2012, Yousef et al. 2012, Zhang et al. 2014, Muanprasat et al. 2015), prebiotic (Lee et al. 2002, Fernandes et al. 2012), or in agriculture applications (Falcón-Rodríguez et al. 2011, Maksimov et al. 2011, Rahman et al. 2015). Bioconversion of chitin and chitosan into CHOS is normally prepared by enzymatic hydrolysis using chitinases and chitosanases to generate short oligomers as the major product (Table 2.3). However, CHOS can also be generated by transglycosylation reaction. So far, a few chitosanase has been shown to possess transglycosylation activity (Tanabe et al. 2003, Hsiao et al.

2008) (Table 2.4). In addition, few studies have described the generation of engineered family 18 chitinases through site directed mutagenesis to reduce the hydrolysis and improve transglycosylation activity in order to produce long chain CHOS (Table 2.4). When conserved Trp167 at the -3 subsite of *Serratia marcescens* QMB1466 was substituted with alanine, the transglycosylation activity of the enzyme was enhanced (Aronson et al. 2006). Long oligosaccharides, i.e., (GINAc)<sub>5</sub> and (GINAc)<sub>6</sub> were produced when (GINAc)<sub>4</sub> was used as substrate, and (GINAc)<sub>6</sub> and (GINAc)<sub>7</sub> could be formed from (GINAc)<sub>5</sub>. In addition, Zakariassen et al reported transglycosylation activity of double mutant chitinase, chiA-D313N-F396W from *Serratia marcescens* (Zakariassen et al. 2011). The mutation of Asp to Asn at conserve diagnostic DxDxE motif at catalytic domain and exchanged Phe to Trp could affect the transglycosylation activity of the enzyme. The long oligosaccharide products (GINAc)<sub>5</sub> to (GINAc)<sub>8</sub> were detected when using (GINAc)<sub>4</sub> as substrate. Recently, (Bhuvanachandra et al. 2018) has created mutated chitinases StmChiA at catalytic domain (D464N) and glycon binding site (W306A and W679A) and it was reveal that the mutants of the glycon binding site (W306A and W679A) appear to produce long-chain CHOS more efficiently than the catalytic mutant D464N.

**Table 2.4** Bioconversion of chitin and chitosan into CHOS by transglycosylation activity of chitinolytic enzyme.

Enzyme	Enzyme source	Substrate	Condition	DP of end products	Reference
Chitosanase	<i>Streptomyces griseus HUT 6037</i>	(Gln) <sub>5</sub> (GlnAc) <sub>3</sub>	37 °C, 8 h	(Gln) <sub>2</sub> (GlnAc) <sub>3</sub> , (Gln) <sub>3</sub> (GlnAc) <sub>3</sub> , (Gln) (GlnAc) <sub>3</sub> .	(Tanabe et al. 2003)
Chitinase A, <i>SmChiA</i> <sup>W167A</sup> GH family 18	<i>Serratia marcescens QMB1466</i> ( <i>E. coli</i> system)	- (GlnAc) <sub>4</sub> - (GlnAc) <sub>5</sub>	On ice temperature for 10 min	-DP5, DP6 from (GlnAc) <sub>4</sub> - DP6, DP7 from (GlnAc) <sub>5</sub>	(Aronson et al. 2006)
Chitinase, ChiA-D313N-F396W GH family 18 (double mutant)	<i>Serratia marcescens</i> ( <i>E. coli</i> system)	(GlnAc) <sub>4</sub>	37 °C, 5 min	DP3-DP8	(Zakariassen et al. 2011)
Chitinase, <i>StmChiA</i> -W306A, W679A (glycon binding site) -D464N (catalytic)	<i>Stenotrophomonas maltophilia</i> ( <i>E. coli</i> system)	(GlnAc) <sub>4</sub> (GlnAc) <sub>5</sub>	40 °C, 0-720 min	DP2-DP6	(Bhuvanachandra et al. 2018)

### 2.5.3 Auxiliary activity

Lytic polysaccharide monooxygenases (LPMOs), a group of carbohydrate active enzymes has been classified as auxiliary activities (AA) from CAZy database (Levasseur et al. 2013), occurring in families 9 (previously GH 61) (Quinlan et al. 2011), 10 (previously CBM 33) (Forsberg et al. 2011), 11 (Hemsworth et al. 2014) 13, 14 and 15. LPMOs are copper dependent enzymes that use molecular oxygen and external electron donor to oxidize on surface of recalcitrant polysaccharide and cleavage glycosidic bonds of chitin and cellulose. Recently, (Vaaje-Kolstad et al. 2010) and (Bissaro et al. 2018) reported advance technique including computational, biophysical, and biochemical methods. These enzymes generate oxidized chain ends, thus boosting the degradation by chitinase (Vaaje-Kolstad et al. 2010). There has been reported about the degradation of insoluble  $\alpha$ - and  $\beta$ - chitin using LPMOs (Table 2.5). Nakagawa et al (Nakagawa et al. 2013) reported the degradation of  $\alpha$ - and  $\beta$ - chitin by CBP 21. The oxidized CHOS with DP 4-6 were produced when using  $\alpha$ - chitin as substrate, while

CHOS with DP 4-10 were detected when using  $\beta$ - chitin as substrate. Moreover, they also studied the synergy of CBP21 and chitinases (ChiB and ChiC) for the degradation of various particle size of crystalline  $\alpha$ -chitin (mechanical pretreatment), the study showed that this enzyme acts synergistically with chitinases. In addition, the individual and synergistic activity with chitinase of LPMO (SgLPMO10F) from *Streptomyces griseus* has been studied (Nakagawa et al. 2015). The individual SgLPMO10F showed activity on both  $\alpha$ - and  $\beta$ -chitin, although the enzyme was active on  $\beta$ -chitin more than  $\alpha$ - chitin. The synergistic activity of *Serratia marcescens* GH18 chitinase and SgLPMO10F could improve the chitin solubilization yield. Other LPMOs that are active on insoluble chitin such as BlAA10A from *Bacillus licheniformis* (Forsberg et al. 2014) and CjLPMO10A from *Cellvibrio japonicus* have also been reported. Moreover, LPMOs have been used for component in enzymes cocktail for chitin degradation. The enzyme cocktails for saccharification of chitin using five mono-component enzymes from *Serratia marcescens* including SmLPMO10A (CBP21), three chitinases (*SmChiA*, *SmChiB*, *SmChiC*) and a beta-*N*-acetylhexosaminidase, *SmCHB* (chitobiase) have been developed by (Mekasha et al. 2017).

**Table 2.5** Bioconversion of chitin into CHOS by recombinant Lytic Polysaccharide Monoxygenase (LPMO). Products detected upon incubation with chitin were CHOS oxidized aldonic acids (i.e. products oxidized at the C1 carbon)

Enzyme	Enzyme source	Substrate	Condition	DP of dominating end products	Reference
LPMO, CBP21	<i>Serratia marcescens</i>	$\alpha$ - and $\beta$ - chitin	37 °C	- CHOS DP 4-6 from $\alpha$ - chitin - CHOS DP 4-10 from $\beta$ - chitin	(Nakagawa et al. 2013)
LPMO, BIAA10A	<i>Bacillus licheniformis</i> ( <i>E. coli</i> system)	squid pen $\beta$ -chitin	37 °C, 16 h	CHOS DP6-9 (C1-oxidized)	(Forsberg et al. 2014)
LPMO, SgLPMO10F	<i>Streptomyces griseus</i> ( <i>Brevibacillus choshinensis</i> SP3)	$\alpha$ - and $\beta$ - chitin	40 °C, 150 min	- CHOS DP4-6 from $\alpha$ -chitin - CHOS DP4-8 from $\beta$ -chitin	(Nakagawa et al. 2015)
Chitin-active LPMO, CjLPMO10A	<i>Cellvibrio japonicus</i> ( <i>E. coli</i> system)	Shrimp shell $\alpha$ -chitin and squid pen $\beta$ - chitin	37 °C, 24 h	CHOS DP4-DP6	(Forsberg et al. 2016)
LPMO, SmAA10A or CBP21	<i>Serratia marcescens</i> ( <i>E. coli</i> system)	$\beta$ - chitin	40 °C, 60 min	CHOS DP4-6	(Bissaro et al. 2018)

## 2.6 Conclusion

Bioconversion of marine shell wastes into value-added chitin, chitosan and CHOS using microbial and enzymatic methods have been researched for many years. To extract the chitin from the crustacean shell, pretreatment the shell wastes using microbial fermentation by lactic acid bacteria and protease producing bacteria has been performed for demineralization and deproteinization. For bioconversion of chitosan, chitin or chitin-oligomer can be converted into chitosan or chitosan oligomers by chitin deacetylase. CHOS production from chitin and chitosan involve GH families of chitinase and chitosanase, respectively. The major products from hydrolysis reaction of chitinase and chitosanase currently are short oligomers (DP ranging from 1-12), depends on substrate specificity of the enzymes (Table 2.3). To produce longer chain CHOS, engineered chitinase with improved transglycosylation and reduced hydrolytic activity have been used. LPMOs are emerging enzyme for the bioconversion of

chitin/chitosan. However, mechanochemical pretreatment for reduction of crystallinity of chitin is also essential for direct enzymatic degradation by LPMOs and/or chitinases.

## 2.7 References

- Aam, B. B., Heggset, E. B., Norberg, A. L., Sørli, M., Vårum, K. M. and Eijsink, V. G. H. (2010). Production of chitooligosaccharides and their potential applications in medicine. **Marine Drugs** 8(5): 1482-1517.
- Alfonso, C., Nuero, O. M., Santamaria, F. and Reyes, F. (1995). Purification of a heat-stable chitin deacetylase from *Aspergillus nidulans* and its role in cell wall degradation. **Curr Microbiol** 30(1): 49-54.
- Andrés, E., Albesa-Jové, D., Biarnés, X., Moerschbacher, B. M., Guerin, M. E. and Planas, A. (2014). Structural Basis of Chitin Oligosaccharide Deacetylation. **Angewandte Chemie International Edition** 53(27): 6882-6887.
- Aronson, N. N., Jr., Halloran, B. A., Alexeyev, M. F., Zhou, X. E., Wang, Y., Meehan, E. J. and Chen, L. (2006). Mutation of a conserved tryptophan in the chitin-binding cleft of *Serratia marcescens* chitinase A enhances transglycosylation. **Biosci Biotechnol Biochem** 70(1): 243-251.
- Aye, K. N. and Stevens, W. F. (2004). Improved chitin production by pretreatment of shrimp shells. **Journal of Chemical Technology & Biotechnology** 79(4): 421-425.
- Bhuvanachandra, B., Madhuprakash, J. and Podile, A. R. (2018). Active-site mutations improved the transglycosylation activity of *Stenotrophomonas maltophilia* chitinase A. **Biochimica et Biophysica Acta (BBA) - Proteins and Proteomics** 1866(3): 407-414.

- Bissaro, B., Isaksen, I., Vaaje-Kolstad, G., Eijsink, V. G. H. and Røhr, Å. K. (2018). How a Lytic Polysaccharide Monooxygenase Binds Crystalline Chitin. **Biochemistry**.
- Blair, D. E., Hekmat, O., Schüttelkopf, A. W., Shrestha, B., Tokuyasu, K., Withers, S. G. and van Aalten, D. M. F. (2006). Structure and mechanism of chitin deacetylase from the fungal pathogen *Colletotrichum lindemuthianum*. **Biochemistry** 45(31): 9416-9426.
- Cai, J., Yang, J., Du, Y., Fan, L., Qiu, Y., Li, J. and Kennedy, J. F. (2006). Purification and characterization of chitin deacetylase from *Scopulariopsis brevicaulis*. **Carbohydrate Polymers** 65(2): 211-217.
- Carlström, D. (1957). The Crystal Structure of  $\alpha$ -chitin (Poly-*N*-Acetyl-D-Glucosamine). **The Journal of Biophysical and Biochemical Cytology** 3(5): 669-683.
- Chang, K. L. B., Tsai, G., Lee, J. and Fu, W.-R. (1997). Heterogeneous *N*-deacetylation of chitin in alkaline solution. **Carbohydrate Research** 303(3): 327-332.
- Chen, X., Zhai, C., Kang, L., Li, C., Yan, H., Zhou, Y., Yu, X. and Ma, L. (2012). High-level expression and characterization of a highly thermostable chitosanase from *Aspergillus fumigatus* in *Pichia pastoris*. **Biotechnology Letters** 34(4): 689-694.
- Falcón-Rodríguez, A. B., Costales, D., Cabrera, J. C. and Martínez-Téllez, M. Á. (2011). Chitosan physico-chemical properties modulate defense responses and resistance in tobacco plants against the oomycete *Phytophthora nicotianae*. **Pesticide Biochemistry and Physiology** 100(3): 221-228.

- Fernandes, J. C., Eaton, P., Franco, I., Ramos, Ó. S., Sousa, S., Nascimento, H., Gomes, A., Santos-Silva, A., Xavier Malcata, F. and Pintado, M. E. (2012). Evaluation of chitoligosaccharides effect upon probiotic bacteria. **International Journal of Biological Macromolecules** 50(1): 148-152.
- Ferrer, J., Paez, G., Marmol, Z., Ramones, E., Garcia, H. and Forster, C. F. (1996). Acid hydrolysis of shrimp-shell wastes and the production of single cell protein from the hydrolysate. **Bioresource Technology** 57(1): 55-60.
- Forsberg, Z., Nelson, C. E., Dalhus, B., Mekasha, S., Loose, J. S. M., Crouch, L. I., Røhr, Å. K., Gardner, J. G., Eijsink, V. G. H. and Vaaje-Kolstad, G. (2016). Structural and functional analysis of a lytic polysaccharide monooxygenase important for efficient utilization of chitin in *Cellvibrio japonicus*. **The Journal of Biological Chemistry** 291(14): 7300-7312.
- Forsberg, Z., Røhr, Å. K., Mekasha, S., Andersson, K. K., Eijsink, V. G. H., Vaaje-Kolstad, G. and Sørli, M. (2014). Comparative study of two chitin-active and two cellulose-active AA10-type lytic polysaccharide monooxygenases. **Biochemistry** 53(10): 1647-1656.
- Forsberg, Z., Vaaje-Kolstad, G., Westereng, B., Buaes, A. C., Stenstrom, Y., MacKenzie, A., Sorlie, M., Horn, S. J. and Eijsink, V. G. (2011). Cleavage of cellulose by a CBM33 protein. **Protein Sci** 20(9): 1479-1483.
- Ghorbel-Bellaaj, O., Hajji, S., Younes, I., Chaabouni, M., Nasri, M. and Jellouli, K. (2013). Optimization of chitin extraction from shrimp waste with *Bacillus pumilus* A1 using response surface methodology. **Int J Biol Macromol** 61: 243-250.

- Hackman, R. H. and Goldberg, M. (1965). Studies on chitin. VI. The nature of alpha- and beta-chitins. **Aust J Biol Sci** 18(4): 935-946.
- Hayes, M., Carney, B., Slater, J. and Bruck, W. (2008). Mining marine shellfish wastes for bioactive molecules: chitin and chitosan--Part A: extraction methods. **Biotechnol J** 3(7): 871-877.
- Heggset, E. B., Dybvik, A. I., Hoell, I. A., Norberg, A. L., Sørli, M., Eijsink, V. G. H. and Vårum, K. M. (2010). Degradation of Chitosans with a Family 46 Chitosanase from *Streptomyces coelicolor* A3(2). **Biomacromolecules** 11(9): 2487-2497.
- Heggset, E. B., Hoell, I. A., Kristoffersen, M., Eijsink, V. G. H. and Vårum, K. M. (2009). Degradation of Chitosans with Chitinase G from *Streptomyces coelicolor* A3(2): Production of chito-oligosaccharides and insight into subsite specificities. **Biomacromolecules** 10(4): 892-899.
- Heggset, E. B., Tuveng, T. R., Hoell, I. A., Liu, Z., Eijsink, V. G. H. and Vårum, K. M. (2012). Mode of action of a family 75 chitosanase from *Streptomyces avermitilis*. **Biomacromolecules** 13(6): 1733-1741.
- Hekmat, O., Tokuyasu, K. and Withers, S. G. (2003). Subsite structure of the endo-type chitin deacetylase from a Deuteromycete, *Colletotrichum lindemuthianum*: an investigation using steady-state kinetic analysis and MS. **Biochemical Journal** 374(2): 369.
- Hemsworth, G. R., Henrissat, B., Davies, G. J. and Walton, P. H. (2014). Discovery and characterization of a new family of lytic polysaccharide mono-oxygenases. **Nature chemical biology** 10(2): 122-126.

- Hirano, T., Sugiyama, K., Sakaki, Y., Hakamata, W., Park, S.-Y. and Nishio, T. (2015). Structure-based analysis of domain function of chitin oligosaccharide deacetylase from *Vibrio parahaemolyticus*. **FEBS Letters** 589(1): 145-151.
- Horn, S. J., Sørbotten, A., Synstad, B., Sikorski, P., Sørli, M., Vårum, K. M. and Eijsink, V. G. H. (2006). Endo/exo mechanism and processivity of family 18 chitinases produced by *Serratia marcescens*. **FEBS Journal** 273(3): 491-503.
- Hoßbach, J., Bußwinkel, F., Kranz, A., Wattjes, J., Cord-Landwehr, S. and Moerschbacher, B. M. (2018). A chitin deacetylase of *Podospora anserina* has two functional chitin binding domains and a unique mode of action. **Carbohydrate Polymers** 183: 1-10.
- Hsiao, Y.-C., Lin, Y.-W., Su, C.-K. and Chiang, B.-H. (2008). High degree polymerized chitooligosaccharides synthesis by chitosanase in the bulk aqueous system and reversed micellar microreactors. **Process Biochemistry** 43(1): 76-82.
- Jeon, Y.-J. and Kim, S.-K. (2000). Production of chitooligosaccharides using an ultrafiltration membrane reactor and their antibacterial activity. **Carbohydrate Polymers** 41(2): 133-141.
- Jo, Y.-Y., Jo, K.-J., Jin, Y.-L., Kim, K.-Y., Shim, J.-H., Kim, Y.-W. and Park, R.-D. (2003). Characterization and Kinetics of 45 kDa Chitosanase from *Bacillus* sp. P16. **Bioscience, Biotechnology, and Biochemistry** 67(9): 1875-1882
- Jung, W. J., Jo, G. H., Kuk, J. H., Kim, K. Y. and Park, R. D. (2006). Extraction of chitin from red crab shell waste by cofermentation with *Lactobacillus paracasei* subsp. tolerans KCTC-3074 and *Serratia marcescens* FS-3. **Appl Microbiol Biotechnol** 71(2): 234-237.

- Kafetzopoulos, D., Martinou, A. and Bouriotis, V. (1993). Bioconversion of chitin to chitosan: purification and characterization of chitin deacetylase from *Mucor rouxii*. **Proceedings of the National Academy of Sciences** 90(7): 2564.
- Kaur, S. and Dhillon, G. S. (2015). Recent trends in biological extraction of chitin from marine shell wastes: a review. **Crit Rev Biotechnol** 35(1): 44-61.
- Krolicka, M., Hinz, S. W. A., Koetsier, M. J., Joosten, R., Eggink, G., van den Broek, L. A. M. and Boeriu, C. G. (2018). Chitinase Chi1 from *Myceliophthora thermophila* C1, a thermostable enzyme for chitin and chitosan depolymerization. **Journal of Agricultural and Food Chemistry** 66(7): 1658-1669.
- Lacombe-Harvey, M. E., Fukamizo, T., Gagnon, J., Ghinet, M. G., Denhart, N., Letzel, T. and Brzezinski, R. (2009). Accessory active site residues of *Streptomyces* sp. N174 chitosanase - variations on a common theme in the lysozyme superfamily. **FEBS J** 276: 857 - 869.
- Lee, H.-W., Park, Y.-S., Jung, J.-S. and Shin, W.-S. (2002). Chitosan oligosaccharides, dp 2–8, have prebiotic effect on the *Bifidobacterium bifidum* and *Lactobacillus* sp. **Anaerobe** 8(6): 319-324.
- Levasseur, A., Drula, E., Lombard, V., Coutinho, P. M. and Henrissat, B. (2013). Expansion of the enzymatic repertoire of the CAZy database to integrate auxiliary redox enzymes. **Biotechnology for Biofuels** 6: 41-41.
- Liu, Z., Gay, L. M., Tuveng, T. R., Agger, J. W., Westereng, B., Mathiesen, G., Horn, S. J., Vaaje-Kolstad, G., van Aalten, D. M. F. and Eijsink, V. G. H. (2017). Structure and function of a broadspecificity chitin deacetylase from *Aspergillus nidulans* FGSC A4. **Sci Rep** 7(1): 1746.

- Lombard, V., Golaconda Ramulu, H., Drula, E., Coutinho, P. M. and Henrissat, B. (2014). The carbohydrate-active enzymes database (CAZy) in 2013. **Nucleic Acids Res** 42(Database issue): D490-495.
- Maksimov, I. V., Valeev, A. S. and Safin, R. F. (2011). Acetylation degree of chitin in the protective response of wheat plants. **Biochemistry (Moscow)** 76(12): 1342-1346.
- Marcotte, E. M., Monzingo, A. F., Ernst, S. R., Brzezinski, R. and Robertas, J. D. (1996). X-ray structure of an anti-fungal chitosanase from *Streptomyces* N174. **Nature Structural Biology** 3: 155 - 162.
- Mekasha, S., Byman, I. R., Lynch, C., Toupalová, H., Anděra, L., Næs, T., Vaaje-Kolstad, G. and Eijsink, V. G. H. (2017). Development of enzyme cocktails for complete saccharification of chitin using mono-component enzymes from *Serratia marcescens*. **Process Biochemistry** 56: 132-138.
- Muanprasat, C. and Chatsudthipong, V. (2017). Chitosan oligosaccharide: Biological activities and potential therapeutic applications. **Pharmacology & Therapeutics** 170: 80-97.
- Muanprasat, C., Wongkrasant, P., Satitsri, S., Moonwiriyaakit, A., Pongkorpsakol, P., Mattaveewong, T., Pichyangkura, R. and Chatsudthipong, V. (2015). Activation of AMPK by chitosan oligosaccharide in intestinal epithelial cells: Mechanism of action and potential applications in intestinal disorders. **Biochemical Pharmacology** 96(3): 225-236.
- Nakagawa, Y. S., Eijsink, V. G. H., Totani, K. and Vaaje-Kolstad, G. (2013). Conversion of  $\alpha$ -chitin substrates with varying particle size and crystallinity reveals substrate preferences of the chitinases and lytic polysaccharide

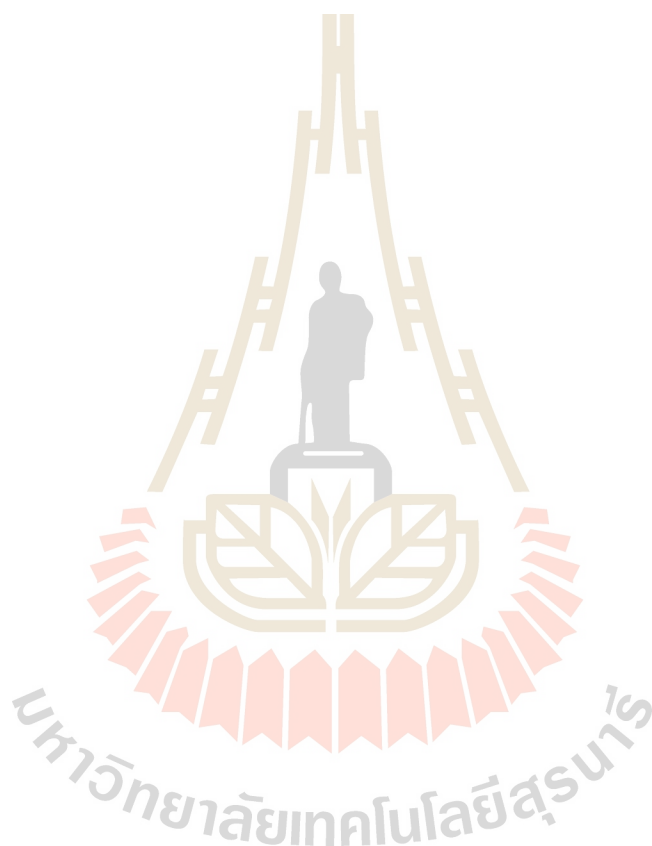
- monooxygenase of *Serratia marcescens*. **Journal of Agricultural and Food Chemistry** 61(46): 11061-11066.
- Nakagawa, Y. S., Kudo, M., Loose, J. S. M., Ishikawa, T., Totani, K., Eijsink, V. G. H. and Vaaje-Kolstad, G. (2015). A small lytic polysaccharide monooxygenase from *Streptomyces griseus* targeting  $\alpha$ - and  $\beta$ -chitin. **The FEBS Journal** 282(6): 1065-1079.
- Naqvi, S., Cord-Landwehr, S., Singh, R., Bernard, F., Kolkenbrock, S., El Gueddari, N. E. and Moerschbacher, B. M. (2016). A recombinant fungal chitin deacetylase produces fully defined chitosan oligomers with novel patterns of acetylation. **Applied and Environmental Microbiology** 82(22): 6645-6655.
- Nguyen, H.-M., Mathiesen, G., Stelzer, E. M., Pham, M. L., Kuczkowska, K., Mackenzie, A., Agger, J. W., Eijsink, V. G. H., Yamabhai, M., Peterbauer, C. K., Haltrich, D. and Nguyen, T.-H. (2016). Display of a  $\beta$ -mannanase and a chitosanase on the cell surface of *Lactobacillus plantarum* towards the development of whole-cell biocatalysts. **Microbial Cell Factories** 15(1): 169.
- Oh, K.-T., Kim, Y.-J., Nguyen, V. N., Jung, W.-J. and Park, R.-D. (2007). Demineralization of crab shell waste by *Pseudomonas aeruginosa* F722. **Process Biochemistry** 42(7): 1069-1074.
- Pechsrichuang, P., Lorentzen, S. B., Aam, B. B., Tuveng, T. R., Hamre, A. G., Eijsink, V. G. H. and Yamabhai, M. (2018). Bioconversion of chitosan into chito-oligosaccharides (CHOS) using family 46 chitosanase from *Bacillus subtilis* (BsCsn46A). **Carbohydrate Polymers** 186: 420-428.

- Prashanth, K. V. H. and Tharanathan, R. N. (2007). Chitin/Chitosan:modification and their unlimited application potential-an overview. **Trends in food Science & Technology** 18: 117-131.
- Qin, Z., Chen, Q., Lin, S., Luo, S., Qiu, Y. and Zhao, L. (2018). Expression and characterization of a novel cold-adapted chitosanase suitable for chitooligosaccharides controllable preparation. **Food Chemistry** 253: 139-147.
- Quinlan, R. J., Sweeney, M. D., Lo Leggio, L., Otten, H., Poulsen, J. C., Johansen, K. S., Krogh, K. B., Jorgensen, C. I., Tovborg, M., Anthonsen, A., Tryfona, T., Walter, C. P., Dupree, P., Xu, F., Davies, G. J. and Walton, P. H. (2011). Insights into the oxidative degradation of cellulose by a copper metalloenzyme that exploits biomass components. **Proc Natl Acad Sci U S A** 108(37): 15079-15084.
- Rahman, M. H., Hjeljord, L. G., Aam, B. B., Sørli, M. and Tronsmo, A. (2015). Antifungal effect of chito-oligosaccharides with different degrees of polymerization. **European Journal of Plant Pathology** 141(1): 147-158.
- Rudall, K. M. (1963). The Chitin/Protein Complexes of Insect Cuticles. In Beament, J. W. L., Treherne, J. E. and Wigglesworth, V. B. (Eds.), **Advances in Insect Physiology** (Vol. 1, pp. 257-313): Academic Press.
- Sedaghat, F., Yousefzadi, M., Toiserkani, H. and Najafipour, S. (2017). Bioconversion of shrimp waste *Penaeus merguensis* using lactic acid fermentation: An alternative procedure for chemical extraction of chitin and chitosan. **International Journal of Biological Macromolecules** 104: 883-888.
- Songsiriritthigul, C., Lapboonrueng, S., Pechsrichuang, P., Pesatcha, P. and Yamabhai, M. (2010). Expression and characterization of *Bacillus licheniformis* chitinase

- (ChiA), suitable for bioconversion of chitin waste. **Bioresource Technology** 101(11): 4096-4103.
- Songsiriritthigul, C., Pesatcha, P., Eijsink, V. G. H. and Yamabhai, M. (2009). Directed evolution of a *Bacillus chitinase*. **Biotechnology Journal** 4(4): 501-509.
- Sørbotten, A., Horn, S. J., Eijsink, V. G. H. and Vårum, K. M. (2005). Degradation of chitosans with chitinase B from *Serratia marcescens*. **FEBS Journal** 272(2): 538-549.
- Tanabe, T., Morinaga, K., Fugamizo, T. and Mitsutomi, M. (2003). Novel Chitosanase from *Streptomyces griseus* HUT 6037 with Transglycosylation Activity. . **Bioscience, Biotechnology, and Biochemistry** 67(2): 354-364.
- Tanaka, T., Fukui, T., Fujiwara, S., Atomi, H. and Imanaka, T. (2004). Concerted Action of Diacetylchitobiose Deacetylase and Exo- $\beta$ -D-glucosaminidase in a Novel Chitinolytic Pathway in the Hyperthermophilic *Archaeon Thermococcus kodakaraensis* KOD1. **Journal of Biological Chemistry** 279(29): 30021-30027.
- Tsigos, I., Martinou, A., Kafetzopoulos, D. and Bouriotis, V. (2000). Chitin deacetylases: new, versatile tools in biotechnology. **Trends Biotechnol** 18(7): 305-312.
- Tsigos, I., Zydowicz, N., Martinou, A., Domard, A. and Bouriotis, V. (1999). Mode of action of chitin deacetylase from *Mucor rouxii* on *N*-acetylchitooligosaccharides. **European Journal of Biochemistry** 261(3): 698-705.
- Vaaje-Kolstad, G., Westereng, B., Horn, S. J., Liu, Z., Zhai, H., Sørli, M. and Eijsink, V. G. H. (2010). An oxidative enzyme boosting the enzymatic conversion of recalcitrant polysaccharides. **Science** 330(6001): 219.

- Wu, H., Aam, B. B., Wang, W., Norberg, A. L., Sørli, M., Eijsink, V. G. H. and Du, Y. (2012). Inhibition of angiogenesis by chitooligosaccharides with specific degrees of acetylation and polymerization. **Carbohydrate Polymers** 89(2): 511-518.
- Yin, H., Zhao, X. and Du, Y. (2010). Oligochitosan: A plant diseases vaccine—A review. **Carbohydrate Polymers** 82(1): 1-8.
- Yousef, M., Pichyangkura, R., Soodvilai, S., Chatsudthipong, V. and Muanprasat, C. (2012). Chitosan oligosaccharide as potential therapy of inflammatory bowel disease: Therapeutic efficacy and possible mechanisms of action. **Pharmacological Research** 66(1): 66-79.
- Zakariassen, H., Hansen, M. C., Joranli, M., Eijsink, V. G. and Sorlie, M. (2011). Mutational effects on transglycosylating activity of family 18 chitinases and construction of a hypertransglycosylating mutant. **Biochemistry** 50(25): 5693-5703.
- Zhang, H., Yun, S., Song, L., Zhang, Y. and Zhao, Y. (2017). The preparation and characterization of chitin and chitosan under large-scale submerged fermentation level using shrimp by-products as substrate. **International Journal of Biological Macromolecules** 96: 334-339.
- Zhang, P., Liu, W., Peng, Y., Han, B. and Yang, Y. (2014). Toll like receptor 4 (TLR4) mediates the stimulating activities of chitosan oligosaccharide on macrophages. **International Immunopharmacology** 23(1): 254-261.
- Zhao, Y., Park, R.-D. and Muzzarelli, R. A. A. (2010). Chitin Deacetylases: Properties and Applications. **Marine Drugs** 8(1): 24.

Zhou, Z., Zhao, S., Wang, S., Li, X., Su, L., Ma, Y., Li, J. and Song, J. (2015). Extracellular Overexpression of Chitosanase from *Bacillus* sp. TS in *Escherichia coli*. **Applied Biochemistry and Biotechnology** 175(7): 3271-3286.



# CHAPTER III

## EXPRESSION OF RECOMBINANT *BACILLUS SUBTILIS* CHITOSANASE IN *E. COLI* EXPRESSION SYSTEM

### 3.1 Abstract

The production of secreted recombinant proteins from *E. coli* is pivotal to the biotechnological industry because it reduces the cost of downstream processing. Proteins destined for secretion contain an N-terminal signal peptide that is cleaved by secretion machinery in the plasma membrane. The resulting protein is released in an active mature form. In this study, *Bacillus subtilis* chitosanase was used as a model protein to compare the effect of two signal peptides on the secretion of heterologous recombinant protein. The results showed that the *E. coli* secretion machinery could recognize both native bacillus and *E. coli* signal peptides. However, only the native bacillus signal peptide could generate the same N-terminal sequence as in the wild type bacteria. When the recombinant Csn constructs contained the *E. coli* OmpA signal peptide, the secreted enzymes were heterogeneous, comprising a mixed population of secreted enzymes with different N-terminal sequences. Nevertheless, the *E. coli* OmpA signal peptide was found to be more efficient for high expression and secretion of bacillus Csn. These findings may be used to help engineer other recombinant proteins for secretory production in *E. coli*.

Keywords: Secretion, Recombinant, *E. coli*, Expression, Signal peptide, OmpA, *Bacillus*, Chitosanase

## 3.2 Introduction

The production of secreted recombinant proteins from *E. coli* is pivotal to the biotechnological industry because it reduces the cost of downstream processing associated with non-secreted proteins (Mergulhão et al. 2005). Secreted proteins are usually properly folded and more stable than cytosolic protein because of lower protease levels in the periplasm or culture medium. Proteins destined for secretion carry an N-terminal signal peptide that is cleaved in the plasma membrane by different mechanisms. The resulting protein is released in an active mature form (Mergulhão et al. 2005). *E. coli* is the most commonly used cell factory for the expression and secretion of recombinant enzymes and other biologically active proteins (Mergulhão et al. 2005). Since secreted recombinant proteins are fused with an *E. coli* signal peptide, the cleavage site is often unknown and hard to predict because it does not have to be the same as for the natural protein. This trivial issue can have a significant effect on biological activity and protein expression. Despite the importance of this aspect of protein engineering for secretion, there have been only a few reports on the effect of signal peptides on protein expression and subsequent processing in *E. coli*. The aim of this study was to investigate the effect of two different signal peptides on recombinant protein expression and N-terminal processing using chitosanase (Csn) from *Bacillus subtilis* as a model protein. This enzyme is biotechnologically important because it converts chitosan, a recalcitrant waste product from the seafood industry, into value-added chito-oligosaccharides, which have been shown to have excellent health and agricultural benefits (Pechsrichuang et al. 2013, Zhou et al. 2015). It is a relatively small, 28-kDa extracellular enzyme that is secreted from *Bacillus subtilis*, a Gram positive bacteria (Pechsrichuang et al. 2013). To analyze the effect of different signal

peptides, a gene encoding mature Csn together with its native signal peptide and a gene encoding recombinant Csn with its native signal peptide replaced with OmpA, a signal peptide from the Gram-negative bacteria *E. coli*, were cloned into a *Ptac* based expression vector and over-expressed in *E. coli* TOP10 cells (Figure 3.1). Protein expression levels and enzymatic activity at different time points, in various compartments, and the sequence of the N-terminus of the secreted proteins were determined. In this article, we show that the type of signal peptide can affect both the structure of the N-terminus and the expression level of recombinant proteins that are secreted from an *E. coli* expression system.

### 3.3 Materials and Methods

#### 3.3.1 Bacterial strains and plasmids

*Bacillus subtilis* strain 168 (ATCC23857) was obtained from the American Type Culture Collection. The bacteria were grown on NA agar at 30 °C. *E. coli* DH5 $\alpha$  (Life Technologies, USA) and TOP10 (Invitrogen, USA) were used as a cloning and expression host, respectively. The plasmid pMY202, which was used for cloning and expression of the *B. subtilis* chitosanase gene, was modified from pFLAG-CTS (Sigma, USA) by replacing the multiple cloning sites (MCS) between *Hind*III and *Sal*I of the pFLAG-CTS in a way that the *Sal*I was destroyed after ligation (Yamabhai et al. 2011).

#### 3.3.2 Substrate

Low molecular weight chitosan [product number 448869 (75–85 % DDA)] was purchased from Sigma-Aldrich and soluble chitosan (10 mg/mL) was prepared by dissolving 10 g of chitosan in 400 mL of distilled water and 90 mL of 1 M acetic acid. The chitosan solution was adjusted to pH 5.5 with 1 M sodium acetate

to a final volume of 1 L with distilled water.

### 3.3.3 Molecular cloning

The genes encoding Csn from *B. subtilis* 168 containing the native signal peptide (Nat-Csn) or the mature enzyme fused with the *E. coli* OmpA signal peptide (OmpA-Csn) were cloned by PCR-based methods into the pMY202 vector, according to a previously published protocol (Songsiriritthigul et al. 2010). The primers were designed from the published database of the DNA sequence of the Csn gene of *B. subtilis* 168 (NCBI accession number: NC\_000964 REGION: complement (2747984..2748817)). The primers, B.subCsnNdeIFw: 5' CTG TGC CAT ATG AAA ATC AGT ATG CAA AAA GCA GAT TTT TGG 3' and B.subCsnBamHIRv: 5' GCA CAG GGA TCC TTT GAT TAC AAA ATT ACC GTA CTC GTT TGA AC 3' were used for PCR amplification of the *B. subtilis* Csn gene containing the native signal peptide (Nat-Csn). The PCR products were cut with *NdeI* and *BglIII* and cloned into *NdeI* and *BglIII* sites on the pMY202 plasmid. For the construction of the recombinant chitosanase gene, of which the native signal peptide was replaced with the *E. coli* OmpA signal peptide (OmpA-Csn), primers B.subCsnOmpAHindIIIFw: 5' CTGTGCAAG CTT CGG CGG GAC TGA ATA AAG ATC AAA AGC3' and B.subCsnBamHIRv: 5' GCA CAG GGA TCC TTT GAT TAC AAA ATT ACC GTA CTC GTT TGA AC 3' were used in the PCR reaction. The PCR products were cut with *HindIII* and *BamHI* and ligated into a pMY202 vector that had been digested with the same enzymes. The recombinant constructs of *B. subtilis* Csn containing either the native or the OmpA signal peptide were designated Nat-Csn/pMY202 and OmpA Csn/pMY202, respectively. The integrity of the constructs was confirmed by automated DNA sequencing (Macrogen, Korea).

### **3.3.4 Expression and preparation of recombinant chitosanases from various compartments**

Four colonies of freshly transformed *E. coli* TOP10 harboring appropriate constructs were transferred into 20 mL Luria–Bertani (LB) broth containing 100 µg/mL ampicillin (LB-Amp) and grown overnight at 37 °C. Then, 2 % of the overnight cultures were added into 200 mL LB-Amp broth and grown at 37 °C with shaking until an optical density at 600 nm (OD<sub>600</sub>) of 0.6–0.7 was reached. Isopropyl-β-d-thiogalactopyranoside (IPTG) was added into the culture broth to a final concentration of 0.1 mM (for purification as shown in Figure 3.3) or 0.5 mM (for determination of enzyme activities in various compartments as reported in Table 3.1), and the incubation was continued at ambient temperature (27–28 °C) with shaking. Fifty mL of culture was collected after induction for 4 and 20 h and centrifuged at 4000×g for 30 min at 4 °C. Preparation of periplasmic extract and cell lysate (cytosolic fraction) was done as previously described (Yamabhai et al. 2008).

### **3.3.5 SDS-PAGE**

Denaturing sodium dodecylsulfate-polyacrylamide gel electrophoresis (SDS-PAGE) was performed according to the method of Laemmli (Laemmli 1970). Protein bands were stained by Coomassie brilliant blue R-250. Protein ladder (10–200 kDa) was purchased from Fermentas (St.Leon, Germany) and Bio-Rad. The protein samples were briefly heated (3 min) in loading buffer (Laemmli buffer) with reducing agent (100 mM β-mercaptoethanol) at 100 °C, using a heat block before loading onto the gel. Enzyme activity assay on agar plates.

### 3.3.6 Chitosanase activity assay on chitosan agar plate

The activity of recombinant chitosanase was assayed on LB agar plates containing 100 µg/mL ampicillin and 0.1 % (w/v) of low MW chitosan. Various concentrations of IPTG (0, 0.1, 0.5 mM) were spread onto the plate before freshly transformed cells were spotted onto the plates and incubated at 37 °C. Hydrolytic clear zones were observed and the diameters of the clear zones were measured at various time points. The experiments were done in triplicate. The average diameters with SD values were reported.

### 3.3.7 Chitosanase activity assay

Standard Csn activity was determined using the 3,5-dinitrosalicylic acid (DNS) method (Miller 1959). The reaction mixture consisted of 40 µL of enzyme (0.4 µg) and 160 µL of 0.5 % (w/v) of soluble chitosan in 200 mM sodium acetate buffer, pH5.5. The reaction was incubated in a Thermomixer Comfort (Eppendorf AG, Hamburg, Germany) at 50 °C for 5 min, with mixing at 900 rpm. The reaction was stopped by adding 200 µL of DNS solution and centrifuged at 12,000×g for 5 min to precipitate the remaining chitosan. Then, the color was developed by heating at 100 °C for 20 min and cooled on ice. The concentration of reducing sugar in the supernatant was determined by measuring the OD at 540 nm, using d-glucosamine (1–5 µmol/mL) as a standard. One unit of Csn activity was defined as the amount of enzyme that released 1 µmol of *D*-glucosamine per minute under standard assay conditions. The experiments were performed in duplicate.

### 3.3.8 Purification of recombinant chitosanase

Recombinant 10x His-tagged Csn proteins were purified from culture supernatant and cell lysate by immobilized metal affinity chromatography (IMAC),

using Ni-NTA agarose (Qiagen, Germany) as previously described (Juajun et al. 2011). The enzyme was eluted with 250 mM imidazole. The eluted enzyme was passed through Vivaspin6 columns ( $M_r$  cut-off 10 kDa; GE Healthcare, Sweden) to remove imidazole and concentrate the protein. The purified enzyme was stored at 4 °C until further use. Protein concentrations were determined by the method of Bradford (Bradford 1976) using a Bio-Rad protein assay kit and bovine serum albumin (BSA) as the standard. The standard calibration curve was constructed from 0.05 to 0.5 mg/mL BSA.

### **3.3.9 N-terminal sequencing**

1.25  $\mu$ g samples of purified OmpA-Csn and Nat-Csn were separated by SDS-PAGE on 15 % gels and electroblotted onto polyvinylidenedifluoride (PVDF) membrane (Bio-Rad, USA) in 50 mM borate buffer containing 10 % (v/v) methanol, pH 9. After blotting, the membrane was stained with Coomassie blue for 3 min, followed by destaining of the membrane with destaining solution (40 % (v/v) methanol and 10 % (v/v) acetic acid). N-terminal sequences were commercially analyzed using Edman degradation on an Applied Biosystems Procise 492 protein sequencer (Protein Micro-Analysis Facility, Medical University of Innsbruck, Austria).

### **3.3.10 MALDI-TOF MS**

Protein samples were loaded into Zeba™ Spin Desalting Columns (Thermo Scientific Inc., USA) pre-equilibrated with water. The columns were centrifuged at 1500 rpm for 2 min and the desalted fraction was precipitated overnight with 2 volumes of cold acetone at -20 °C. After centrifugation at 12,000 rpm for 15 min, the protein pellet was resuspended in 0.1 % TFA/50 % ACN to a final concentration of 10  $\mu$ g/ $\mu$ L. The protein was mixed with MALDI matrix solution (10

mg sinapinic acid in 1 mL of 50 % acetonitrile containing 0.1 % trifluoroacetic acid), directly spotted onto the MALDI target (MTP 384 ground steel, Bruker Daltonik, GmbH), and allowed to dry at room temperature. MALDI-TOF MS spectra were collected using Ultraflex III TOF/TOF (Bruker Daltonik, GmbH) in linear positive mode with a mass range of 5,000–100,000 Da. Five hundred shots were accumulated with a 200-Hz laser for each sample. MS spectra were analyzed by FlexAnalysis software (Bruker Daltonik, GmbH). Bovine insulin, equine cytochrome C and equine apomyoglobin were used as external protein calibrations.

### 3.4 Results

#### 3.4.1 Cloning and secretion of recombinant Csn containing two different signal peptides on agar plates

The *tac* promoter was used to control the expression of the two recombinant Csn forms, and protein over-expression was induced with IPTG. The recombinant enzymes were fused with 10x histidine tags at the C-termini to facilitate one-step affinity purification using IMAC, which allowed for accurate determination of production yield and the sequence of N-terminal amino acids. For the Nat-Csn construct, the native *Bacillus* signal peptide (35 amino acids) was retained by cloning the entire *B. subtilis* Csn gene into the pMY202 vector, which had been previously digested with *Nde*I and *Bgl*III. The PCR products (~831 bp) were digested with *Nde*I and *Bgl*III and cloned into corresponding restriction sites on the pMY202 plasmid (Figure 3.1, left panel). For the OmpA-Csn construct, the native signal peptide of *B. subtilis* Csn was replaced with that of the *E. coli* OmpA signal peptide. The PCR products (~726 bp) were digested with *Hind*III and *Bam*HI and cloned into

corresponding restriction sites on the pMY202 plasmid, which contained the OmpA gene. This resulted in the fusion of the *E. coli* OmpA signal peptide with the mature enzyme (Figure 3.1, right panel). The DNA sequences of the two constructs were confirmed by automated DNA sequencing (Macrogen, Korea). The theoretical molecular mass of the Nat-Csn and OmpA-Csn constructs were 33.23 and 31.26 kDa, respectively. To compare the effect of the signal peptide on Csn secretion on agar plates, a single colony of *E. coli* TOP10 harboring pMY202 containing either OmpA-Csn or Nat-Csn was grown on LB-Amp agar containing 0.1 % low MW chitosan, and 0, 0.1 or 0.5 mM IPTG, and incubated at 37 °C. Clearing zones from different conditions were measured at different time points and plotted as shown in Figure 3.2, left panel. Representative clearing zones are shown on the right panel. While no clearing zones were observed in *E. coli* expressing empty vector, the size of clearing zones of *E. coli* expressing OmpA-Csn were significantly larger than those from Nat-Csn-expressing *E. coli* after 48 h. These results suggest that homologous OmpA is more efficient than the native signal peptide at directing the secretion of heterologous enzyme in *E. coli*. Moreover, these results indicated that over-expression of *ptac* promoter could be induced by increasing concentration of IPTG. The observation of clear zones in the absence of IPTG was an indication that the promoter was leaky.

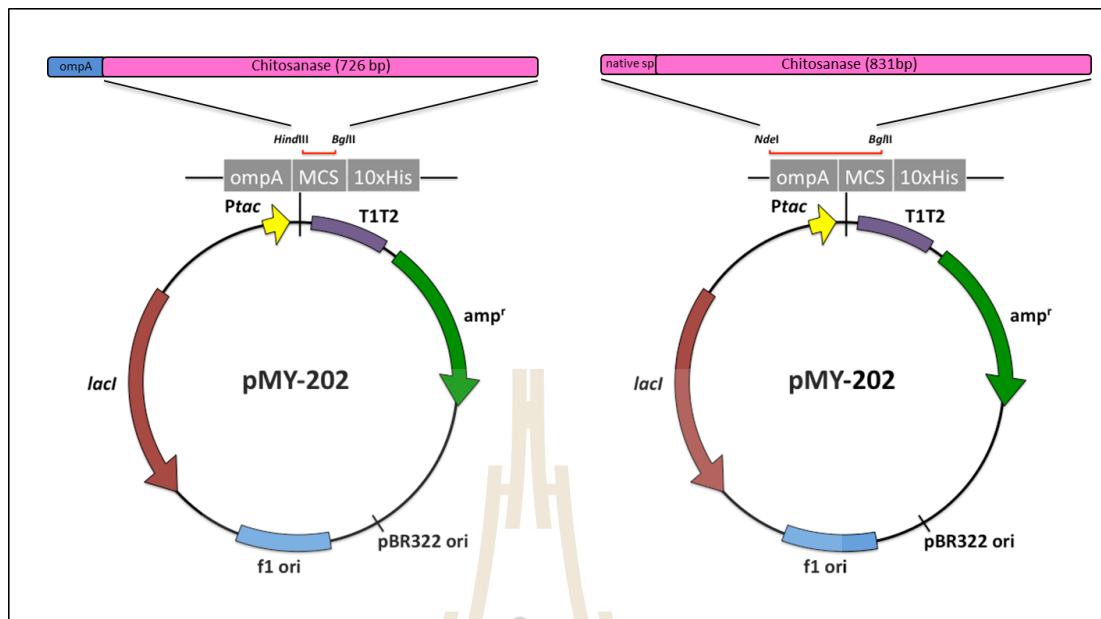


**Figure 3.1** Map of constructs used in this study. Nat-Csn (construct on left) was used for secretory expression of Csn via its native bacillus signal peptide, while OmpA-Csn (construct on right), comprised of the mature enzyme fused with the *E. coli* OmpA signal peptide that is a component of the pMY202 vector.

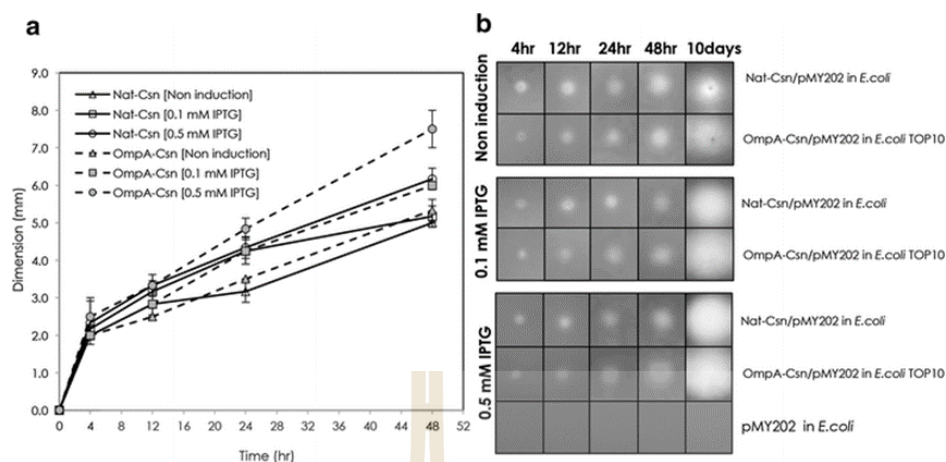


**Figure 3.2** Secretion of recombinant Csn. Mean clear zones diameters (from three colonies of *E. coli* expressing recombinant Nat-Csn and OmpA-Csn) at 0, 4, 12, 24 and 48 h are shown in the panel **a** along with standard error. Representative clear zones from different conditions at 4, 12, 24, 48, and 10 days are shown in the panel **b**. No clear zone was detected around colonies of *E. coli* expressing empty vector (bottom row).

### 3.4.2 Effect of signal peptides on yield and secretion efficiency of recombinant Csn containing two different signal peptides in an *E. coli* expression system

To further evaluate the effect of the signal peptides on the expression and secretion of Csn from *E. coli*, the recombinant proteins were collected from three different compartments (cytoplasm, periplasmic space, and culture broth) and their enzyme activities were analyzed at different time points. The total enzyme activity in the compartments and the secretion efficiency at different time points are reported in Table 3.1. These results indicate that the yield of the construct containing the *E. coli* signal peptide was approximately two folds to ten folds higher than the yield of

constructs with the native signal peptide, but was dependent on induction time and compartment. At 20 h after induction, both total yield and secretion efficiency of constructs with the OmpA signal peptide were approximately two fold higher than those with the native signal peptide. Moreover, the enzyme activities in the periplasm and culture broth were both approximately five fold higher when OmpA was used as the signal peptide. At 4 h after induction, when periplasmic leakage should be insignificant (Rinas and Hoffmann 2004, Albiniak et al. 2013) the use of the OmpA signal peptide resulted in as much as a ten fold higher Csn activity in the periplasm. The differences in yield and secretion efficiency were not observed at time 0, when the gene expression was not induced by IPTG.

**Table 3.1** Enzyme activity and secretion efficiency.

	Induction time (h)	Enzymatic activity (Total units <sup>a</sup> )		Fold change <sup>b</sup>
		Native Sp	OmpA Sp	
Broth	0	85.5±2.00	98.0±2.92	1.15
	4	115±1.5	244±5.1	2.12
	20	265±2.00	1,386±2.6	5.23
Periplasm	0	0.93±0.02	0.99±0.01	1.06
	4	2.03±0.01	22.2±0.20	10.9
	20	4.90±0.09	27.6±0.69	5.63
Cytosal	0	21.3±0.02	20.5±0.35	0.96
	4	338±2.6	561±12.8	1.45
	20	528±5.1	564±0	1.07
Total	0	108±2.0	119±3.3	1.1
	4	505±1.2	828±7.5	1.64
	20	798±3.0	1,978±3.2	2.48
Secretion Efficiency (%) <sup>c</sup>	0	79.3±0.39	82.0±0.21	1.03
	4	22.7±0.34	29.5±0.88	1.3
	20	33.2±0.38	70.1±0.01	2.11

Expression and secretion of *B. subtilis* Csn into different compartments of the *E. coli*

host harboring Nat-Csn/pMY202 or OmpA-Csn/pMY202, which contain native (Native Sp) or OmpA (OmpA Sp) signal peptides.

<sup>a</sup>Total enzyme activity from 50-mL culture. The experiments were done in duplicate and the average values with standard deviations are reported.

<sup>b</sup>Fold change indicates the relative values of the yields or secretion efficiencies of constructs with different signal peptides from different compartments (OmpA Sp divided by native Sp).

<sup>c</sup>Secretion efficiency was calculated from the percentage of the enzyme activity from culture broth plus periplasmic space divided by the total enzyme activities from all three compartments.

However, leaky expression from the *tac* promoter could be observed as shown in an assay on agar plates. Under these conditions, the secretion efficiency of constructs containing either the *E. coli* or the native signal peptide was equally high. To accurately determine the yield and activity of recombinant Csn, secreted enzymes were purified from culture broth to homogeneity (Figure 3.3a, b). The expected size of secreted recombinant Csn was approximately 32 kDa. The SDS-PAGE analysis of crude secreted enzymes from culture broth or cell lysate (periplasm plus cytosol) are illustrated in Figure 3.3c. Routinely, approximately 18.5 and 0.4 mg/L of purified OmpA-Csn and Nat-Csn could be purified from culture supernatant of shake-flask cultivation, respectively (Table 3.2). Both purified recombinant Csn proteins had specific activities of approximately 300-400 U/mg. These results are consistent with previous results on agar plates that the OmpA signal peptide is not only more efficient at directing recombinant *Bacillus* Csn secretion via the Sec dependent pathway in an *E. coli* expression system, but it also allows for increased protein expression upon induction with IPTG.

**Table 3.2** Purification of Nat-Csn/pMY202 and OmpA-Csn/pMY202 from culture broth or cell lysate

Sample	Protein mg/mL <sup>1)</sup>	Total protein mg/L <sup>2)</sup>	Activity (U/mL)	Total activity U/L	Specific act. (U/mg)	Purity (fold) <sup>3)</sup>	%Yield <sup>4)</sup>
<b>Csn-OmpA</b>							
Crude broth	0.22	216	48.7	48700	225	1.00	100
Purify broth	2.64	18.5	1370	9600	519	2.31	19.7
Crude Lysate	1.20	60.2	140	7020	117	1.00	100
Purify Lysate	0.56	2.9	253	1301	456	3.92	18.5
<b>Csn-Native</b>							
Crude broth	0.09	89.4	6.1	6095	68	1.00	100
Purify broth	0.14	0.38	37.9	106	280	4.10	1.74
Crude Lysate	3.68	184	704	35200	191	1.00	100
Purify Lysate	1.49	5.97	530	2120	355	1.86	6.02

<sup>1)</sup> Protein concentration (mg/ml) was determined by Bradford method as described in material and method. <sup>2)</sup>Total of protein in 1L from culture volume 100 mL. <sup>3)</sup>Purity refers to the increase in the specific activity, that calculated by specific activity of pure enzyme divided by specificity of crude enzyme. <sup>4)</sup> Yield refers to the recovery of the enzymatic activity after each purification step. The yield (%) was calculated from the total activity (U/L) at purified enzyme divided by the total activity (U/L) in crude enzyme, multiplied by 100.

### 3.4.3 N-terminal sequencing of secreted recombinant Csn

When proteins are secreted via the *E. coli* secretory pathway, the signal peptide is cleaved by membrane bound signal peptidases before the mature enzyme is released into the extracellular environment (Choi and Lee 2004). Since most recombinant proteins are foreign to *E. coli*, the cleavage sites can be predicted (Bendtsen et al. 2004, Zhang and Henzel 2004) but may differ from the actual cleavage sites that are often unknown. The secreted recombinant Csn were subjected to N-terminal sequencing to investigate whether changes in the structure of signal peptide could lead to alterations in amino acid sequence at the N-terminus. To do this,

secreted enzymes were purified from culture broth, transferred onto PVDF (Figure 3.3d) and submitted for N-terminal sequencing.

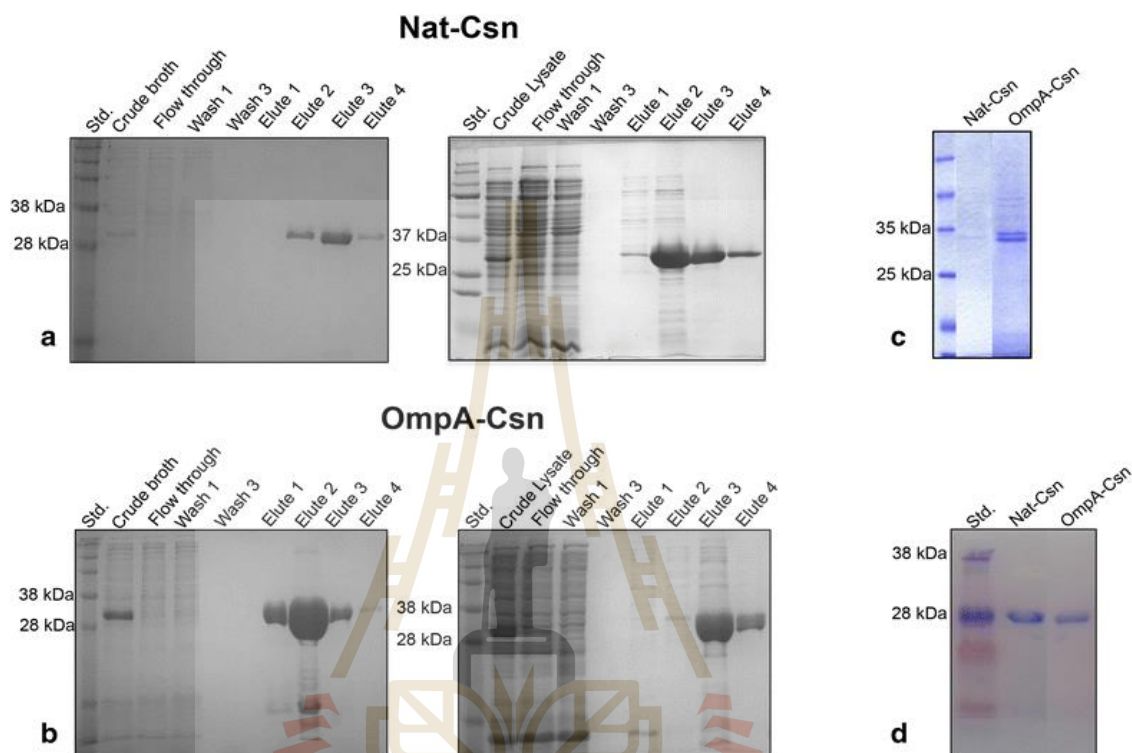


**Figure 3.3** Expression and purification of secreted Nat-Csn and OmpA-Csn from culture supernatant and cell lysate. SDS-PAGE analysis of constructs containing native (a) or OmpA (b) signal peptides from culture supernatant (*left panel*) and cell lysate (*right panel*) at various purification steps are shown. Equal volumes (15  $\mu\text{L}/\text{lane}$ ) of samples were loaded into lanes, except for crude lysate, of which 5  $\mu\text{L}/\text{lane}$  was loaded. c The comparison of crude enzymes obtained from culture broth after 20 h of induction with 0.1 mM IPTG. Equal volumes of culture broth (15  $\mu\text{L}/\text{lane}$ ) were loaded into *each lane*. Purified proteins from culture broth were separated by SDS-PAGE on 15 % gels and transferred onto PVDF membrane for N-terminal amino acid sequencing (d).



#### 3.4.4 MALDI-TOF mass spectrometry of secreted recombinant Csn

To confirm and further analyze the heterogeneous population of Csn secreted via the OmpA signal peptide, purified secreted Csn-OmpA protein was subjected to MALDI-TOF-MS for determination of intact molecular mass. Two intense mass signals corresponding to 30,339.71 and 31,150.36 Da were detected (Figure 3.5). The m/z ratio of these two signals corresponded well with amino acids 13–287 (cleavage site 1) and 22–287 (cleavage site 2), which encode proteins that are 275 and 266 amino acids, respectively. These mass determinations for purified Csn-OmpA were consistent and reproducible following several separate experiments. Since the sensitivity of MALDI TOF-MS is in the femtogram range, therefore, we could only confirm the presence of two heterogeneous products of secreted bacillus Csn using the OmpA signal peptide. Taken together these results indicated that even though the OmpA signal peptide could efficiently direct the secretion of the recombinant protein, the site of signal peptide cleavage might not have been accurate, resulting in a heterogeneous population of secreted proteins. In addition, our data indicated that the secretory machinery and the N-terminal signal peptidases of Gram-negative *E. coli* and Gram-positive *Bacillus* are highly similar, even if the structure of their cell walls are significantly different, because the *E. coli* translocation machinery could efficiently process and transport native *Bacillus* enzyme with native signal peptide.

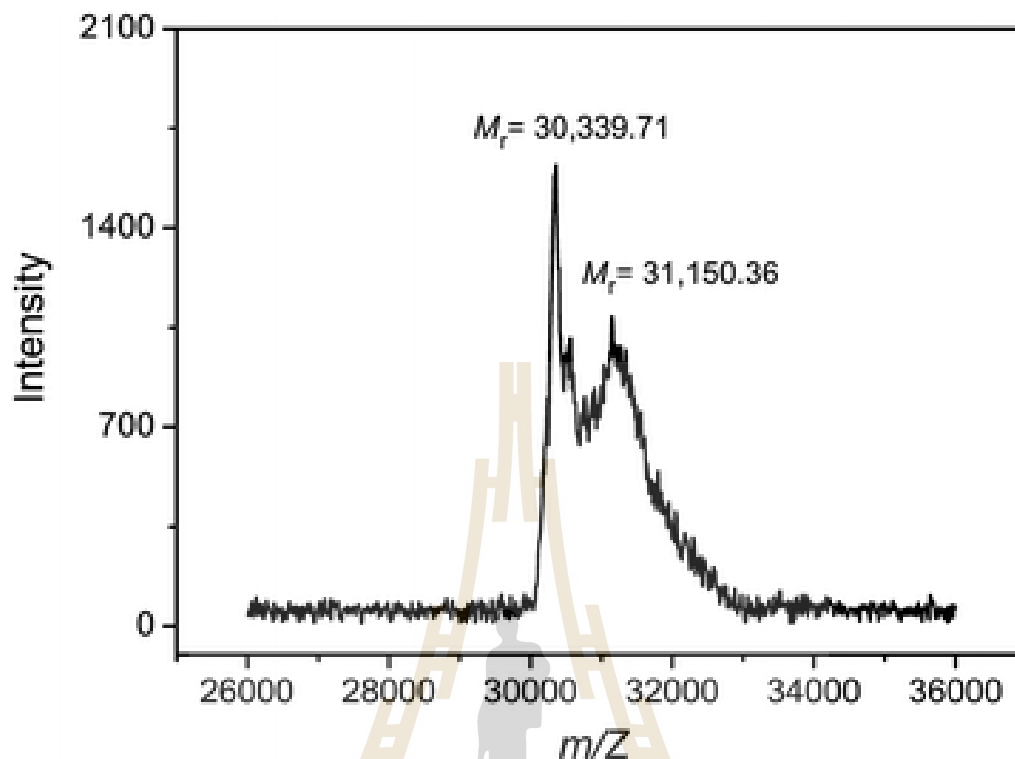


**Figure 3.5** MALDI-TOF MS analysis of the recombinant OmpA-Csn. Two mass signals with molecular mass ( $m/z$ ) of 30,339.71 and 31,150.36 Da as measured in a linear positive mode were indicated. Bovine insulin, equine cytochrome C, and equine apomyoglobin were used as external calibrated standard.

### 3.5 Discussion

Despite a substantial amount of information about secretion mechanisms, types of signal peptides and the effect of signal peptides on the secretion of different enzymes in various expression systems (Nakamura et al. 1989, Mathiesen et al. 2008, Degering et al. 2010), little information on the structure of the N-termini of the secreted recombinant proteins in *E. coli* has been reported. Even though many online databases and software programs can be used to predict signal peptides and cleavage sites, these

algorithms are not always accurate (Zhang and Henzel 2004), as demonstrated in this study. It has been previously shown that in addition to the signal peptide, the protein domain adjacent to the signal sequence, called the export initiation domain, is critical for protein translocation across the inner membrane of *E. coli* (Andersson and Heijne 1991). *Bacillus Csn* was selected as a model in this study because it is an extracellular enzyme and therefore contains an export initiation domain that favors secretion. As such, *Bacillus Csn* was well suited for the purpose of this study, where mainly the effect of the signal peptide was compared. While native *Bacillus* signal peptide can be recognized by *E. coli* secretion machinery, the secretion efficiency was not as high as when the OmpA signal peptide was used. In the presence of the *Bacillus* signal peptide, the secretion efficiency was 33.8 % at 20 h after induction, indicating that two-thirds of the recombinant proteins were retained in the cell. However, the N-terminal signal peptide had identical cleavage sites as in native *Bacillus* strains, indicating that N-terminal signal peptide processing is very accurate. This result indicates that both *E. coli* OmpA and native *Bacillus Csn* signal peptides direct the export of proteins via similar Sec-dependent secretion machinery. In addition, our data suggests that *Bacillus* and *E. coli* signal peptidases are functionally similar, even though their cell wall structures are very different. These data support the previous observation that the major components of the Sec machinery, which are required for protein secretion in both *Bacillus* and *E. coli*, are quite similar (Yuan et al. 2010). Both gram-positive and gram-negative employ a similar type I signal peptidase (SPase), a membrane-bound exported pre-enzymes during the late stages of the transport process (Roosmalen et al. 2004, Paetzel 2014). The consensus SPase recognition sequence is Ala-X-Ala at positions -1 and -3 relative to the cleavage site in preproteins (Paetzel 2014). *B. subtilis* proteomics

analysis revealed that 71 % of the corresponding signal peptides contain the consensus Ala-X-Ala recognition sequence; while 18 % of the identified extracellular proteins contain a Val-X-Ala recognition sequence (Roosmalen et al. 2004). Therefore, native *Bacillus* SP could be cleaved precisely after VFA sequence, generating precise N-terminus as indicated in Figure 3.4. As for construct containing OmpA signal peptide, there were two Ala-XAla sequences, which was artificially created by genetic engineering, consequently we detected two cleavage sites after the two Ala-X-Ala sequences (cleavage site 2 and 3). The cleavage site 1 was unusual as it was situated in the middle of hydrophobic region of signal peptide, before a helix-breaking glycine residue. This cleavage might have occurred via a different secretory pathway due to the incompatibility between the export initiation domain of *Bacillus* Csn and Gram-negative OmpA signal peptide. This result suggested that, one should avoid creating more than one Ala-X-Ala sequence at the junction between signal peptide and mature protein, when engineering a recombinant protein for secretory production. The two signal peptides had significantly different effects on the secretory production of recombinant proteins in *E. coli*. As shown in Table 3.1, the OmpA signal peptide led to significantly higher yields of recombinant enzyme, compared with the native signal peptide. Codon optimization analysis, using OPTIMIZER, an online application for improving expression levels, indicated that the codon adaptation index (CAI) based on codon usage of predicted highly expressed genes of the N-terminus of the native *Bacillus* signal peptide, was only 0.537 (1.0 is the highest) (Puigbo et al. 2007). Therefore one explanation for the higher expression yield could be because the codon of the homologous OmpA sequence located at the 5' end of the gene is more compatible with the *E. coli* translation machinery, especially at the initiation of translation step. Further study by codon optimization of native Csn signal peptide to mimic the codon

usage of *E. coli* will be necessary to test if this could help improve expression levels without compromising the fidelity of signal peptide cleavage. If successful, this may have broader commercial applications in the future.

It is interesting to note that the *ptac* promoter was leaky (Boer et al. 1983), resulting in low protein expression in the absence of induction with IPTG. At this low expression level, both signal peptides had 80 % secretion efficiency. It is possible that the secretion machinery was not fully occupied and still able to process the secretion of both signal peptides (Driessen et al. 2001). However, when IPTG was used to induce protein over-expression, secretion mediated by the native *Bacillus* signal peptide, which was less compatible with the *E. coli* translocase complex, became the rate-limiting step for secretory production much earlier than when OmpA was used (Keyzer et al. 2003). Another possibility is that the signal peptides used different secretion pathways (Muller et al. 2001). Recently, it was shown that a short peptide could serve as a signal peptide and guide heterologous cellulose proteins across both the inner and outer membranes of *E. coli* (Gao et al. 2015). Taken together these results suggest that when the N-terminal sequence of a protein is not critical, the OmpA signal peptide is preferred for the secretion of recombinant proteins in *E. coli*-based systems.

### 3.6 Conclusion

Our results indicated that in an *E. coli* expression system, the *E. coli* OmpA signal peptide was more efficient than the native bacillus signal peptide, for both expression and secretion of *Bacillus* Csn; however, cleavage of the signal peptide was not precise. Moreover, our results also indicated that the secretion machinery of Gram-negative *E. coli* could be used to correctly process the signal sequence and efficiently direct the

secretion of extracellular hydrolytic enzymes from Gram-positive bacteria, despite significant differences between the cell walls of Gram-positive and Gram-negative bacteria. These results can be used for the engineering of other recombinant proteins for secretory production in *E. coli*.

### 3.7 References

- Albiniak, A. M., Matos, C. F., Branston, S. D., Freedman, R. B., Keshavarz-Moore, E. and Robinson, C. (2013). High-level secretion of a recombinant protein to the culture medium with a *Bacillus subtilis* twin-arginine translocation system in *Escherichia coli*. **FEBS J** 280.
- Andersson, H. and Heijne, G. (1991). A 30-residue-long “export initiation domain” adjacent to the signal sequence is critical for protein translocation across the inner membrane of *Escherichia coli*. **Proc Natl Acad Sci U S A** 88.
- Bendtsen, J. D., Nielsen, H., von Heijne, G. and Brunak, S. (2004). Improved Prediction of Signal Peptides: SignalP 3.0. **J Mol Biol** 340: 783 - 795.
- Boer, H. A., Comstock, L. J. and Vasser, M. (1983). The tac promoter: a functional hybrid derived from the trp and lac promoters. **Proc Natl Acad Sci USA** 80.
- Bradford, M. M. (1976). A rapid and sensitive method for the quantitation of microgram quantities of protein utilizing the principle of protein-dye binding. **Anal Biochem** 72.
- Choi, J. H. and Lee, S. Y. (2004). Secretory and extracellular production of recombinant proteins using *Escherichia coli*. **Appl Microbiol Biotechnol** 64.
- Degering, C., Eggert, T., Puls, M., Bongaerts, J., Evers, S., Maurer, K. H. and Jaeger, K. E. (2010). Optimization of protease secretion in *Bacillus subtilis* and

- Bacillus licheniformis* by screening of homologous and heterologous signal peptides. **Appl Environ Microbiol** 76.
- Driessen, A. J., Manting, E. H. and Does, C. (2001). The structural basis of protein targeting and translocation in bacteria. **Nat Struct Biol** 8.
- Gao, D., Wang, S., Li, H., Yu, H. and Qi, Q. (2015). Identification of a heterologous cellulase and its N-terminus that can guide recombinant proteins out of *Escherichia coli*. **Microb Cell Fact** 14.
- Juajun, O., Nguyen, T.-H., Maischberger, T., Iqbal, S., Haltrich, D. and Yamabhai, M. (2011). Cloning, purification, and characterization of  $\beta$ -galactosidase from *Bacillus licheniformis* DSM 13. **Applied Microbiology and Biotechnology** 89(3): 645-654.
- Keyzer, J., Does, C. and Driessen, A. J. (2003). The bacterial translocase: a dynamic protein channel complex. **Cell Mol Life Sci** 60.
- Laemmli, U. K. (1970). Cleavage of structural proteins during the assembly of the head of bacteriophage T4. **Nature** 227.
- Mathiesen, G., Sveen, A., Piard, J. C., Axelsson, L. and Eijsink, V. G. H. (2008). Heterologous protein secretion by *Lactobacillus plantarum* using homologous signal peptides. **Journal of Applied Microbiology** 105(1): 215-226.
- Mergulhão, F. J. M., Summers, D. K. and Monteiro, G. A. (2005). Recombinant protein secretion in *Escherichia coli*. **Biotechnology Advances** 23(3): 177-202.
- Miller, G. L. (1959). Use of dinitrosalicylic acid reagent for determination of reducing sugar. **Anal Chem** 31.

- Muller, M., Koch, H. G., Beck, K. and Schafer, U. (2001). Protein traffic in bacteria: multiple routes from the ribosome to and across the membrane. **Prog Nucleic Acid Res Mol Biol** 66.
- Nakamura, K., Fujita, Y., Itoh, Y. and Yamane, K. (1989). Modification of length, hydrophobic properties and electric charge of *Bacillus subtilis* alpha-amylase signal peptide and their different effects on the production of secretory proteins in *B. subtilis* and *Escherichia coli* cells. **Mol Gen Genet** 216.
- Paetzel, M. (2014). Structure and mechanism of *Escherichia coli* type I signal peptidase. **Biochim Biophys Acta** 1843.
- Pechsrichuang, P., Yoohat, K. and Yamabhai, M. (2013). Production of recombinant *Bacillus subtilis* chitosanase, suitable for biosynthesis of chitosan-oligosaccharides. **Bioresource Technology** 127: 407-414.
- Puigbo, P., Guzman, E., Romeu, A. and Garcia-Vallve, S. (2007). OPTIMIZER: a web server for optimizing the codon usage of DNA sequences. **Nucleic Acids Res** 35.
- Rinas, U. and Hoffmann, F. (2004). Selective leakage of host-cell proteins during high-cell-density cultivation of recombinant and non-recombinant *Escherichia coli*. **Biotechnol Prog** 20.
- Roosmalen, M. L., Geukens, N., Jongbloed, J. D., Tjalsma, H., Dubois, J. Y., Bron, S., Dijl, J. M. and Anne, J. (2004). Type I signal peptidases of Gram-positive bacteria. **Biochim Biophys Acta** 1694.
- Songsiriritthigul, C., Lapboonrueng, S., Pechsrichuang, P., Pesatcha, P. and Yamabhai, M. (2010). Expression and characterization of *Bacillus licheniformis* chitinase (ChiA), suitable for bioconversion of chitin waste. **Bioresource Technology**

101(11): 4096-4103.

Yamabhai, M., Buranabanyat, B., Jaruseranee, N. and Songsiriritthigul, C. (2011).

Efficient *E. coli* expression systems for the production of recombinant beta-mannanases and other bacterial extracellular enzymes. **Bioeng Bugs** 2.

Yamabhai, M., Emrat, S., Sukasem, S., Pesatcha, P., Jaruseranee, N. and

Buranabanyat, B. (2008). Secretion of recombinant *Bacillus* hydrolytic enzymes using *Escherichia coli* expression systems. **Journal of Biotechnology** 133(1): 50-57.

Yuan, J., Zweers, J. C., Dijl, J. M. and Dalbey, R. E. (2010). Protein transport across and into cell membranes in bacteria and archaea. **Cell Mol Life Sci** 67.

Zhang, Z. and Henzel, W. J. (2004). Signal peptide prediction based on analysis of experimentally verified cleavage sites. **Protein Sci** 13.

Zhou, Z., Zhao, S., Wang, S., Li, X., Su, L., Ma, Y., Li, J. and Song, J. (2015).

Extracellular Overexpression of Chitosanase from *Bacillus* sp. TS in *Escherichia coli*. **Applied Biochemistry and Biotechnology** 175(7): 3271-3286.

## CHAPTER IV

### IN-DEPTH CHARACTERIZATION OF FAMILY 46

#### CHITOSANASE FROM *BACILLUS SUBTILIS* (*BSCSN46A*)

##### 4.1 Abstract

*BsCsn46A*, a GH family 46 chitosanase from *Bacillus subtilis* had been previously shown to have potential for bioconversion of chitosan to chito-oligosaccharides. However, so far, in-depth analysis of both the mode of action of this enzyme and the composition of its products were lacking. In this study, we have employed size exclusion chromatography,  $^1\text{H}$ -NMR, and mass spectrometry to reveal that *BsCsn46A* can rapidly cleave chitosans with a wide-variety of acetylation degrees, using a non-processive endo-mode of action. The composition of the product mixtures can be tailored by varying the degree of acetylation of the chitosan and the reaction time. Detailed analysis of product profiles revealed differences compared to other chitosanases. Importantly, *BsCsn46A* seems to be one of the fastest chitosanases described so far. The detailed analysis of preferred endo-binding modes using  $\text{H}_2^{18}\text{O}$  showed that a hexameric substrate has three productive binding modes occurring with similar frequencies.

Keywords : GH46; chitosanase; bioconversion; chitosan; chito-oligosaccharides;

*Bacillus*

## 4.2 Introduction

Chito-oligosaccharides can be produced by enzymatically or chemically from chitosans, linear heteropolymers of  $\beta(1\rightarrow4)$  linked *N*-acetyl-D-glucosamine (GlcNAc or A) and D-glucosamine (GlcN or D) (Aam et al. 2010). Such chitosans are produced from chitin, one of Nature's primary structural polysaccharides, found in the outer exoskeleton of arthropods (of which crabs, lobster and shrimps are of importance for industrial production of chitosan) and in fungal cell walls. Chitin is an abundant bioresource that needs proper bioremediation, and its value-creating conversion to chitosan and CHOS is thus of major interest (Khoushab and Yamabhai 2010). Chitosans differ in terms of their chain length (degree of polymerization, DP), fraction of acetylation ( $F_A$ ), and pattern of acetylation ( $P_A$ ). The  $F_A$  needs to be below 0.7 for the chitosan to be soluble. Chitosans that are generated by de-*N*-acetylation of chitin under homogeneous conditions have a random distribution of A- and D- subunits (Vårum et al. 1991).

Chitosanases, or chitosan *N*-acetylglucosaminohydrolases (EC 3.2.1.132), catalyzes the hydrolysis of glycosidic bonds in chitosan, and limited hydrolysis will lead to the production of CHOS (Fukamizo et al. 1994). CHOS have various potential applications in the food, agricultural and pharmaceutical industries and there is increasing interest in the conversion of chitin, via chitosan into bioactive CHOS (Aam et al. 2010, Xia et al. 2011). Enzymatic conversion of chitosan is attractive since this leads to clean processes and because there is a wide variety of depolymerizing enzymes with varying cleavage specificities. Thus, by varying the enzyme, different product mixtures can be obtained. Enzymes with chitosanase activity have been found in various glycosyl hydrolase (GH) families according to the CAZy database, and there are three families

that only have chitosanases: GH46, GH75, and GH80. Notably, chitosan contains four types of glycosidic bonds: D-D, A-A, D-A and A-D. Chitosanases will differ in their preferences for these pairs of monomers, and these preferences may also be affected by adjacent sugars. Enzymes with a preference for A-A would be classified as chitinases (families GH18 and GH19), but these enzymes also act on chitosan (Itoh et al. 2002, Sørbotten et al. 2005, Horn et al. 2006, Stefanidi and Vorgias 2008, Purushotham et al. 2012).

In a previous study, we expressed a family 46 chitosanase (Takasuka et al. 2014, Viens et al. 2015) from *Bacillus subtilis* strain 168 (*BsCsn46A*; UniProt: CHIS\_BACSU; locus name BSU26890). Basic characterization of the enzyme revealed industrially relevant properties such as high thermostability and pH-stability, high-level secretory expression in *Escherichia coli*, and the ability to convert chitosan (Pechrichuang et al. 2013). This enzyme belongs to group B of the GH46 chitosanases, according to a phylogenetic analysis carried out by Viens et al. (2015), for which there is not yet a representative that has been characterized in-depth. Because of this and because of promising initial results, we have now carried out an in-depth analysis of the mode of action of this enzyme. Furthermore, we have analyzed its ability to convert chitosan in detail, including an analysis of the composition and sequence of its hydrolytic products. These analyses were carried out using state-of-the-art size exclusion chromatography (SEC), <sup>1</sup>H- NMR and mass spectrometry (MS) methods. We have carried out conversion reactions with various types of chitosans, leading to a variety of product mixtures.

## 4.3 Material and Methods

### 4.3.1 Chitosans

Kitoflokk<sup>TM</sup> chitosan with  $F_A$  0.15 and an average DP ( $DP_n$ ) of approximately 206 (corresponding to an average molecular weight ( $MW_n$ ) of 37 kDa) was provided by Teta Vannrensing (Kløfta, Norway). Chitosan with  $F_A$  0.3 and  $DP_n > 1000$ , ( $MW_n = 200-400$  kDa) was purchased from Heppe Medical chitosan GmbH (Halle, Germany). Highly acetylated chitosan with  $F_A$  0.6 was prepared by homogenous de-*N*-acetylation of chitin from shrimp shells (Chitonor, Senjahopen, Norway), according to a previously described method (Sannan et al. 1975, Vårum et al. 1991). Briefly, 4 g of chitin flakes was mixed with 100 g of 40% (w/w) NaOH and incubated at 4 °C overnight. Then, 300 g of ice was added and the solution was stirred until homogeneous. Undissolved chitin was removed by centrifugation (10,000×g at 4 °C). After sparging with nitrogen gas for 10 minutes to remove oxygen, the solution was incubated at 25 °C (water bath) for 42 h to deacetylate chitosan. The deacetylation reaction was stopped by adding 280 g of ice. The solution was stirred until it was homogeneous, followed by addition of HCl until the pH reached 4.5. The chitosan sample was dialyzed against water using a dialysis membrane with 12-14 kDa cut-off (SpectrumLabs, Texas, USA) to remove salt. The water was changed several times until the conductivity reached 3 µS. The resulting chitosan solution was then filtered (Whatman filters, first 1.2 µM, then 0.8 µM; Millipore) and lyophilized.

### 4.3.2 Expression of recombinant *BsCsn46A* gene in *E. coli*

A gene fragment encoding *BsCsn46A* was engineered for secretory production in *E. coli*, as previously described (Pechsrichuang et al. 2013, Pechsrichuang et al. 2016). To produce the enzyme, a single colony of freshly transformed *E. coli*

TOP10 harboring the OmpA-Csn/pMY202 (Pechsrichuang et al. 2016) was grown in Luria Bertani (LB) broth containing 100 µg/ml ampicillin (LB-Amp) overnight, at 37 °C, with shaking at 180 rpm. Five ml of the overnight cultures was used to inoculate 0.5 L of ampicillin containing TB medium, and bacteria grown in airlift fermenter (Harbinger Biotechnology and Engineering, Ontario, Canada) at 37 °C until the OD<sub>600</sub> reached 1.0. At that point, isopropyl-β-D-thiogalactopyranoside (IPTG) was added to a final concentration of 0.1 mM, and the incubation was continued at 28 °C for 20 h. The culture broth was collected by centrifugation at 4000×g for 30 min at 4 °C and concentrated using a VivaFlow 200 system equipped with a filter with a molecular weight cut-off (MWCO) of 10,000 Da. The recombinant chitosanase, containing C-terminal His<sub>10</sub> tag, was purified by immobilized metal affinity chromatography (IMAC), using Ni-NTA agarose, according to the manufacturer's instruction (Qiagen, Hilden, Germany).

#### 4.3.3 Enzymatic degradation of chitosan

Chitosans with different fractions of acetylation (F<sub>A</sub> 0.15, 0.3 and 0.6) were dissolved in 40 mM sodium acetate buffer, pH 5.5, containing 100 mM NaCl and 0.1 mg BSA/ml of chitosan. Chitosan solutions F<sub>A</sub> 0.15 and 0.3 (final concentration of 10 mg/ml) were pre-incubated in an incubator shaker at 37 °C, and the degradation reactions were started by adding 0.05 µg of *BsCsn46A* per mg of chitosan. Samples were taken from the reactions at various time points from 10 min to 2880 min. The reaction was stopped by adding 150 µl of 1 M HCl followed by heating at 100 °C for 3 mins. Then, the samples were concentrated and dried by using a vacuum concentrator. Before <sup>1</sup>H-NMR, the samples were dissolved in D<sub>2</sub>O and the pD was adjusted to 4.5. Alternatively, the samples were dissolved in 0.15 M ammonium acetate, pH 4.5, for SEC. To increase the degrees of scission (α) of chitosans, additional *BsCsn46A* was

added at 0.05  $\mu\text{g}$  per mg of chitosan after incubation for 1440 min, and the degradation reaction was continued for 1,440 min.

For highly acetylated chitosan ( $F_A$  0.6), the degradation reactions were started by adding 4  $\mu\text{g}$  of the enzyme per mg of chitosan and incubated at 50  $^\circ\text{C}$  for 1,440 min. To increase the  $\alpha$ -values of chitosan, more enzyme (4  $\mu\text{g}$  per mg of chitosan) was added and further incubated for 1,440 min.

#### 4.3.4 Size-exclusion chromatography

SEC was used for baseline separation of CHOS as previously described (Sørbotten et al. 2005). Three XK 26 columns were connected in series and packed with Superdex™ 30 (Pharmacia Biotech, Uppsala, Sweden), with an overall dimension of 2.60 x 180 cm. The mobile phase, (0.15 M ammonium acetate, pH 4.5) was pumped through the system using an LC-10ADvp pump (Shimadzu GmbH, Duisburg, Germany) at a flow rate of 0.8 ml/min. Products were detected using a refractive index (RI) detector (Shodex RI-101, Shodex Denko GmbH, Dusseldorf, Germany) coupled to a CR 510 Basic Data logger (Campbell Scientific Inc., Logan, UT). Fractions of 4 ml were collected using a fraction collector for CHOS sequence analysis.

#### 4.3.5 NMR spectroscopy

Samples for  $^1\text{H}$ -NMR analysis were dissolved in  $\text{D}_2\text{O}$ , and then  $\text{DCl}$  or  $\text{NaOD}$  were used to adjust the pD to 4.3 - 4.6.  $^1\text{H}$ -NMR spectra were obtained at 400 MHz at a temperature of 85  $^\circ\text{C}$ , as previously described (Vårum et al. 1991). The degree of scission ( $\alpha$ ), which equals the fraction of cleaved glycosidic linkages, was calculated as the inverse value of  $\text{DP}_n$  (average degree of polymerization). The  $\text{DP}_n$  was calculated as previously described (Sørbotten et al. 2005), using the formula  $\text{DP}_n = (\text{A}\alpha + \text{A}\beta + \text{D}\alpha + \text{D}\beta + \text{A} + \text{D}) / (\text{A}\alpha + \text{A}\beta + \text{D}\alpha + \text{D}\beta)$ .  $\text{A}\alpha$ ,  $\text{A}\beta$ ,  $\text{D}\alpha$  and  $\text{D}\beta$  equal the integrals of the

reducing end signals of  $\alpha$  and  $\beta$  anomers of GlcNAc and GlcN, respectively, and A and D equal the integrals of the peaks representing sugars in internal positions and at the non-reducing end. The signals for the  $\beta$ -anomers of reducing end sugars are difficult to quantify because they overlap with the internal signals (for D) or because, in the case of A, they appear as two doublets at 4.705 ppm ( $-\text{AA}$ ) and 4.742 ppm ( $-\text{DA}$ ). Therefore, the  $\beta$ -anomer signals were calculated from the  $\alpha$ -anomers signals based on the known  $\alpha/\beta$  anomer ratio of 60:40 (Tsukada and Inoue 1981, Koga et al. 1998, Horn et al. 2006). The internal signals for D were then corrected.

#### **4.3.6 Analysis of CHOS by mass spectrometry (MS)**

Identification of isolated CHOS was performed with Matrix-Assisted Laser Desorption Ionization mass spectrometry (MALDI TOF/TOF MS). MS spectra were acquired using an Ultraflex<sup>TM</sup> TOF/TOF mass spectrometer (Bruker Daltonik GmbH, Bremen, Germany) with gridless ion optics under the control of Flexcontrol. For sample preparation, 1  $\mu\text{l}$  of sample was mixed with 1  $\mu\text{l}$  of 10 % (w/v) 2,5-dihydroxybenzoic acid (DHB) in 30% acetonitrile and spotted onto a MALDI target plate (Bahrke et al. 2002). The MS experiments were conducted using an accelerating potential of 20 kV in reflectron mode.

#### **4.3.7 CHOS sequencing**

Approximately 20 mg of CHOS obtained from degradation of  $F_A$  0.3 chitosan to a degree of scission of 0.14 or 0.26 were dried using a vacuum concentrator and separated by SEC as described above. The individual fractions of CHOS obtained from the SEC experiment were lyophilized using a freeze dryer. Then, the CHOS (from DP2 to DP6) were labeled with 2-aminoacridone (Bahrke et al. 2002) and purified using a C-18 column (Starata C18E, Phenomenex, CA, USA) (Morelle et al. 2006), as follows.

The CHOS, typically 0.5 mg, were dissolved in 10  $\mu\text{L}$  of 0.1 M of AMAC and 10  $\mu\text{L}$  of 1 M natriumcyanoborhydride (NCBH). The samples were heated at 90  $^{\circ}\text{C}$  for 30 min (in the dark), cooled to -20  $^{\circ}\text{C}$ , and dried using a vacuum concentrator. The dried samples were dissolved in 100  $\mu\text{L}$  of 70% methanol and centrifuged at 10,000 $\times g$  for 30 min to remove undissolved CHOS. Then, the samples were dried using the vacuum concentrator and dissolved in 100  $\mu\text{L}$  deionized water. After centrifugation for 5 minutes to remove potential insoluble the sample was applied to a C-18 column (Starata C18E, Phenomenex, CA, USA), which was used for purification of AMAC-labeled CHOS. The eluted AMAC-labeled CHOS were dried using the vacuum concentrator and stored at -20  $^{\circ}\text{C}$  until analysis. Before analysis the samples were dissolved in 50  $\mu\text{L}$  of 50 % methanol. Analysis was performed using an LTQ-Velos Pro ion trap mass spectrometer (Thermo Scientific, Bremen, Germany) connected to an Ultimate 3000 RS HPLC (Dionex, CA, USA), using a setup for direct injection without a column. The pump delivered 200  $\mu\text{L}/\text{min}$  of 0.03  $\mu\text{M}$  formic acid in 70 % acetonitrile and the data was acquired for 24 seconds after injection. The capillary voltage was set to 3.5 kV and the scan range was  $m/z$  150-2000 using two micro scans for the MS. The automatic gain control was set to 10,000 charges and a maximum injection time of 20 milliseconds. For fragmentation of desired precursor masses by MS2, the normalized collision energy was set to 37 and three micro scans were used. The data were recorded with Xcalibur version 2.2.

#### **4.3.8 Hydrolysis of (GlcN)<sub>5</sub> and (GlcN)<sub>6</sub> in H<sub>2</sub><sup>18</sup>O for subsite mapping**

To determine preferred binding modes for the substrate, hydrolysis of (GlcN)<sub>5</sub> and (GlcN)<sub>6</sub> was carried out in H<sub>2</sub><sup>18</sup>O (Larodan Fine Chemicals, Malmö, Sweden), as previously described (Hekmat et al. 2010, Eide et al. 2013). In accordance

with the previously published protocols, reactions were set up to reach approximately 20 % substrate conversion in short reaction times (up to two minutes). Short reaction times are needed to avoid non-enzymatic incorporation of  $^{18}\text{O}$ , as described by Eide et al. (2013). The enzyme concentration was adjusted to ensure that 20% substrate conversion happened within the first two minutes. The enzyme stock solutions were highly concentrated to keep the volume of added enzyme and, thus, unlabeled  $\text{H}_2\text{O}$ , below 2 % of the total reaction volume (Hekmat et al. 2010). The hydrolysis was performed at  $37^\circ\text{C}$  and 600 rpm in  $\text{H}_2^{18}\text{O}$  containing 50 mM sodium acetate buffer (pH 5.5) and 5 mM  $(\text{GlcN})_5$  or  $(\text{GlcN})_6$ . Reactions were started by adding enzyme to a final concentration of  $1.8\ \mu\text{M}$  and  $1.4\ \mu\text{M}$  for the reactions with  $(\text{GlcN})_5$  and  $(\text{GlcN})_6$ , respectively. Samples of  $1\ \mu\text{l}$  were taken at several time points within the first 120 s of the reaction. The reactions were immediately quenched by mixing with a DHB solution (15 mg/ml DHB in 30% ethanol), spotted directly on the MALDI target and dried. The hydrolysis products were then analyzed by MALDI-TOF-MS as previously described (Eide et al. 2013). Data were analyzed for the time point where approximately 20 % of the substrate had been converted. The minor errors caused by the presence of unlabeled water and non-enzymatic incorporation of  $^{18}\text{O}$  were neglected.

## 4.4 Results and discussion

### 4.4.1 Hydrolysis of chitosan

$^1\text{H-NMR}$  spectroscopy was used to analyze the time course of the degradation of chitosan with  $F_A$  0.15 or  $F_A$  0.3. NMR spectra of the product mixtures were recorded at several time points during the degradation reaction and were assigned as described in Sørbotten et al. (2005) (see also (Ishiguro et al. 1992) and the Materials

and Methods section for further details). The spectra, depicted in Figure 4.1, show that the new reducing ends generated early in the reaction were almost exclusively deacetylated (D). At early time points, the spectra show signals at 5.43 ppm and 4.92 ppm, representing the  $\alpha$  and  $\beta$  anomers of a reducing end D, respectively, while signals representing acetylated reducing ends (A; 5.19 ppm and 4.742 ppm) only appeared after more extensive degradation ( $\alpha$ -values above 0.1). Thus, *BsCsn46A* has an expected preference for D-units in the -1 subsite, although the enzyme can also hydrolyze glycosidic linkages following an A-unit. Reducing end A units give multiple signals: the  $\alpha$ -anomer resonates at 5.19 ppm, whereas the  $\beta$ -anomer of a reducing end A resonates at 4.705 or 4.742 ppm, depending on whether the preceding unit is an A or a D, respectively (Sørbotten et al. 2005). The fact that only the 4.742 ppm signal was observed indicates that cleavage after an A only occurs if the preceding unit is deacetylated.



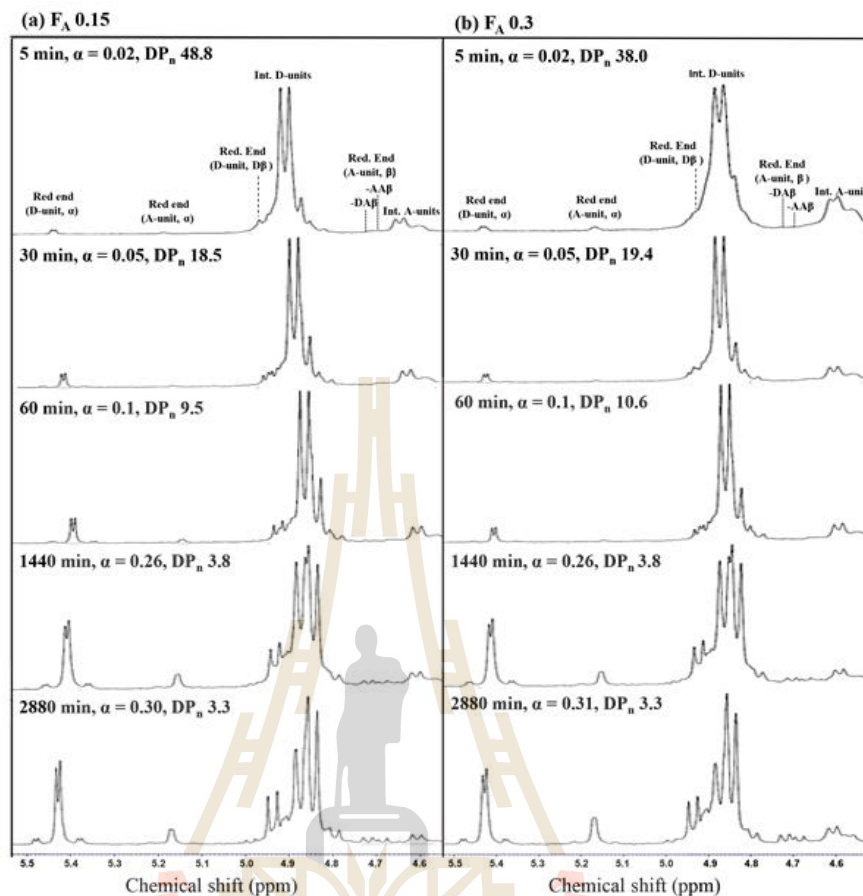


**Figure 4.1** Product formation over time during degradation of chitosans with  $F_A$  0.15 (left) or  $F_A$  0.3 (right) with *BsCsn46A*, analyzed by  $^1\text{H-NMR}$ . The figure shows  $^1\text{H-NMR}$  spectra of the anomer region of chitosans with  $F_A$  0.15 or  $F_A$  0.3 at various time points during degradation with *BsCsn46A*. The  $\alpha$ -values (degree of scission) and the  $DP_n$  (average chain length in the product mixture) at each time point are indicated. A reducing end D-unit resonates at 5.43 ppm ( $\alpha$ -anomer) and 4.92 ppm ( $\beta$ -anomer). The  $\alpha$ -anomer of a reducing end A-unit resonates at 5.19, while the  $\beta$ -anomer appears as two doublets at 4.705 ppm ( $-AA$ ) and 4.742 ppm ( $-DA$ ), depending on whether the preceding sugar unit is an A or a D, respectively. Internal D-units resonate at

4.8-4.95 ppm, whereas internal A-units resonate at 4.55-4.68. See Sørbotten et al. (2005) and the Materials and Methods section for more details concerning the interpretation and quantification of these spectra.

Progress curves for the degradation of the chitosans, i.e. curves showing the increase in  $\alpha$  over time (Figure 4.2), showed a rapid linear phase until the  $\alpha$ -values reached 0.15-0.20, followed by a slower second phase at higher  $\alpha$ -values. Reactions set-up to yield maximum degradation of the chitosans gave maximum  $\alpha$ -values of 0.30 and 0.31 for  $F_A$  0.15 and  $F_A$  0.3, respectively, which means that about 1 in 3 of the glycosidic bonds had been cleaved. Interestingly, the maximum  $\alpha$ -value obtained with the  $F_A$  0.3 chitosan is considerably lower than the maximum  $\alpha$ -value of 0.44 obtained when degrading a  $F_A$  0.32 chitosan with ScCsn46A, a family 46 chitosanase from *Streptomyces coelicolor* A3(2) (Heggset et al. 2010).

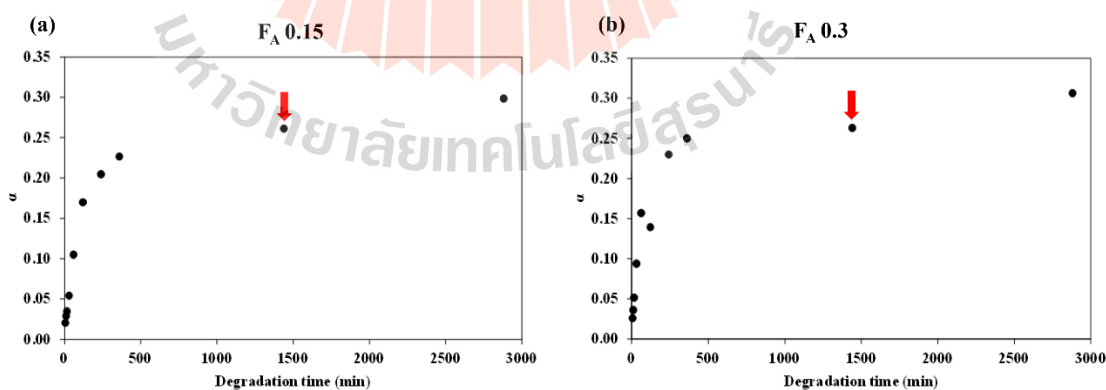


**Figure 4.2** Time-course for the increase in  $\alpha$  during degradation of chitosans with  $F_A$  0.15 (left) or  $F_A$  0.3 with *BsCsn46A*. The graph shows the degree of scission ( $\alpha$ ) determined by  $^1\text{H-NMR}$  in reactions containing 10 mg/ml chitosan, 0.05  $\mu\text{g}$  of *BsCsn46A* per mg of chitosan in 40 mM sodium acetate buffer, pH

5.5, containing 100 mM NaCl and 0.1 mg BSA/ml. In an attempt to reach maximum conversion of the chitosans, additional *BsCsn46A* was added at 0.05  $\mu\text{g}$  per mg of chitosan after incubation for 1440 min (red arrow), and the degradation reaction was continued for another 1440 min.

Using five data points recorded during the first hour of the reaction (Figure 4.3), the initial specific activity was then calculated as previously described (Heggset et al. 2009). The initial specific activity of *BsCsn46A* was  $5.5 \times 10^3$  and  $8.4 \times 10^3 \text{ min}^{-1}$  for  $F_A$  0.15 and  $F_A$  0.3, respectively. The initial rates displayed by *BsCsn46A* are remarkably high. Previous studies have shown that degradation of a chitosan with  $F_A$  0.32 by *ScCsn46A* (Heggset et al. 2010) or of a chitosan with  $F_A$  0.31 by *SaCsn75A* from *Streptomyces avermitilis* (Heggset et al. 2012) have initial rates of  $325 \text{ min}^{-1}$  and  $6.5 \text{ min}^{-1}$ , respectively. This result confirms indications from previous studies which concluded that *BsCsn46A* has high potential for biotechnological applications (Pechsrichuang et al. 2013, Pechsrichuang et al. 2016). It is remarkable that the initial specific activity of *BsCsn46A* against  $F_A$  0.3 chitosan was approximately 1.5 times higher compared to the  $F_A$  0.15 chitosan. Likewise, it was unexpected that the enzyme reaches almost identical  $\alpha$ -values for the two substrates, despite the difference in acetylation. This could be due to binding preferences of the enzyme for certain sequences containing acetylated sugars, but could also reflect a difference in the substrates. The substrates may differ in terms of the randomness of the distribution of acetylated units and this can affect hydrolysis yields. Notably, when increasing the  $F_A$  to 0.6, hydrolysis yields in terms of maximum  $\alpha$  decreased to approximately 0.18 as indicated by SEC experiment in the next section (Figure 4.4c), in line with the notion that *BsCsn46A* is a chitosanase and not a chitinase.

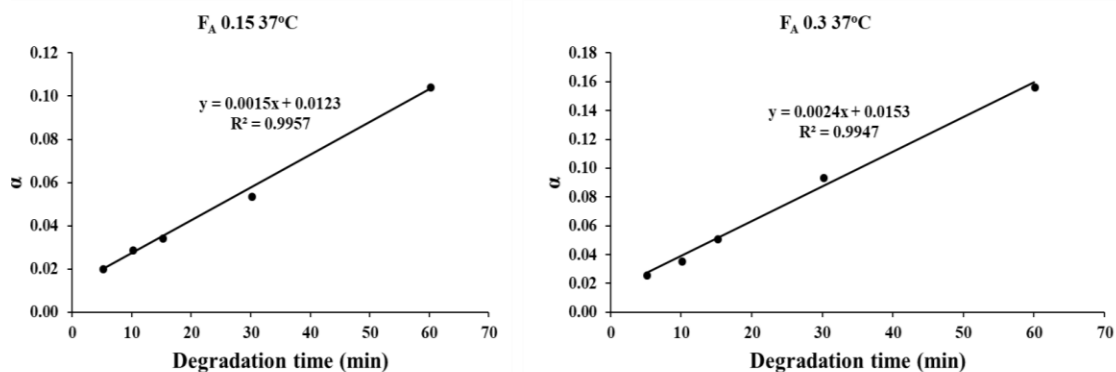


**Figure 4.3** Time-course analysis of the initial phase of degradation. The initial phase of degradations of chitosans with  $F_A$  0.15 or 0.3 by *BsCsn46A* at 37 °C at various time points are illustrated. The graph shows the degree of scission determined by  $^1\text{H-NMR}$  in reactions containing 10 mg/ml chitosan,  $0.05 \mu\text{g}$  of *BsCsn46A* per mg of chitosan in 40 mM sodium acetate buffer, pH 5.5, 100 mM NaCl and 0.1 mg BSA/ml. These time courses were used to estimate the initial rates of the degradation reaction, as indicated.

#### 4.4.2 Size distribution of CHOS obtained after degradation of chitosans with varying degrees of acetylation

CHOS mixtures were separated by size exclusion chromatography (SEC) as shown in Figure 4.4. The chromatograms indicated size distributions of oligomers obtained after degradation of chitosans with  $F_A$  0.15, 0.3 or 0.6 at two  $\alpha$ -values, one intermediate value and one at approximately maximum  $\alpha$ . The DP of the peaks was assigned using MALDI-TOF MS. The chromatograms showed rapid disappearance of the polymer peak (not shown) and production of a continuum of odd- and even-numbered oligomers, indicating that *BsCsn46A* is a non-processive endo-acting enzyme, similar to *ScCsn46A* and *SaCsn75A* (Heggset et al. 2010, Heggset et al. 2012).

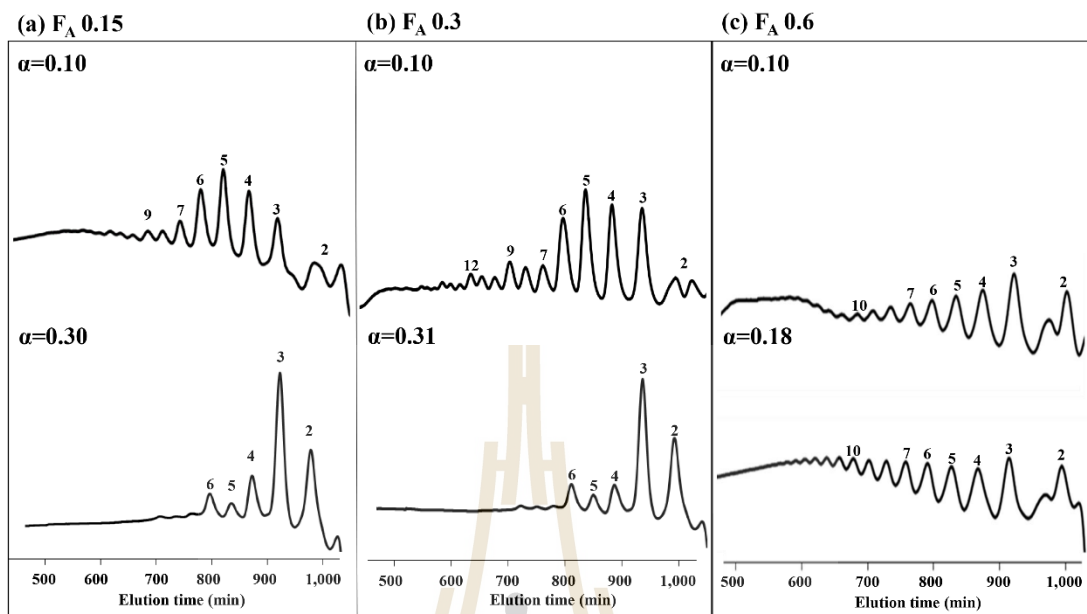


**Figure 4.4** Product analysis by size exclusion chromatography (SEC). Size distribution of CHOS after degradation of three different chitosans at 37 °C for  $F_A 0.15$  and  $F_A 0.3$  chitosans and 50 °C for  $F_A 0.6$  chitosan using  $B_sCsn46A$ . For each chitosan an intermediate product mixture ( $\alpha = 0.10$ ) and a final product mixture (varying  $\alpha$ ) is shown. The peaks are labeled with the DP values.

In the initial phase of the reactions with chitosans with  $F_A 0.15$  and  $F_A 0.3$  the dominating products were oligomers in the DP3 - DP6 range, whereas DP2 and longer oligomers up to a DP of approximately 15 were also produced. After extensive degradation, the amount of the short oligomers increased and the main products were dimers and trimers. No monomers were observed, confirming previous TLC analyses (Pechsrichuang et al. 2013). Interestingly, the chromatograms showed that, at the end of the reaction, the amount of DP6 was higher than the amount of DP5. This product

profile is unique to *BsCsn46A* and further illustrates the difference with *ScCsn46A* (Heggset et al. 2010), which produces more pentamer than hexamer, is slower and reaches higher  $\alpha$ -values.

Hydrolysis of the  $F_A$  0.6 chitosan yielded a continuum of products reaching from DP3 to DP > 10 (Figure 4.4c). Clearly, *BsCsn46A* generates many longer non-cleavable oligomeric products. In this case, as expected (Heggset et al. 2010), the dimer top was clearly split into two, reflecting the presence of considerable amounts of acetylated dimers.

#### **4.4.3 Chemical composition of CHOS fractions obtained after degradation of chitosans with varying $F_A$**

The chemical compositions of individual CHOS fractions obtained after degradation of chitosans with  $F_A$  values of 0.15, 0.3, or 0.6 were analyzed by MALDI-TOF-MS and the results are summarized in Table 4.1. For the chitosans with  $F_A$  0.15 and  $F_A$  0.3, fully deacetylated oligomers were the dominating products in the early phase of the reaction, whereas A-containing products became more dominant after extensive degradation, while D5, D6 and D7 disappeared (Table 4.1). The dimer peaks contained a mixture of primarily D2 and DA and a small amount of A2, both in the initial rapid phase and at the end of the reaction. The trimer fraction contained approximately equal amounts of D3 and D2A1 and a small amount of D1A2 both in the initial phase and at the end of the reactions, indicating that *BsCsn46A* cannot cleave these oligomers. The product compositions obtained upon degradation of the  $F_A$  0.15 and  $F_A$  0.3 chitosans were slightly different, with several A-rich products only being detected in product mixtures generated from the  $F_A$  0.3 chitosan. It is interesting to note that the product

mixtures seem to contain pentamers and hexamers that contain only one A. So, in some cases, one internal A unit apparently hampers hydrolysis by *BsCsn46A*, which is yet another difference of this enzyme compared to *ScCsn46A*.

**Table 4.1** Chemical composition of CHOS fractions \*

DP	F <sub>A</sub> 0.15		F <sub>A</sub> 0.3		F <sub>A</sub> 0.6
	$\alpha = 0.12$	$\alpha = 0.30$	$\alpha = 0.11$	$\alpha = 0.31$	$\alpha = 0.18$
2	<b>D2</b> , DA, A2	<b>D2</b> , DA, A2	<b>D2</b> , DA, A2	<b>D2</b> , DA, A2	<b>DA</b> , A2, D2
3	<b>D3</b> , <b>D2A1</b> , D1A2	<b>D3</b> , <b>D2A1</b> , D1A2	<b>D3</b> , <b>D2A1</b> , D1A2	<b>D3</b> , <b>D2A1</b> , D1A2	<b>D2A1</b> , D1A2, D3, A3
4	<b>D4</b> , D3A1, D2A2, D1A3	<b>D4</b> , D3A1, D2A2	<b>D4</b> , D3A1, D2A2, D1A3	<b>D3A1</b> , D4, D2A2, D1A3	<b>D2A2</b> , D1A3, D3A1
5	<b>D5</b> , D4A1, D3A2, D2A3	<b>D4A1</b> , D3A2, D2A3	<b>D5</b> , D4A1, D3A2, D2A3, D1A4	<b>D4A1</b> , D3A2, D2A3	<b>D2A3</b> , D3A2, D1A4, D4A5
6	<b>D6</b> , D5A1, D4A2, D3A3, D2A4	<b>D5A1</b> , D4A2, D3A3	<b>D6</b> , D5A1, D4A2, D3A3	<b>D5A1</b> , D4A2, D3A3, D2A4	<b>D3A3</b> , D2A4, D4A2, D1A5
7	<b>D7</b> , D6A1, D5A2	NA.	<b>D7</b> , D6A1, D5A2, D4A3, D3A4	NA.	<b>D3A4</b> , D4A3, D5A2, D1A6

\*Chemical composition of CHOS fractions obtained after size exclusion chromatography of product mixtures generated by *BsCsn46A* from chitosans with varying F<sub>A</sub>. The bold letters represent seemingly dominant products, defined by using the signal intensities of MS (height of the peak). NA, not analyzed.

As expected, products obtained after extensive degradation of the highly acetylated F<sub>A</sub> 0.6 chitosan, contained relatively many acetylated sugars and were longer. Fully deacetylated products longer than D3 were not observed.

#### 4.4.4 CHOS sequences

To determine the sequences of hydrolytic products, CHOS were produced by degrading F<sub>A</sub> 0.3 chitosan to  $\alpha$ -values of 0.14 and 0.26, using the same condition as described in section 4.3.3, followed by SEC (Figure 4.5). The CHOS were derivatized by reductive amination of the reducing end with 2-aminoacridone, and the resulting compounds were analyzed by MS/MS, giving insights into CHOS sequences. MS1 and

MS2 spectra of CHOS after degradation of the chitosan to  $\alpha = 0.14$  are shown in Figure 4.6 and 4.7, while Figure 4.8 and 4.9 show MS1 and MS2 spectra for the  $\alpha = 0.26$  sample; the results are summarized in Table 4.2.

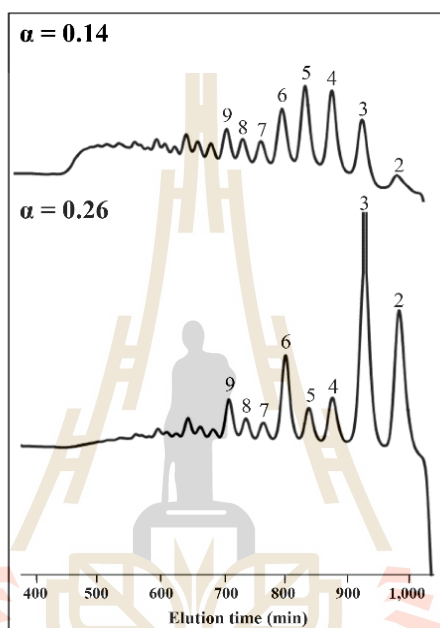


**Figure 4.5** Size distribution of CHOS for sequence analysis. Chromatograms of CHOS products after degradation of chitosan FA 0.3 with *BsCsn46A* to  $\alpha$ -values 0.14 and 0.26 at 37 °C are illustrated. These CHOS fractions were isolated for oligomer sequencing. The peaks are labeled with the DP values.

For DP3, DP4 and DP5, the MS1 spectra (Figure 4.6, 4.8) showed a dominance of fully and highly deacetylated products at  $\alpha = 0.14$  (Figure 4.6), and a shift towards products with a higher degree of acetylation at  $\alpha = 0.26$  (Figure 4.8). MS1 spectra for the hexamer were similar at  $\alpha = 0.14$  and  $\alpha = 0.26$ , with a dominance of products carrying two or three acetylations. This is probably due to the fact that intermediate products of this length (hexameric) and with a higher fraction of D are

good substrates and thus rapidly cleaved. Somewhat unexpectedly, the dominating dimer at  $\alpha = 0.14$  was DA (dominating sequence DA), whereas at  $\alpha = 0.26$  the dominating dimer was DD, as expected. A plausible explanation is that *BsCsn46A* is endo-acting, i.e. has multiple subsites (see section 4.4.5) and may thus not be very active on shorter intermediate substrates, which is needed to generate dimeric products. Additionally, one would have to assume that when the substrates become short the enzyme prefers an A to be bound in its -1 subsite (on polymeric substrates, the enzyme cleaves preferably after D, as clearly shown by  $^1\text{H-NMR}$  in Figure 4.1).

MS2 spectra (Figure 4.7, 4.9) showed that for DP3 and DP4, the reducing ends of mono-acetylated accumulating products primarily contained an A, although small amounts of CHOS with D on the reducing end were also observed (Table 4.2). Similarly, di-acetylated CHOS (D1A2, D2A2) also primarily showed a dominance of acetylated reducing ends (Table 4.2). Apparently, the -1 subsite of this chitosanase can harbor an A quite well, as also shown by the  $^1\text{H-NMR}$  data for samples with  $\alpha > 0.1$  (Figure 4.1). MS2 analysis of DP5 and DP6 CHOS was not performed due to the complexity of these samples.

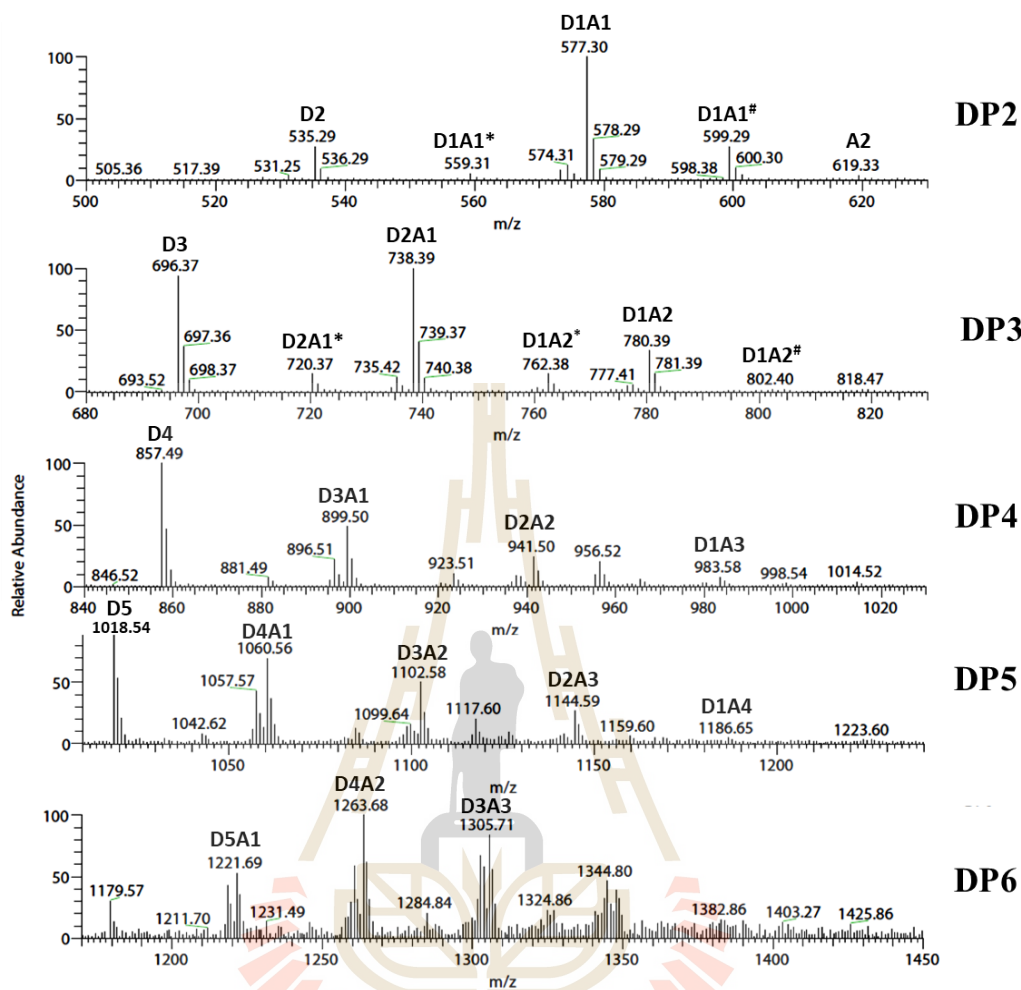


**Figure 4.6** MS1 spectra of AMAC labeled products. Chitosan F<sub>A</sub> 0.3 was degraded to  $\alpha = 0.14$  before the CHOS was separated by SEC. Peaks corresponding to different DP was isolated, labeled at the reducing end with AMAC and analyzed with MS. All masses represent the mass of the CHOS plus hydrogen and AMAC. A \* indicates loss of water, while a # indicates a sodium adduct.

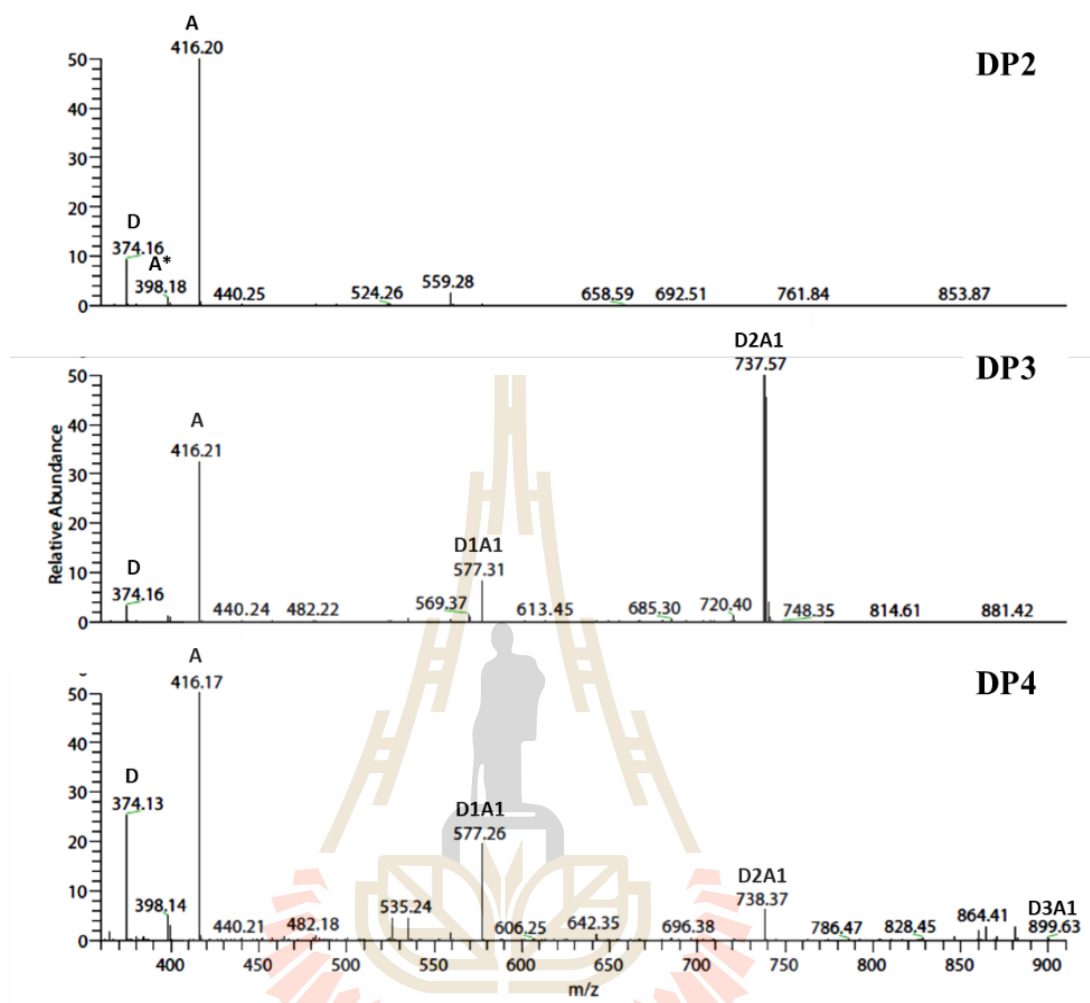


**Figure 4.7** MS2 spectra of AMAC labeled mono-acetylated products. Chitosan  $F_A$  0.3 was degraded to  $\alpha = 0.14$  before SEC. Peaks corresponding to different DP separated the CHOS was isolated, labeled at the reducing end with AMAC and analyzed with MS. Parent ions for mono-acetylated CHOS was isolated and fractionated to decide the sequence. MS2 spectra represented by CHOS with DP2 (parent ion 577.3, D1A1), DP3 (parent ion 738.4, D2A1), and DP4 (parent ion 899.5, D3A1). All masses represent the mass of the CHOS plus hydrogen and AMAC. An asterisk (\*) indicates loss of water.

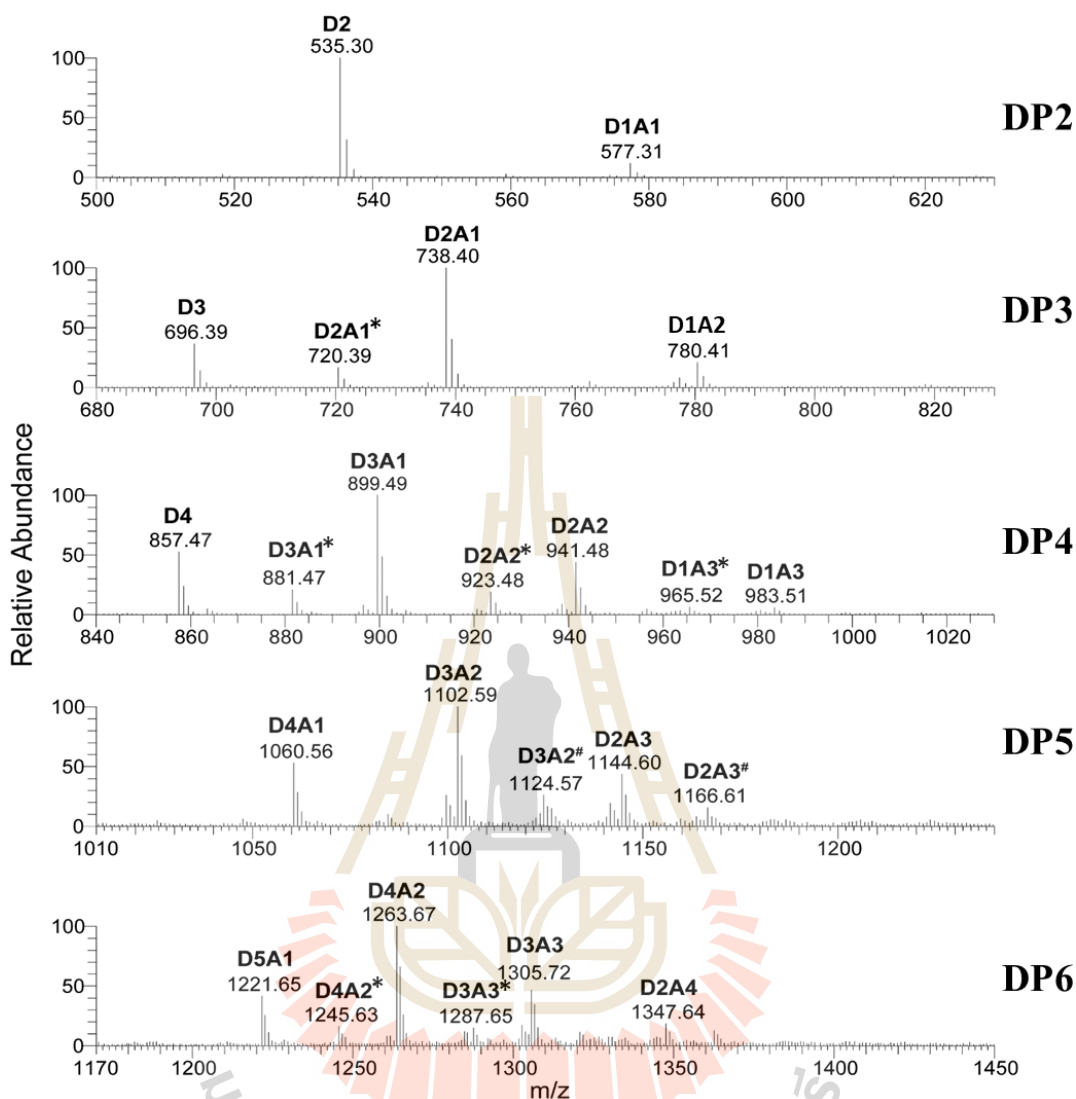


**Figure 4.8** MS1 spectra of AMAC labeled products. Chitosan FA 0.3 was degraded to  $\alpha = 0.26$  before the CHOS was separated by SEC. Peaks corresponding to different DP was isolated, labeled at the reducing end with AMAC and analyzed with MS. All masses represent the mass of the CHOS plus hydrogen and AMAC. A \* indicate loss of water, while a # indicates a sodium adduct.

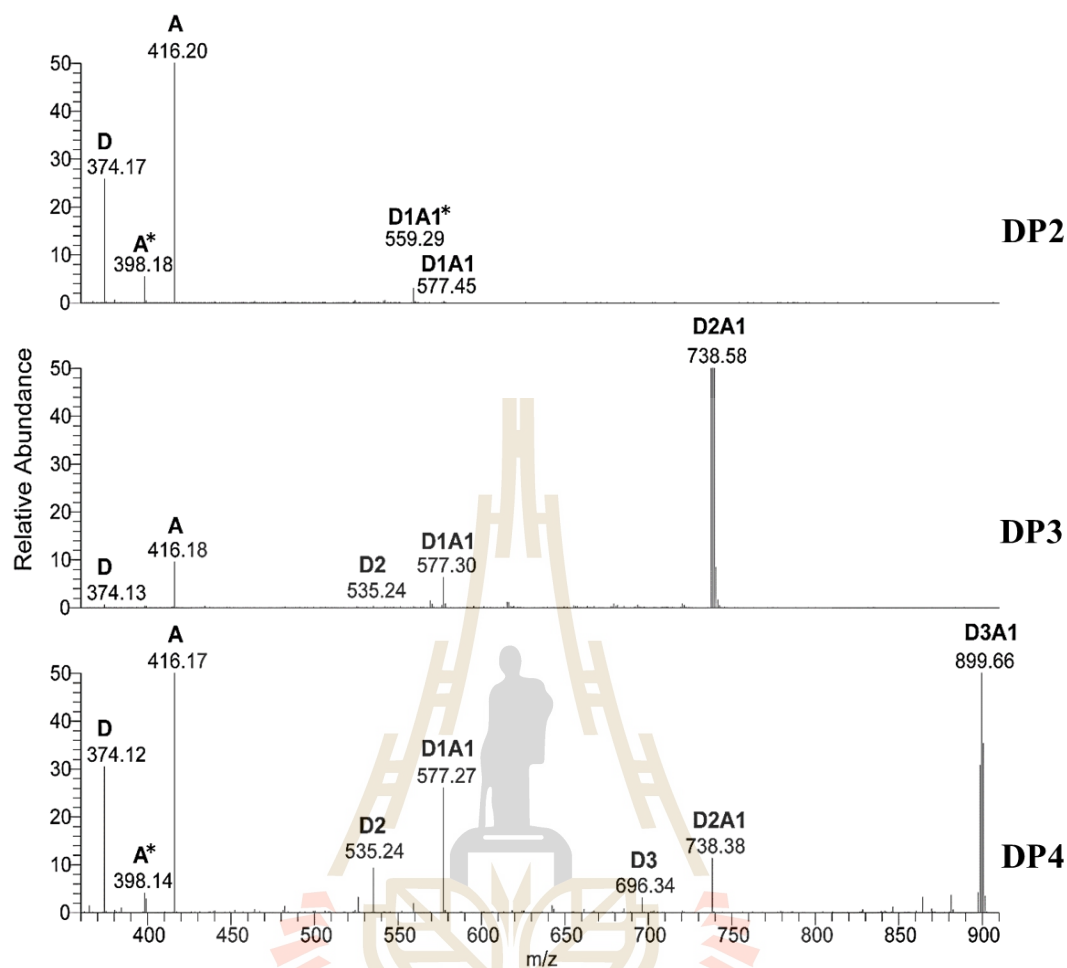


**Figure 4.9** MS2 spectra of AMAC labeled mono-acetylated products. Chitosan  $F_A$  0.3 was degraded to  $\alpha = 0.26$  before SEC. Peaks corresponding to different DP separated the CHOS was isolated, labeled at the reducing end with AMAC and analyzed with MS. Parent ions for mono-acetylated CHOS was isolated and fractionated to decide the sequence. MS2 spectra represented by CHOS with DP2 (parent ion 577.3, D1A1), DP3 (parent ion 738.4, D2A1), and DP4 (parent ion 899.5, D3A1). All masses represent the mass of the CHOS plus hydrogen and AMAC. An asterisk (\*) indicates loss of water.

The sequencing data do not allow firm statements concerning residue preferences in the +1 subsite (i.e. the subsite where the non-reducing end of a to-be formed intermediate product binds). Still, the fact that partially acetylated products

accumulating early in the reaction tend to have an A at their reducing end and a D at their non-reducing end suggests that the +1 subsite has a stronger preference for D than the -1 subsite.

**Table 4.2** Sequences of isolated CHOS\*

Degree of scission ( $\alpha$ )	Degree of polymerization								
	DP2		DP3		DP4		DP5	DP6	
	MS1 peak	Sequence from MS2	MS1 peak	Sequence from MS2	MS1 peak	Sequence from MS2	MS1 peak	MS1 peak	
0.14	D1A1	<b>DA</b> AD	D2A1	<b>DDA</b> DAD	D4	<b>DDDD</b> <b>DDDA</b>	D5 D4A1	<b>D4A2</b> D3A3	
	D2	DD		ADD	D3A1	DDAD			D3A2
	A2	AA	D3	<b>DDD</b>		ADDD	D2A3	D6	
	D1A2			D1A2	<b>ADA</b>	D2A2	DADD	D1A4	
					DAA		<b>DADA</b>		
					AAD		<b>DDAA</b>		
							<b>ADDA</b>		
					D1A3	NA.			
0.26	D2	<b>DD</b>	D2A1	<b>DDA</b>	D3A1	<b>DDDA</b>	D3A2 D4A1	<b>D4A2</b> D5A1	
	D1A1	<b>DA</b> AD		ADD		DDAD			D2A3
	D1A2			D1A2	D3	<b>DDD</b>	ADDD	D2A4	
						<b>ADA</b>	<b>AADA</b>		
						DAA	<b>ADAA</b>		
						AAD	<b>AAAD</b>		
						D1A3	<b>ADDA</b> <b>DDAA</b> <b>DADA</b>		
					D2A2	ADAD DAAD			
					D4	<b>DDDD</b>			

\*Analysis of CHOS sequences obtained after size exclusion chromatography of  $F_A$  0.3 chitosan hydrolyzed with *BsCsn46A* to  $\alpha$ -value 0.14 and 0.26. The isolated CHOS (DP2 to DP6) were labeled with AMAC. The oligomer sequences were determined using MS. Sequences in bold are the dominating sequences based on the

relative intensity of MS2 signals. MS2 sequence analysis of DP5 and DP6 CHOS was not performed due to the complexity of these samples.

#### 4.4.5 Substrate positioning in the active site of *BsCsn46A*

The preferred productive binding modes of *BsCsn46A* were studied by degradation of (GlcN)<sub>5</sub> and (GlcN)<sub>6</sub> in H<sub>2</sub><sup>18</sup>O followed by product detection using MALDI-TOF-MS (Figure 4.10). Product analysis was carried out when approximately 20% of the substrate was converted, and reactions were set up such as to minimize reaction and sample handling times to prevent anomeric equilibrium being reached. During the hydrolysis reaction, an <sup>18</sup>O atom is incorporated into the anomeric center (C1) of the newly formed reducing end, i.e. the sugar bound in subsite -1. Short reaction and sample handling times are needed because, due to the anomeric equilibrium, eventually all reducing ends will carry <sup>18</sup>O (Hekmat et al. 2010). Comparison of the ratios of otherwise identical <sup>18</sup>O- and <sup>16</sup>O-containing products in the MALDI-TOF MS analysis will therefore provide insight into how the substrate was bound while being cleaved. The trimer generated from (GlcN)<sub>5</sub> was almost exclusively (GlcN)<sub>3</sub> <sup>18</sup>O (Figure 4.10, right panel) indicating that the productive binding mode is mainly from subsite -3 to +2 (Figure 4.11, upper panel). For (GlcN)<sub>6</sub>, the mass spectrometry data indicated three productive binding modes, from subsite -4 to +2, -3 to +3 and -2 to +4. It must be noted that, while we use “subsite -4” and “subsite +4” for convenience, such subsites, extending beyond subsites -3 to +3, have not been described for GH46 chitosanases and are thus hypothetical; these “subsites” may in fact be regions of weak affinity for the substrate rather than true subsite-like binding pockets for a sugar unit. Comparison of the signals for (GlcN)<sub>4</sub>-<sup>18</sup>O and (GlcN)<sub>4</sub>-<sup>16</sup>O indicates that productive binding in subsites -4 to +2 is more common than productive binding in subsites -2 to +4, with an

approximate 60:40 ratio (Figure 4.11, lower panel). Thus, there seems to be some difference in substrate binding affinity between these hypothetical -4 and +4 subsites. Equal amounts of  $(\text{GlcN})_3\text{-}^{16}\text{O}$  and  $(\text{GlcN})_3\text{-}^{18}\text{O}$  indicate productive binding of  $(\text{GlcN})_6$  to subsites -3 to +3. While it is not possible to make a direct quantitative comparison of the three binding modes (since the MS is not fully quantitative), the data shown in Figure 4.10 suggest that the three binding modes, involving subsites -4 to +2, -3 to +3 or -2 to +4, have quite similar frequencies. To our knowledge the present study is the first example of subsite mapping in a chitosanase using  $^{18}\text{O}$ -labelled water.

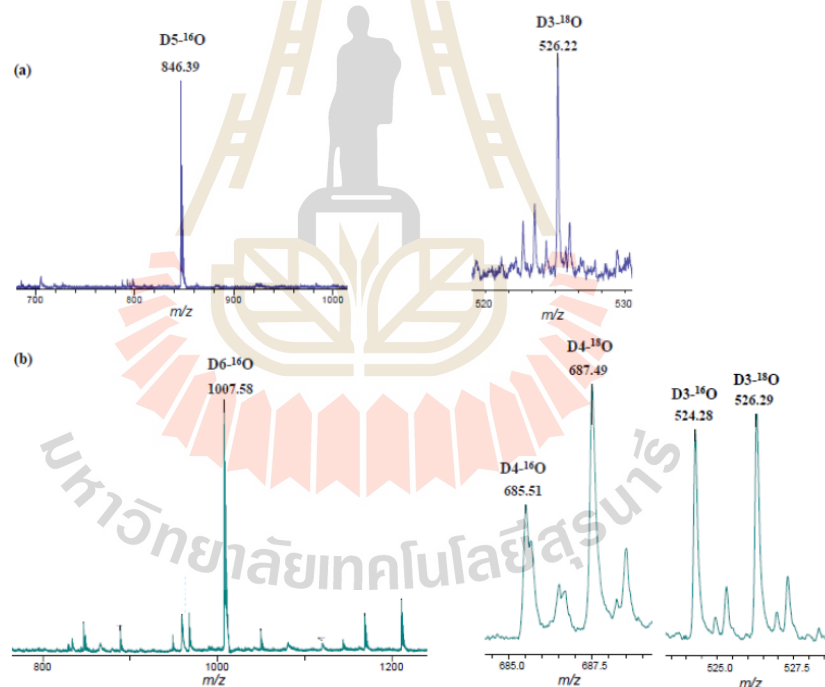


**Figure 4.10** MALDI-TOF-MS analysis of  $(\text{GlcN})_5$  and  $(\text{GlcN})_6$  degradation. Products generated from  $(\text{GlcN})_5$  (panel a) and  $(\text{GlcN})_6$  (panel b) in  $\text{H}_2^{18}\text{O}$  are illustrated. The left panel shows the substrate, while key hydrolysis products with  $^{16}\text{O}$  and  $^{18}\text{O}$  are shown in the right panel. GlcN is abbreviated as D. All labeled peaks are sodium adducts. Dimeric products were not shown.

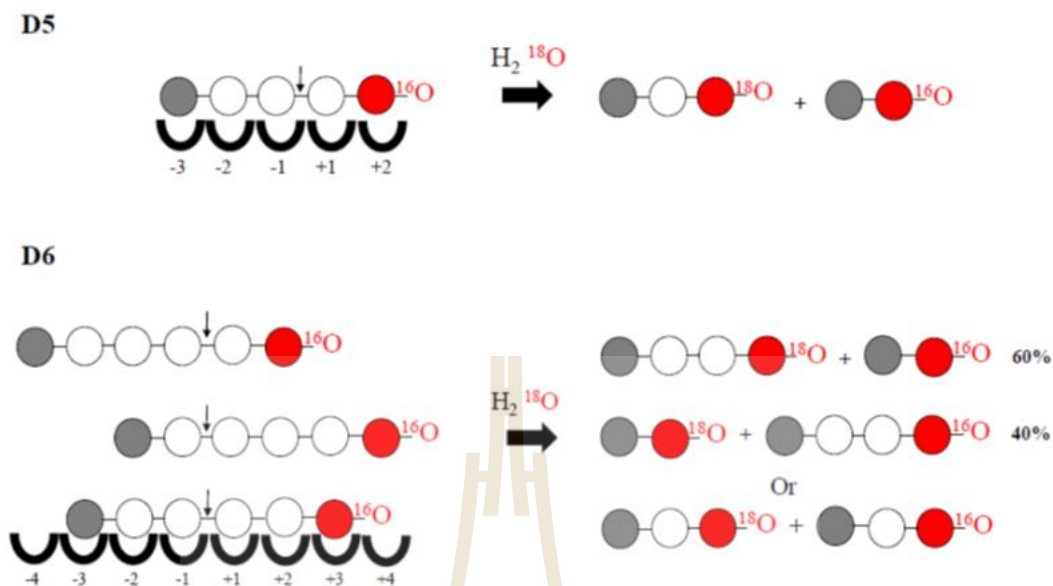


**Figure 4.11** Productive binding modes of *BsCsn46A*. Cleavages of (GlcN)<sub>5</sub> and (GlcN)<sub>6</sub> as derived from experiments with H<sub>2</sub><sup>18</sup>O are depicted. The proposed binding modes and their frequencies were derived from signal intensities (height of the peak) in MALDI-TOF-MS. Grey, red and white circles represent non-reducing end, reducing end and internal GlcN units.

## 4.5 Conclusions

*BsCsn46A* can efficiently convert chitosans with different degrees of acetylation into mixtures of CHOS with varying chain lengths and compositions, depending on the substrate and the reaction conditions. There are clear functional differences between *BsCsn46A* and other chitosanases, including the well-characterized and closely related *ScCsn46A* and a clearly different enzyme from the GH75 family, *SaCsn75A*. Several of these differences are discussed above and Table 4.3 provides a summary of key properties of the three enzymes, which all act in a non-processive endo fashion.

Importantly, *BsCsn46A* is easy to produce (Pechsrichuang et al. 2016) and displays high specific activity. Thus, as suggested before, this enzyme seems a useful tool for industrial conversion of chitosans to different CHOS composition, which may have a variety of biological activities (Aam et al. 2010, Muanprasat and Chatsudthipong 2017) and may find several applications.

**Table 4.3** Properties of three well-characterized chitosanases

Enzyme	Reference	GH family	Subsite specificity <sup>1)</sup>			Initial dominating tetramer <sup>2)</sup>	Degradation of chitosan $F_A$ 0.31-0.32 <sup>3)</sup>		
			-2	-1	+1		Initial rate (min <sup>-1</sup> )	Maximum $\alpha$ -value	DP of dominating end products <sup>4)</sup>
<i>BsCsn46A</i>	This study	46	D/A	D/A	D/A	DDDD	$8.4 \times 10^3$	0.31	2-3
<i>ScCsn46A</i>	(Heggset et al., 2010)	46	D/A	D/A	D/A	DDDD	325	0.44	1-3
<i>SaCsn75A</i>	(Heggset et al., 2012)	75	D/A	A/D	D	DDDA	6.5	0.27	2-4

<sup>1)</sup> In the cases where both A- and D-units productively bind to a subsite, the preferred sugar is printed in a larger font. Note that the enzymes show subtle variations in subsite specificity that are not visible in this Table; more details can be found in the references.

<sup>2)</sup> *BsCsn46A*,  $F_A = 0.30$  chitosan,  $\alpha = 0.11$ ; *ScCsn46A*,  $F_A = 0.32$  chitosan,  $\alpha = 0.10$ ; *SaCsn75A*,  $F_A = 0.31$  chitosan,  $\alpha = 0.07$ . <sup>3)</sup> The chitosans used had slightly varying  $F_A$ , as indicated in footnote 2. <sup>2)</sup> The range shown comprises the highest peak in the SEC chromatogram and its two neighbouring peaks. In the case of *BsCsn46A*, no monomer was detected whereas the tetramer peak was very low; hence a range of 2-3.

## 4.6 References

- Aam, B. B., Heggset, E. B., Norberg, A. L., Sørli, M., Vårum, K. M. and Eijsink, V. G. H. (2010). Production of chitooligosaccharides and their potential applications in medicine. **Marine Drugs** 8(5): 1482-1517.
- Bahrke, S., Einarsson, J. M., Gislason, J., Haebel, S., Letzel, M. C., Peter-Katalinić, J. and Peter, M. G. (2002). Sequence analysis of chitooligosaccharides by matrix-assisted laser desorption ionization postsorce decay mass spectrometry. **Biomacromolecules** 3(4): 696-704.
- Eide, K. B., Lindbom, A. R., Eijsink, V. G. H., Norberg, A. L. and Sørli, M. (2013). Analysis of productive binding modes in the human chitotriosidase. **FEBS Letters** 587(21): 3508-3513.
- Fukamizo, T., Ohkawa, T., Ikeda, Y. and Goto, S. (1994). Specificity of chitosanase from *Bacillus pumilus*. **Biochimica et Biophysica Acta (BBA)/Protein Structure and Molecular Enzymology** 1205: 183-188.
- Heggset, E. B., Dybvik, A. I., Hoell, I. A., Norberg, A. L., Sørli, M., Eijsink, V. G. H. and Vårum, K. M. (2010). Degradation of Chitosans with a Family 46 Chitosanase from *Streptomyces coelicolor* A3(2). **Biomacromolecules** 11(9): 2487-2497.
- Heggset, E. B., Hoell, I. A., Kristoffersen, M., Eijsink, V. G. H. and Vårum, K. M. (2009). Degradation of Chitosans with Chitinase G from *Streptomyces coelicolor* A3(2): Production of chito-oligosaccharides and insight into subsite specificities. **Biomacromolecules** 10(4): 892-899.
- Heggset, E. B., Tuveng, T. R., Hoell, I. A., Liu, Z., Eijsink, V. G. H. and Vårum, K. M. (2012). Mode of Action of a Family 75 Chitosanase from *Streptomyces avermitilis*. **Biomacromolecules** 13(6): 1733-1741.

- Hekmat, O., Lo Leggio, L., Rosengren, A., Kamarauskaite, J., Kolenova, K. and Stålbrand, H. (2010). Rational Engineering of Mannosyl Binding in the Distal Glycone Subsites of *Cellulomonas fimi* Endo- $\beta$ -1,4-mannanase: Mannosyl Binding Promoted at Subsite -2 and Demoted at Subsite -3. **Biochemistry** 49(23): 4884-4896.
- Horn, S. J., Sørbotten, A., Synstad, B., Sikorski, P., Sørli, M., Vårum, K. M. and Eijsink, V. G. H. (2006). Endo/exo mechanism and processivity of family 18 chitinases produced by *Serratia marcescens*. **FEBS Journal** 273(3): 491-503.
- Horn, S. J., Sørli, M., Vaaje-Kolstad, G., Norberg, A. L., Synstad, B., Vårum, K. M. and Eijsink, V. G. H. (2006). Comparative studies of chitinases A, B and C from *Serratia marcescens*. **Biocatalysis and Biotransformation** 24(1-2): 39-53.
- Ishiguro, K., Yoshie, N., Sakurai, M. and Inoue, Y. (1992). A  $^1\text{H}$  NMR study of a fragment of partially *N*-deacetylated chitin produced by lysozyme degradation. **Carbohydrate Research** 237(Supplement C): 333-338.
- Itoh, Y., Kawase, T., Nikaidou, N., Fukada, H., Mitsutomi, M., Watanabe, T. and Itoh, Y. (2002). Functional Analysis of the Chitin-binding Domain of a Family 19 Chitinase from *Streptomyces griseus* HUT6037: Substrate-binding Affinity and Dominant Increase of Antifungal Function. **Bioscience, Biotechnology, and Biochemistry** 66(5): 1084-1092.
- Khoushab, F. and Yamabhai, M. (2010). Chitin Research Revisited. **Marine Drugs** 8(7): 1988.
- Koga, D., Yoshioka, T. and Arakane, Y. (1998). HPLC Analysis of Anomeric Formation and Cleavage Pattern by Chitinolytic Enzyme. **Bioscience, Biotechnology, and Biochemistry** 62(8): 1643-1646.

- Morelle, W., Canis, K., Chirat, F., Faid, V. and Michalski, J.-C. (2006). The use of mass spectrometry for the proteomic analysis of glycosylation. **Proteomics** 6(14): 3993-4015.
- Muanprasat, C. and Chatsudthipong, V. (2017). Chitosan oligosaccharide: Biological activities and potential therapeutic applications. **Pharmacology & Therapeutics** 170: 80-97.
- Pechsrichuang, P., Songsiriritthigul, C., Haltrich, D., Roytrakul, S., Namvijitr, P., Bonaparte, N. and Yamabhai, M. (2016). OmpA signal peptide leads to heterogenous secretion of *B. subtilis* chitosanase enzyme from E. coli expression system. **SpringerPlus** 5(1): 1200.
- Pechsrichuang, P., Yoohat, K. and Yamabhai, M. (2013). Production of recombinant *Bacillus subtilis* chitosanase, suitable for biosynthesis of chitosan-oligosaccharides. **Bioresource Technology** 127: 407-414.
- Purushotham, P., Sarma, P. V. S. R. N. and Podile, A. R. (2012). Multiple chitinases of an endophytic *Serratia proteamaculans* 568 generate chitin oligomers. **Bioresource Technology** 112(Supplement C): 261-269.
- Sannan, T., Kurita, K. and Iwakura, Y. (1975). Studies on chitin, 1. Solubility change by alkaline treatment and film casting. **Die Makromolekulare Chemie** 176(4): 1191-1195.
- Sørbotten, A., Horn, S. J., Eijsink, V. G. H. and Vårum, K. M. (2005). Degradation of chitosans with chitinase B from *Serratia marcescens*. **FEBS Journal** 272(2): 538-549.
- Stefanidi, E. and Vorgias, C. E. (2008). Molecular analysis of the gene encoding a new chitinase from the marine psychrophilic bacterium *Moritella marina* and

biochemical characterization of the recombinant enzyme. **Extremophiles** 12(4): 541-552.

Takasuka, T. E., Bianchetti, C. M., Tobimatsu, Y., Bergeman, L. F., Ralph, J. and Fox, B. G. (2014). Structure-guided analysis of catalytic specificity of the abundantly secreted chitosanase SACTE\_5457 from *Streptomyces* sp. SirexAA-E. **Proteins: Structure, Function, and Bioinformatics** 82(7): 1245-1257.

Tsukada, S. and Inoue, Y. (1981). Conformational properties of chito-oligosaccharides: titration, optical rotation, and carbon-13 N.M.R. studies of chito-oligosaccharides. **Carbohydrate Research** 88(1): 19-38.

Vårum, K. M., Antohonsen, M. W., Grasdalen, H. and Smidsrød, O. (1991). Determination of the degree of *N*-acetylation and the distribution of *N*-acetyl groups in partially *N*-deacetylated chitins (chitosans) by high-field n.m.r. spectroscopy. **Carbohydrate Research** 211(1): 17-23.

Viens, P., Lacombe-Harvey, M.-È. and Brzezinski, R. (2015). Chitosanases from Family 46 of Glycoside Hydrolases: From Proteins to Phenotypes. **Marine Drugs** 13(11): 6566.

Xia, W., Liu, P., Zhang, J. and Chen, J. (2011). Biological activities of chitosan and chitooligosaccharides. **Food Hydrocolloids** 25(2): 170-179.

# CHAPTER V

## BIOLOGICAL ACTIVITY OF CHITO-OLIGOSACCHARIDE

### 5.1 Abstract

Chito-oligosaccharides (CHOS) are oligomers of D-glucosamine and *N*-acetylglucosamine, derived from chitosan or chitosan degradation. The primary aim of this study is to investigate the modulatory effects of various degrees of acetylation of CHOS on neuroprotection and autophagy modulation in human neuroblastoma SH-SY5Y cells, which has not been previously reported. CHOS with various fractions of acetylation,  $F_A$  (0.15, 0.3 and 0.6) were prepared by enzymatic hydrolysis using recombinant *Bacillus subtilis* chitosanase (*BsCsn46A*) or improved mutant of *Bacillus licheniformis* chitinase (*ChiA3*). The CHOS products were characterized by  $^1\text{H-NMR}$ , size exclusion chromatography, and mass spectrometry. *In vitro* analysis on a model cell line for neuronal function and differentiation, SH-SY5Y indicated that CHOS at concentrations ranging from 100-1,000  $\mu\text{g/ml}$  showed no cytotoxicity to the cells. The influence of CHOS on oxidative stress and apoptosis was also examined. SH-SY5Y cells were pretreated with CHOS for 24 hours prior to challenging with 0.7 mM paraquat (neurotoxic agent) for another 12 hours. The pretreatment of CHOS resulted in the reduction of apoptotic cells and intracellular reactive oxidation species. In addition, the mRNA expression level of anti-apoptotic gene *BCL2* was increased when compared with paraquat. Besides, the expression of antioxidant gene, superoxide dismutase (*SOD*)

was also upregulated after pretreatment with CHOS for 6 hours. Investigation of the effect of CHOS on autophagy indicated that the expression of autophagy-associated genes were altered upon the CHOS treatment for 6 h. SH-SY5Y treated with F<sub>A</sub> 0.3 CHOS showed an increase in the mRNA expression of *ATG5* and *LC3 I/II*. Moreover, the structural protein of autophagosomal membrane (*LC3I/II*) was detected by immunofluorescence staining. Detection of the structural protein of autophagosomal membrane (*LC3I/II*) by immunofluorescent staining indicated that CHOS treatment led to high fluorescence intensity when compared with the untreated. Moreover, autophagosome accumulation was also detected by using monodansylcadaverine (MDC) staining and the results indicated that autophagosome was accumulated after incubated with various acetylated CHOS at a concentration of 100 and 1,000 µg/ml. Analysis of autophagic flux by immunoblotting of *LC3 I/II* and *P62* demonstrated that CHOS with F<sub>A</sub> 0.6 shows the highest effect. In conclusion, this study suggested that CHOS could upregulate autophagy and effectively protect human neuroblastoma SH-SY5Y cells from a neurotoxic agent and CHOS with different degree of acetylation could have different effects. This highlights the potential use of CHOS as a neuroprotective agent in the future.

**Keywords:** Chitooligosaccharides, Neuroblastoma, Autophagy, Antioxidant, Apoptosis

## 5.2 Introduction

Chitooligosaccharides or chitosan oligomers can be produced enzymatically or chemically from chitosans. Chitosans are linear heteropolymers of  $\beta$  (1 $\rightarrow$ 4) linked *N*-acetyl-D-glucosamine and its deacetylated counterpart D-glucosamine (GlcN). Enzymatic methods for the hydrolysis of chitosan involve the use chitosanases and chitinase. This method is performed in gentle conditions and the MW distribution of the CHOS mixtures could be controlled.

Chitosanases and chitinases are chitosan- and chitin-degrading enzymes. Chitosanase or chitosan *N*-acetylglucosaminohydrolase (EC 3.2.1.132) catalyzes the hydrolysis of glycosidic bond of chitosan into chitooligosaccharide. Chitinase (EC3.2.1.14) is the enzymes responsible for chitin degradation. Both of the enzyme can hydrolyze D-A and A-D linkages. However, chitinases have the ability to hydrolyzed A-A linkage, but not D-D linkage and this property distinguishes these enzymes from chitosanases (Heggset et al. 2009, Aam et al. 2010, Heggset et al. 2010, Pechsrichuang et al. 2018). These hydrolytic enzymes vary with regard to their specific cleavage sites, which are determined by sequences in heteropolymers of A and D units. Thus, different patterns of chitosans and hydrolytic enzymes will produce CHOS mixtures with different both length and sequence. In this study, we prepared CHOS with various fractions of acetylation,  $F_A$  (0.15, 0.3 and 0.6) by enzymatic hydrolysis using recombinant *Bacillus subtilis* chitosanase (*BsCsn46A*) (Pechsrichuang et al. 2018) or mutated *Bacillus licheniformis* chitinase (*ChiA3*), which has been improved by DNA shuffling technique (Songsiriritthigul et al. 2009).

CHOS have received growing attention because these oligosaccharides have low viscosity, biocompatible, water soluble at the neutral pH and possess numerous potential

interesting biological properties (Muanprasat and Chatsudthipong 2017) . However, most of the molecular mechanisms behind these bioactivities are still unknown. It has been suggested that the properties of CHOS such as degree of deacetylation (DDA), degree of polymerization (DP), charge distribution, and nature of chemical modification are important factors influencing the biological activities of CHOS (Aam et al., 2010).

Autophagy is an intracellular self-degradation process conserved from yeast to mammals (Levine and Klionsky 2004). Autophagy occurs as a cellular response including nutrient or growth factor deprivation, hypoxia, reactive oxygen species, DNA damage, protein aggregates, damaged organelles or intracellular pathogens (Kroemer et al. 2010). It can be classified into different types such as macroautophagy, microautophagy and chaperone-mediated autophagy (Mizushima and Komatsu 2011). A predominant form of autophagy is macroautophagy (henceforth called autophagy) that degrades cytoplasmic components including proteins, organelles, and even some invasive bacteria (Horie et al. 2017). Autophagy can be morphologically characterized by formation of double-membrane formation autophagosomes, cup-shaped autophagosome (Menzies et al. 2017). During autophagy activation, the autophagosome encloses cytoplasmic materials and fuses with lysosome and then degrade enclosed cytoplasmic materials, allowing cells to eliminate damaged or harmful components through catabolism and recycling to maintain nutrient and energy homeostasis (Li et al. 2013). Therefore, autophagy is necessary to maintain the normal function of the central nervous system, preventing the accumulation of misfolded and aggregated proteins. Impairment of autophagy in neurons can result in accumulation of misfolded and aggregated proteins, which stimulate the inclusion bodies or extracellular plaques. Cellular aggregations of misfolded proteins are cause of many neurodegenerative

diseases, including Alzheimer's disease, Parkinson's disease and Huntington's disease (Ciechanover and Kwon 2015). The neuroprotective effect of CHOS has been tested in neuron cells (Zhou et al. 2008, Dai et al. 2013, Huang et al. 2015). In this study, we investigated the neuroprotective effect of various degrees of acetylation of CHOS from paraquat induced neurotoxicity and its mechanism of autophagy modulation in SH-SY5Y cells.

## 5.3 Material and Method

### 5.3.1 Chitosans

Chitosan  $F_A$  0.15, molecular weight (MW<sub>n</sub>) of approximately 37 kDa, was provided by Tera Vennrensing (Kløfta, Norway). Chitosan  $F_A$  0.3, MW<sub>n</sub> approximately 200-400 kDa., was purchased from Heppe Medical chitosan GmbH (Germany). Highly acetylated chitosan  $F_A$  0.6 was prepared by homogenous de-*N*-acetylation of chitin from shrimp shells (Chitonor, Senjahopen, Norway) according to previously described method (Sannan, Kurita et al. 1975, Vårum, Antohonsen et al. 1991).

### 5.3.2 Chitoooligosaccharide production and analysis

CHOS with various fractions of acetylation,  $F_A$  (0.15, 0.3 and 0.6) were prepared by enzymatic hydrolysis using recombinant *Bacillus subtilis* chitosanase (*BsCsn46A*) (Pechsrichuang et al. 2013) or recombinant mutated *Bacillus licheniformis* chitinase (*ChiA3*) (Songsiriritthigul et al. 2009). Production of CHOS was modified from our previous work (Pechsrichuang et al. 2018). Briefly, one gram of chitosans with different degree of acetylation ( $F_A$  0.15, 0.3 and 0.6) were dissolved in 1% HCl containing 0.1 mg BSA/mL substrate. Then, pH was adjusted to 5.5 using 1M NaOH. Chitosan solutions (final concentration of 10 mg/mL) were pre-incubated in incubator

shaker at 37 °C. The degradation reactions  $F_A$  0.15 and  $F_A$  0.3 chitosan were started by adding 0.5  $\mu\text{g}$  of chitosanase from *Bacillus subtilis* (*BsCsn46A*) per mg of chitosan. To obtain the maximum degradation of chitosans and degrade all of polymer, same amount of enzyme was added more at 6 and 24 h and further incubated for 24 h. For high acetylated  $F_A$  0.6 chitosan, the degradation reactions were started by adding 0.1  $\mu\text{g}$  of mutated chitinase from *Bacillus licheniformis* ChiA3 per mg of chitosan. To obtain the maximum degradation of chitosans, more enzyme (0.1  $\mu\text{g}$  of ChiA3 per mg chitisan) was added at 6 h and further incubated for 18 h.

Samples were taken from the reactions at various time points from 10 min to 2,880 min. The reaction was stopped by adding 1M HCl and heated at 100°C for 3 mins. Then, the samples were concentrated and dried by using speed vacuum. Next, the samples were dissolved in D<sub>2</sub>O (Deuterium oxide or heavy water) or 0.15 M ammonium acetate, pH 4.5 for further <sup>1</sup>H-NMR or size exclusion chromatography (SEC) analysis, respectively. To obtain the maximum degradation of chitosans, 0.5  $\mu\text{g}$  of *BsCsn46A* was added per mg of chitosan and the degradation reaction was incubated at 37°C 1,440 min. The extent of chitosan degradation is given as degree of scission,  $\alpha$  (= 1/average degree of polymerization,  $DP_n$ ), which represents the fraction of glycoside bonds that has been cleaved (Sørbotten et al. 2005).

### 5.3.3 Size exclusion chromatography (SEC)

CHOS were separated on three XK 26 columns connected in series and packed with (Pharmacia Biotech, Uppsala, Sweden), with an overall dimension of 2.60 × 180 cm. The elution buffer used was 0.15 M ammonium acetate, pH 4.5. The elution buffer was pumped through the system using an LC-10ADvp pump (Shimadzu GmbH, Duisburg, Germany), delivering the elution buffer at a flow rate of 0.8 mL/min. The

relative amounts of oligomers were monitored with a refractive index (RI) detector (Shodex RI-101, Shodex Denko GmbH, Dusseldorf, Germany) coupled to a CR 510 Basic Data logger (Campbell Scientific Inc., Logan, UT). To characterize the isolated CHOS, fractions of 4 mL were collected using a fraction collector. For quantitative studies of degradation, typically 10 mg of degraded chitosan was injected.

#### **5.3.4 NMR spectroscopy**

Samples for  $^1\text{H-NMR}$  analysis were dissolved in  $\text{D}_2\text{O}$ , and then 1/10 and 1/100 dilution of concentrated  $\text{DCl}$  or  $\text{NaOD}$  was used to adjust the pD to 4.3 - 4.6, respectively.  $^1\text{H-NMR}$  spectra was obtained at 400 MHz at a temperature of 85 °C, as previously described (Vårum et al. 1991). The degree of scission ( $\alpha$ ) and the  $\text{DP}_n$  was calculated as previously described (Sørbotten et al. 2005).

#### **5.3.5 Analysis of CHOS by Mass spectrometry**

Identification of isolated CHOS was performed with Matrix-Assisted Laser Desorption Ionization mass spectrometry (MALDI TOF/TOF MS). MS spectra were acquired using an Ultraflex<sup>TM</sup> TOF/TOF mass spectrometer (Bruker Daltonik GmbH, Bremen, Germany) with gridless ion optics under the control of Flexcontrol. For sample preparation, 1  $\mu\text{L}$  of the reaction products was mixed with 1  $\mu\text{L}$  of 10% 2,5 dihydroxybenzoic acid (DHB) in 30% acetonitrile and spotted onto a MALDI target plate (Bahrke et al. 2002). The MS experiments were conducted using an accelerating potential of 20 kV in the reflectron mode.

#### **5.3.6 Cell culture**

Human neuroblastoma SH-SY5Y cells were maintained in DMEM (HyClone, Logan, UT) supplemented with 10% (V/V) heat-inactivated fetal bovine

serum (FBS) (HyClone, Logan, UT), 1% (V/V) L-glutamine (Gibco, CA, USA), 1% (V/V) nonessential amino acid (Gibco, CA, USA) and 100 U/ml penicillin/streptomycin (Gibco, CA, USA) in humidified incubator with 37 °C and 5% CO<sub>2</sub>.

### **5.3.7 Measurement of cell viability by (MTT) assay**

The effect of CHOS on cell viability was measured by 3-(4,5-dimethylthiazol-2-yl)-2,5-diphenyltetrazolium bromide (MTT) assay (Invitrogen). SH-SY5Y cells were seeded at  $4 \times 10^3$  cells in 96 well plate and incubated at 37 °C and 5% CO<sub>2</sub> overnight. The cells were treated with 100, 200, 500 and 1,000 µg/ml of CHOS (F<sub>A</sub> 0.15, 0.3 and 0.6) for 24 h. After incubation, culture media was removed and 100 µl of 0.5 mg/mL MTT solution in PBS was added and the cells were further incubated for 3 h. Then, the MTT solution was discarded and purple formazan crystal was dissolved in 100 µl of DMSO. The absorbance was measured at 570 nm, using a microplate reader (BMG Labtech, Ortenberg, Germany). The absorbance of untreated cells was taken as 100% viability. All experiments were performed in triplicate.

### **5.3.8 Apoptosis detection using AnnexinV and 7-AAD staining**

SH-SY5Y cells were seeded at  $4 \times 10^5$  cells in 6 well plate and incubated at 37 °C with 5% CO<sub>2</sub> for overnight. The cells were pre-treated with 1,000 µg/ml of CHOS (F<sub>A</sub> 0.15, 0.3 and 0.6), 20 µM Curcumin and DMEM with 5% FBS (untreated) for 24 h. Curcumin was used as positive control for neuroprotection (Jaronwitschawan et al. 2017). Then, the culture media was discarded and the cells were challenged with 0.7 mM paraquat (neurotoxic agent) for 12 h. The cells were harvested and washed once with PBS. Then, cells were stained with Annexin V conjugated to fluorescein-isothiocyanate (FITC) and 7-amino-actinomycin (7-AAD) (Muse Annexin V and

DeadCell Kit, Merck KGaA, Germany) for 20 minutes at room temperature in the dark. Dead cells, live cells, early and late apoptotic cells were analyzed by flow cytometry (Muse cell analyzer, Merck, Billerica, MA, USA).

### **5.3.9 Real-time quantitative reverse transcription PCR (qPCR)**

SH-SY5Y cells were plated at  $4 \times 10^5$  cells in 6 well plate and incubated at 37 °C and 5% CO<sub>2</sub> for overnight. To analyze autophagy and antioxidant gene expression, the cells were treated with DMEM with 5% FBS (untreated), DMEM without FBS (starvation), 20 µM curcumin, and 1,000 µg/ml of various degrees of acetylated CHOS (F<sub>A</sub> 0.15, 0.3 and 0.6). Starvation condition and curcumin were used as positive control for autophagy activation (Jaronwitchawan et al. 2017). For apoptosis gene expression, the cells were treated using the same condition as described in section 5.3.8. Total RNA was extracted from the treated cells using NucleoSpin RNA kit (Macherey-Nagel, Dueren Germany). According to the manufacturer's protocol, 500 ng of RNA was reverse transcribed to cDNA using RT-PCR quick master mix (Toyobo, Japan). For gene expression analysis, 100 ng of cDNA were used as template for qPCR. The qPCR was performed using the QuantStudio5 Real-Time PCR system (Thermo Fisher Scientific, USA). The relative expression levels of mRNAs were quantified by normalization with the internal control GAPDH gene. Primers used in this experiment show in Table 5.1.

**Table 5.1** qPCR primers of autophagy, antioxidant and apoptosis gene.

Gene	Direction	Primer sequence (5'to 3')
<i>ATG5</i>	Forward	actgtccatctgcagccac
	Reverse	tgcagaagaaaatggatttcg
<i>BECLIN</i>	Forward	ctcctgggtctctcctggtt
	Reverse	tggacacgagttcaagatcc
<i>LC3 I/II</i>	Forward	tatcaccgggattttgggtg
	Reverse	gagaagacctcaagcagcg
<i>P62</i>	Forward	tactctggctcccaaagcaa
	Reverse	tcaaggtccagagaaggtgg
<i>GPX</i>	Forward	ttcccgcaaccagttg
	Reverse	ttacctgcacttctcgaa
<i>CAT</i>	Forward	ttcccaggaagatcctgac
	Reverse	acctggtagatcgaatgg
<i>SOD</i>	Forward	gtgcaggtcctcactttaat
	Reverse	ctttgtcagcagtcacattg
<i>CASPASE 3</i>	Forward	agaactggactgtggcattgag
	Reverse	gcttgcggcatactgtttcag
<i>CASPASE 8</i>	Forward	ctcccaacttgctttatg
	Reverse	aagacccagagcattgtta
<i>BAX</i>	Forward	cttttctactttgccagcaaac
	Reverse	gaggccgtccaaccac
<i>BCL2</i>	Forward	tcgcatcaggaaggctaga
	Reverse	aggaccaggcctccaagct
<i>P53</i>	Forward	tcaacaagatgtttgccaactg
	Reverse	atgtgctgtgactgctttagatg

### 5.3.10 Measurement of intracellular reactive oxidation species (ROS) by

#### DCF assay

The intracellular ROS was detected using DCFH-DA which is cell-permeable and is hydrolyzed intracellularly to the DCFH carboxylate anion that is retained in the cell. The production of intracellular ROS was assessed by DCFH-DA oxidation. DCFH-DA is cleaved intracellularly by nonspecific esterases and turns into

highly fluorescent 2',7'-dichlorofluorescein (DCF) upon oxidation (Kalyanaraman et al. 2012).

The cells were treated using the same condition as described in section 5.3.8. Then, the cells were harvested and incubated with 10  $\mu$ M DCFH-DA in DMEM at 37 °C for 15 minutes. After incubation the culture media was discarded. The fluorescence intensity of DCFH-DA was measured by a fluorescence microplate-reader (Thermo Scientific, USA) at an excitation wavelength of 485 nm and an emission wavelength of 530 nm. Results were expressed as percentage of controls. All experiments were performed in triplicate.

#### **5.3.11 Detection of microtubule-associated protein 1A/1B-light chain 3 (LC3 I/II) by immunofluorescence staining**

SH-SY5Y cells were seeded at  $4 \times 10^4$  cells in 24-well plate with 12 mm glass cover slip for and cultured at 37°C and 5% CO<sub>2</sub> for 1 day. The cells were treated with DMEM with 5% FBS (untreated), DMEM without FBS (starvation), 20  $\mu$ M curcumin, 50  $\mu$ M chloroquine (CQ, autophagy inhibitor) (Redmann et al. 2017) and 1,000  $\mu$ g/ml of various degrees of acetylated CHOS (FA 0.15, 0.3 and 0.6). Starvation condition and curcumin were used as positive control for autophagy activation (Jaronwitchawan et al. 2017) while CQ were use as autophagy inhibitor that block autophagic degradation in lysosomes (Redmann et al. 2017). All of treatments were dissolved in DMEM with 5% FBS. The treated cells were incubated at 37 °C with 5% CO<sub>2</sub> for 6 h, except CQ treated cell were incubated for 3 h. Following the respective treatments, cells were fixed with 4% paraformaldehyde/PBS for 15 min at room temperature and washed 3 times with PBS. The cells were permeabilized and blocked with 0.1% Triton X-100 and 10% FBS in PBS for 1 h at room temperature. The

coverslips were then incubated with 1:1000 diluted anti-LC3I/II-rabbit primary antibody (Merck, Germany) diluted in blocking solution for overnight at 4 °C, followed by washing with PBS 3 times for 5 min each. Then, the cells were stained with anti-rabbit Alexa Flour 488 secondary antibody diluted 1:1000 in PBS and incubated at room temperature for 2 h in the dark. The nuclei were counterstained with DAPI (Vector Laboratories) and the stained cells were observed under a laser scanning confocal microscope (Nikon A1). Images were analyzed using the ImageJ program (NIH).

#### **5.3.12 Detection of autophagosome using monodansylcadaverine (MDC) staining**

SH-SY5Y cells were seeded at  $1 \times 10^4$  cells in 24-well plate with 12 mm glass cover slip and cultured at 37 °C with 5% CO<sub>2</sub> for 1 day. The cells were treated and fixed using the same condition as described in section 5.3.11. To monitor autophagosome, the cells were stained by MDC. MDC preferentially accumulates in autophagosome due to a combination of ion trapping and specific interactions with membrane lipids (Munafó and Colombo 2001). Briefly, the cells were stained with 50 µM MDA and incubated at room temperature for 20 minutes. The stained cells were washed with PBS for 3 times. The stained cells were mounted on a glass slide with a drop of antifade reagent observed under fluorescence microscope (Axioscope, Zeiss, Germany).

#### **5.3.13 Western blot analysis**

SH-SY5Y cells were seeded at  $5 \times 10^5$  cells in 6-well plate and cultured at 37 °C and 5% CO<sub>2</sub> for 1 day. The cells were incubated with DMEM with 5% FBS (untreated), DMEM without FBS (Starvation), 20 µM curcumin, 50 µM chloroquine and 1,000 µg/ml of various degrees of acetylated CHOS (F<sub>A</sub> 0.15, 0.3 and 0.6) for 6 and

24 h. The cells were harvested by adding 100  $\mu$ l of 0.25% Trypsin/EDTA and 400  $\mu$ l PBS and incubated at 37  $^{\circ}$ C, 5% CO<sub>2</sub> for 3 minutes. Then, the cells were washed twice by adding 1ml of cold PBS and collected by centrifugation at 3,000 rpm for 5 min. The cell lysate was extracted by adding 300  $\mu$ l NP40 cell lysis buffer (FNN0021, Invitrogen, USA) containing 1mM PMSF and 1x protease inhibitor cocktail (P-2714, Sigma, USA) and incubated for 30 min on ice with vortexing at 10 minutes interval. The crude lysate was collected by centrifugation at 13,000 g for 10 minutes at 4  $^{\circ}$ C. The protein concentrations were determined by BCA protein assay kit (Pierce) using BSA standards. Then, 20  $\mu$ g of total protein per sample was separated by 12.5% SDS-PAGE, followed by wet electroblotting (Biorad) to a PVDF membrane at voltage 100 V for 2h and western blotting. Anti-LC3-I/II Antibody (ACB293, Merck), P62/SQSTM1 Antibody (MAB8028, R & D systems) and Anti-GAPDH (ABS16, Merck) were used as primary antibodies. Goat Anti-rabbit IgG, HRP-conjugate (12-348, Upstate biotechnology) and Goat anti mouse HRP conjugated (Promega) antibodies were used as secondary antibody. The western blots were developed using selected chemiluminescence (ECL) detection kit (Amersham, Bucks., U.K.).

## 5.4 Results

### 5.4.1 Production and characterization of CHOS

<sup>1</sup>H-NMR spectroscopy was used to determined average degree of polymerization (DP<sub>n</sub>) and the degree of scission ( $\alpha$ ), that is the fraction of glycosidic linkages in the chitosan that has been cleaved by the enzymes (Sørbotten et al. 2005). The time course of hydrolysis of various degrees of acetylated chitosan show in figure 5.2. Chitosans with F<sub>A</sub> 0.15 and 0.3 were hydrolyzed with chitosanase *BsCsn46A* to  $\alpha$ =

0.37 and 0.30, respectively (Figure 5.1A). In addition, the  $F_A 0.6$  chitosan was hydrolyzed by ChiA3 from *Bacillus licheniformis* to  $\alpha = 0.45$  (Figure 5.1B).

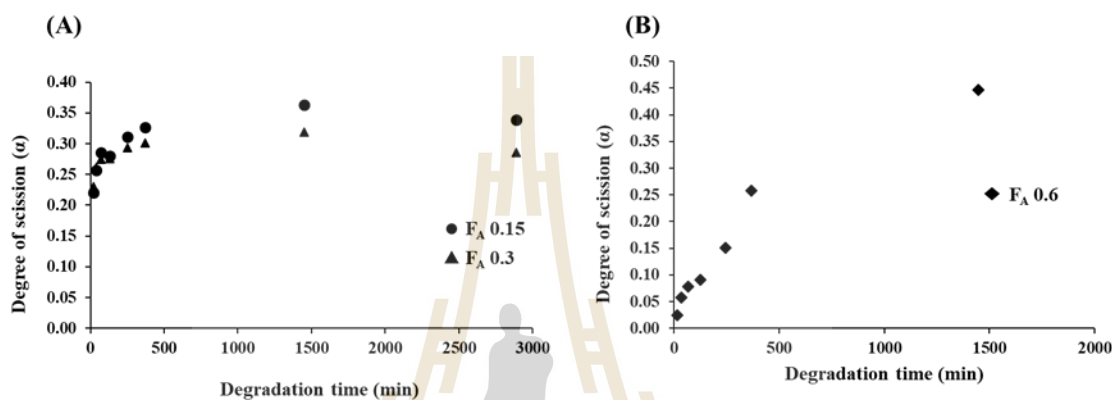


**Figure 5.1** Time-course for the increase in  $\alpha$  during degradation of chitosans with  $F_A 0.15$  or  $F_A 0.3$  with *BsCsn46A* (A) and  $F_A 0.6$  with ChiA3 (B). The graphs show the degree of scission ( $\alpha$ ) determined by  $^1\text{H-NMR}$ .

In addition, information about the identity of the new reducing ends (A- or D- units), which reveals information about the productive binding preference in the -1 subsite of the enzyme was identified proton NMR. The  $^1\text{H-NMR}$  spectra of the anomer region of chitosans with  $F_A 0.15$ ,  $F_A 0.3$  and  $F_A 0.6$  degraded by *BsCsn46A* or ChiA3 show in figure 5.2. The spectra show the large majority of the new reducing end of chitosan with  $F_A 0.15$  and 0.3 hydrolyzed by *BsCsn46A* are D-unit at -1 subsite, while  $F_A 0.6$  cleaved by ChiA3 are A-units.

After enzymatic hydrolysis, CHOS mixtures were separated by size exclusion chromatography (SEC) as show in Figure 5.3. The chromatograms indicated the size distribution of oligomers obtained after degradation of various degrees of

acetylated chitosans at two  $\alpha$ -values. From the SEC chromatograms of  $F_A 0.15$  and  $0.3$  at 1,440 min, the void peak ( $DP > 50$ ) still appears (Figure 5.3, upper panel). To degrade all of polymer, more enzyme was added and further incubated for 24 h. Consequently, the polymer peak disappears as the reaction proceeds. As expected, the major products of  $F_A 0.15$  and  $0.3$  CHOS were DP2-6 (Figure 5.3A, lower panel) and 2-12 (Figure 5.3B, lower panel), respectively. While, the majority of  $F_A 0.6$  CHOS produced from ChiA3 was DP2-6 (Figure 5.3C, lower panel).

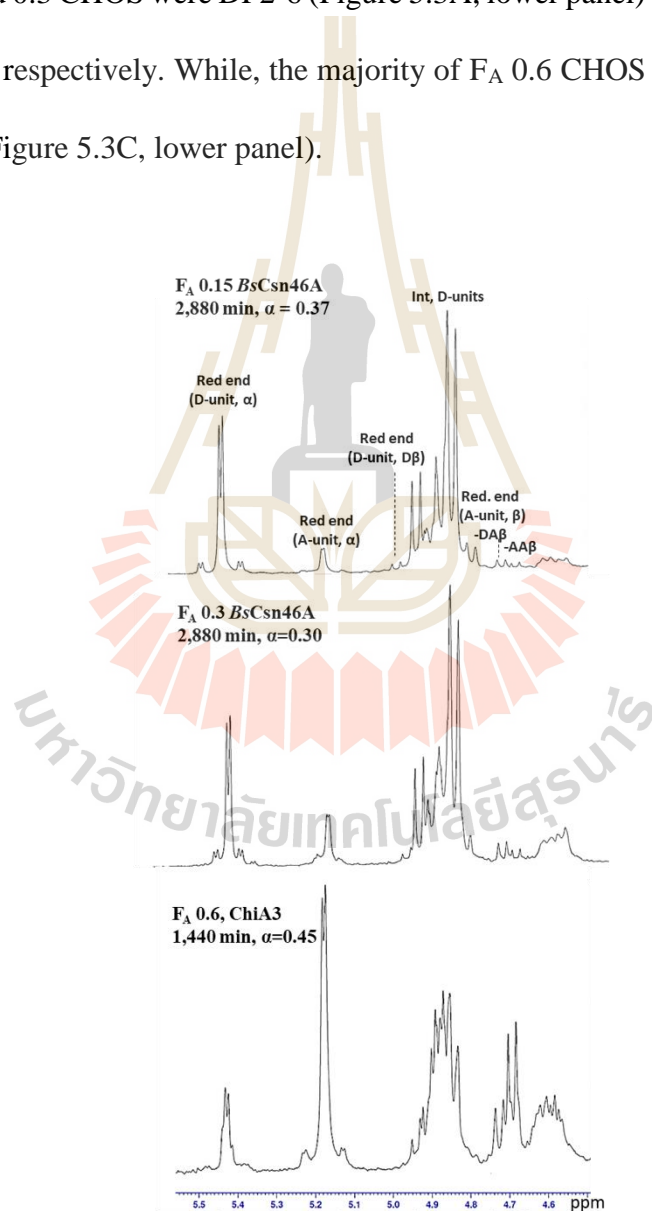


**Figure 5.2**  $^1\text{H-NMR}$  analysis of CHOS preparation.  $^1\text{H-NMR}$  spectra of the anomeric region of chitosans with  $F_A 0.15$ ,  $F_A 0.3$  and  $F_A 0.6$  hydrolyzed by

*BsCsn46A* or *ChiA3*. The  $\alpha$ -values (degree of scission) are indicated. A reducing end D-unit resonates at 5.43 ppm ( $\alpha$ -anomer) and 4.92 ppm ( $\beta$ -anomer). The  $\alpha$ -anomer of a reducing end A-unit resonates at 5.19, while the  $\beta$ -anomer appears as two doublets at 4.705 ppm ( $-AA$ ) and 4.742 ppm ( $-DA$ ), depending on whether the preceding sugar unit is an A or a D, respectively. Internal D-units resonate at 4.8–4.95 ppm, whereas internal A-units resonate at 4.55–4.68 (Sørbotten et al. 2005).

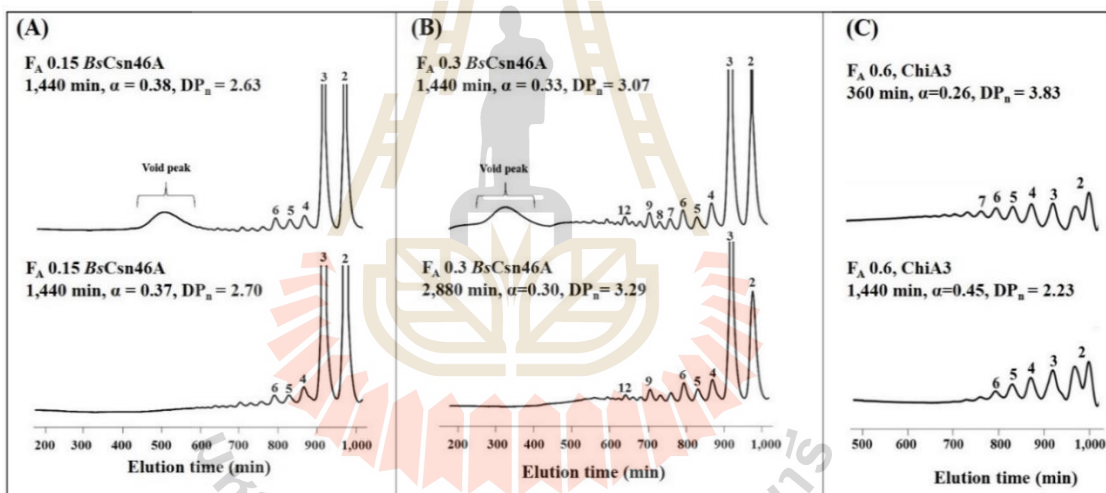


**Figure 5.3** Product analysis by size exclusion chromatography (SEC). Size distribution of CHOS after degradation of three different chitosans at 37 °C using *BsCsn46A* for  $F_A$  0.15 and 0.3, and *ChiA3* for  $F_A$  0.6. The peaks are labeled by numbers indicating the DP.

The chemical compositions of individual CHOS fractions obtained after degradation of chitosans with  $F_A$  values of 0.15, 0.3, or 0.6 were analyzed by MALDI-TOF-MS and the results are summarized in Table 5.2. Confirming our previous reported, the hydrolytic products obtained from of  $F_A$  0.15 and 0.3 chitosan hydrolyzed

by *BsCsn46A* contained fully deacetylated oligomer as the main products and  $F_A$  0.3 chitosan were more A-unit products (Pechsrichuang et al. 2018). For the products obtained from highly acetylated  $F_A$  0.6 chitosan hydrolyzed by ChiA3, contained slightly more A-rich products. However, the difference between *BsCsn46A* and ChiA3 hydrolytic products is the majority of reducing end sugar residues in the oligomeric fractions which are D- and A-unit, respectively.

**Table 5.2** Chemical composition of CHOS fractions<sup>a</sup>.

DP	$F_A$ 0.15	$F_A$ 0.3	ChiA3 $F_A$ 0.6
	$\alpha = 0.37$	$\alpha = 0.30$	$\alpha = 0.45$
2	<b>D2</b> , DA, A2	<b>D2</b> , DA, A2	<b>D2</b> , DA, A2
3	<b>D3</b> , D2A1, D1A2	<b>D2A1</b> , D3, D1A2	<b>D1A2</b> , D2A1, D3, A3
4	<b>D3A1</b> , D2A2, D4, D1A3	<b>D3A1</b> , D2A2, D1A3	<b>D2A2</b> , D3A1, D1A3
5	<b>D4A1</b> , D3A2, D2A3	<b>D3A2</b> , D2A3, D1A4	<b>D3A2</b> , D2A3, D4A1, D1A4
6	<b>D4A2</b> , D3A3, D2A4	<b>D3A3</b> , D2A4, D4A2, D1A5	<b>D4A2</b> , D3A3, D5A1, D2A4
7	<b>D5A2</b> , D4A3, D3A4	<b>D4A3</b> , D3A4	ND

<sup>a</sup>Chemical composition of CHOS fractions obtained after size exclusion chromatography of product mixtures generated by *BsCsn46A* or ChiA3 from chitosans with varying  $F_A$ . The bold letters represent seemingly dominant products, defined by using the signal intensities of MS (height of the peak). NA, not analyzed.

#### 5.4.2 Cytotoxicity of CHOS

Cytotoxicity of CHOS ( $F_A$  0.15, 0.3 and 0.6) were determined using MTT assay. The cells were treated with different concentration of CHOS (100-1,000  $\mu\text{g/ml}$ ) for 24 h. MTT result shows that the cells remained their viability similar to untreated cells (Figure 5.4A). Therefore, those concentrations of CHOS were used for all experiments.

### 5.4.3 CHOS reduced paraquat-induced intracellular ROS and apoptosis in SH-SY5Y cells

To examine the pretreatment of CHOS affected on the generation of intracellular ROS induced by paraquat, the intracellular ROS level was assessed by using DCFH-DA. SH-SY5Y cells were pretreated with 1,000  $\mu\text{g}/\text{ml}$  CHOS for 24 hours prior to challenging with 0.7 mM paraquat for another 12 hours. The pretreatment of CHOS resulted in a significant reducing the intracellular ROS induced by paraquat when compared with paraquat alone (Figure 5.4B). Moreover, the apoptotic cells death also reduced, from 9.5% of paraquat alone to 3.42%, 3.74% and 5.82% after pretreated the cells with  $F_A$  0.15, 0.3 and 0.6 CHOS, respectively (Figure 5.4C).

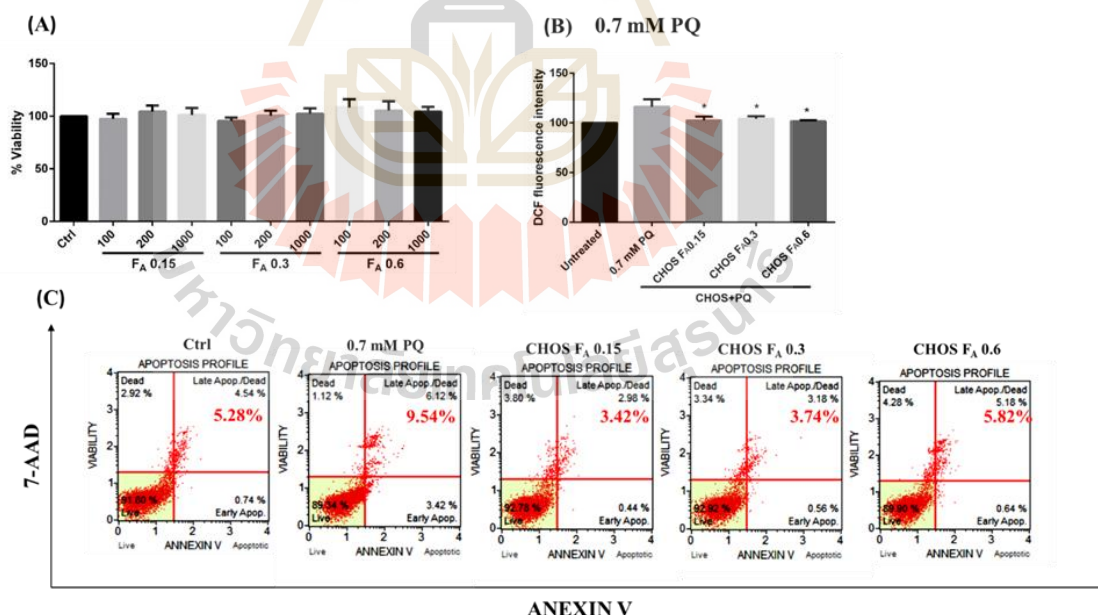


**Figure 5.4** Protective effect of CHOS on paraquat-induced neuronal cell death in SH-SY5Y cell. (A) Cells were treated with 100-1,000  $\mu\text{g}/\text{ml}$  CHOS ( $F_A$  0.15, 0.3 and 0.6) for 24 h. Cell viability was detected by MTT assay. (B) Cell were pretreated with 1,000  $\mu\text{g}/\text{ml}$  CHOS and exposed to 0.7 mM paraquat.

The intracellular reactive species was measured by DCF assay and the percentage of apoptotic cell was measured by using AnnexinV and 7-AAd staining. The data were represented as mean  $\pm$ SD (n=3). \*p<0.05 versus untreated. (C) Apoptosis detection using AnnexinV and 7-AAd staining.

#### **5.4.4 Effect of CHOS on apoptosis related gene expression exposed to paraquat and antioxidant gene expression in SH-SY5Y**

SH-SY5Y cells were pretreated with 1,000  $\mu$ g/ml CHOS ( $F_A$  0.15, 0.3 and 0.6) for 24 h prior to challenging with 0.7 mM paraquat for another 12 h. After the cells were treated, the relative expression of apoptosis genes, *P53*, *BAX*, *CASPASE8*, *CASPASE3* and *BCL2* were determined by qPCR. The gene expression level of apoptosis related genes including *P53*, *BAX*, *CASPASE8*, *CASPASE3* and *BCL2* were increased in all treatments when compared with control (Figure 5.5A-E). However, the ratio of *BAX* (a pro-apoptotic) gene and *BCL2* (anti-apoptotic gene) was significantly decreased (Figure 5.5F) when pretreated with various degrees of acetylated CHOS, indicating that the apoptosis was inhibited.

The expression of the key antioxidant genes including, *SOD* (superoxide dismutase), *CAT* (catalase) and *GPX* (glutathione peroxidase) also determined. The result shows that *SOD* upregulated after the cells were treated with various acetylated CHOS with concentrations 100 or 1,000  $\mu$ g/ml for 6 hours (Figure 5.6 A). While, *CAT* increased when treated with 1,000  $\mu$ g/ml  $F_A$  0.15 CHOS and *GPX* expression was not difference from the control (Figure 5.6 B,C). These results indicated that CHOS could be reduced apoptotic cell death of SH-SY5Y cells from paraquat through apoptosis inhibition and its functioned as antioxidant.

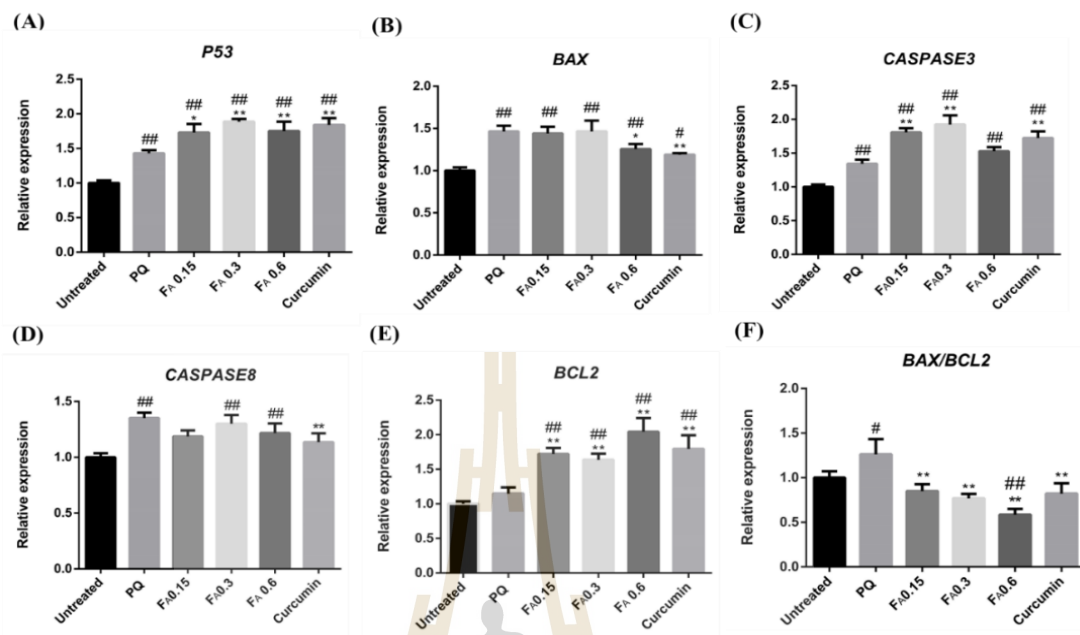


**Figure 5.5** Protective effect of CHOS on paraquat-induced neuronal cell death in SH-SY5Y cell. SH-SY5Y cell were pretreated with DMEM with 5% FBS (untreated), 1,000  $\mu\text{g/ml}$  of CHOS (FA 0.15, 0.3 and 0.6) and 20  $\mu\text{M}$  curcumin for 24 h and challenged with 0.7 mM paraquat for 12 h. The relative expression of apoptosis genes, *P53*, *BAX*, *CASPASE8*, *CASPASE3* and *BCL2* were calculated by using *GAPDH* as a reference gene. The data were represented as mean  $\pm$ SD (n=3). #p<0.05, ##p<0.01 versus untreated. \*p<0.05, \*\*p<0.01 versus the group exposed to paraquat alone.

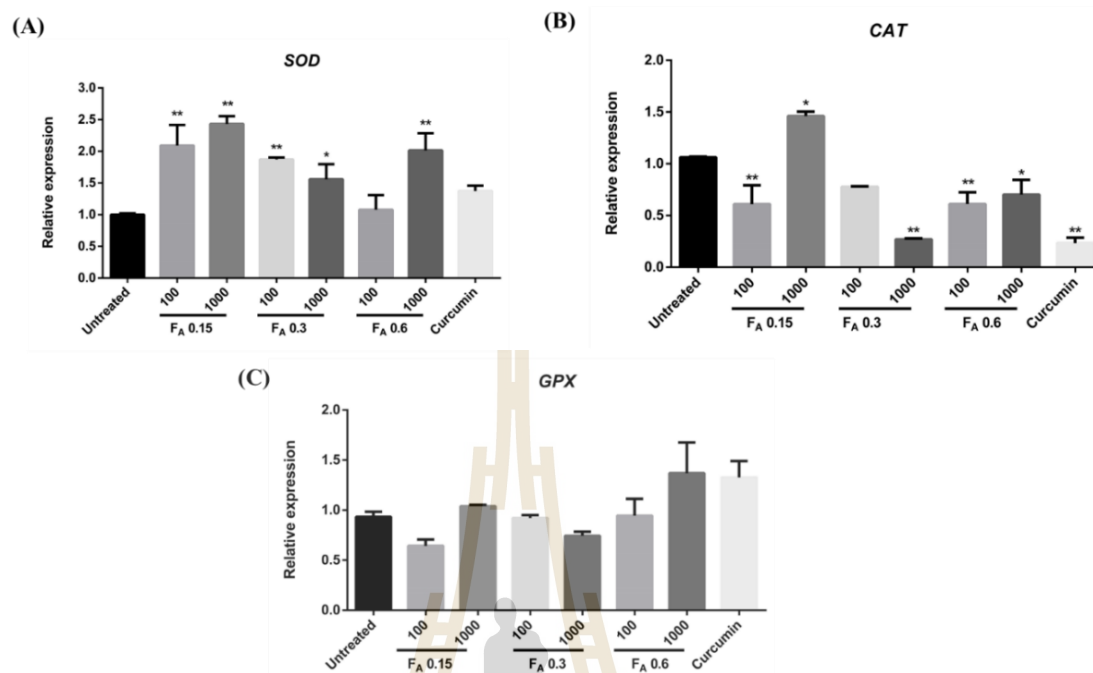


**Figure 5.6** Analysis of antioxidant gene expression by qPCR. SH-SY5Y cells were treated with DMEM with 5% FBS (untreated), 100 and 1,000 µg/ml of CHOS (F<sub>A</sub> 0.15, 0.3 and 0.6) and 20 µM curcumin for 6 h. The relative expression of *SOD*, *CAT* and *GPX* were calculated by using *GAPDH* as a reference gene. The data were represented as mean ±SD (n=3). \*p<0.05, \*\*p<0.01 versus untreated.

#### 5.4.5 CHOS induced autophagy in SH-SY5Y cells

Autophagy (or self-eating) was first described by Christian de Duve in 1963 as a lysosome-mediated degradation process for non-essential or damaged cellular constituents (De Duve 1963). Autophagy breaks down macromolecules and recycles their components not only to preserve cellular energy but also to clear damaged proteins and mitochondria (Dodson et al. 2013). Impairment of autophagy is cause many pathologies, including neurodegenerative diseases (Schapira and Gegg 2011). To

examine the effect of CHOS on autophagy, SH-SY5Y cells were incubated with 1,000  $\mu\text{g/ml}$  of various degrees of acetylated CHOS ( $F_A 0.15$ , 0.3 and 0.6).

The autophagy related genes including *ATG5*, *BECLIN*, *LC3 I/II* and *P62* were monitored by using qPCR. We observed that the cells treated with  $F_A 0.3$  CHOS significantly increased the mRNA expression of *ATG5* and *LC3 I/II*. While,  $F_A 0.3$  and 0.6 CHOS was not different from the untreated cell (Figure 5.7).

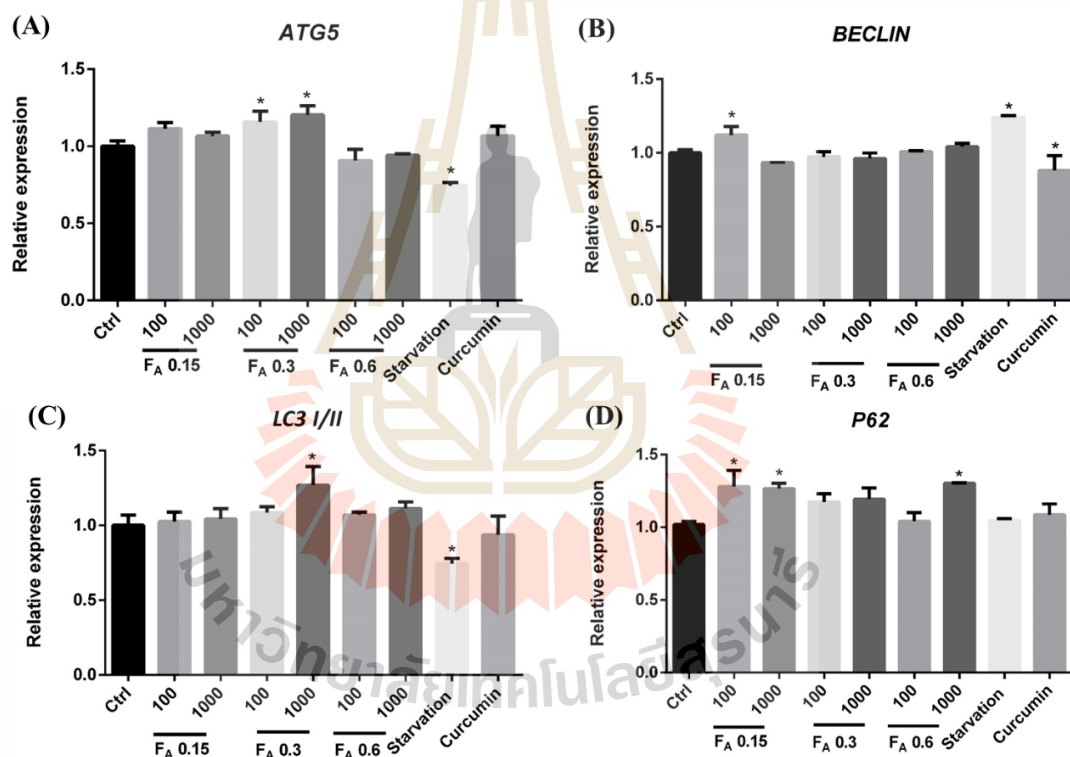


**Figure 5.7** Analysis of autophagy gene expression by qPCR. SH-SY5Y cells were treated with DMEM with 5% FBS (untreated), 100 and 1,000  $\mu\text{g/ml}$  of CHOS ( $F_A 0.15$ , 0.3 and 0.6), DMEM without FBS (starvation) and 20  $\mu\text{M}$  Curcumin for 6 h. The relative expression of *ATG5*, *BECLIN*, *LC3 I/II* and *P62* were calculated by using *GAPDH* as a reference gene. The data were represented as mean  $\pm$ SD (n=3). \*p<0.05 versus untreated.

However, the structural protein of autophagosomal membrane (*LC3/III*) was detected by immunofluorescence staining (Figure 5.8A). The result shows that all CHOS treated SH-SY5Y cells presented high fluorescence intensity when compared with the untreated cells (Figure 5.8B). The cells treated with CQ showed an enhanced *LC3/III* protein accumulation, indicating a defective autophagy. While, CHOS, curcumin and DMEM without serum (starvation) treated SH-SY5Y cells exhibited an enhancement and well organization of *LC3/III* protein.

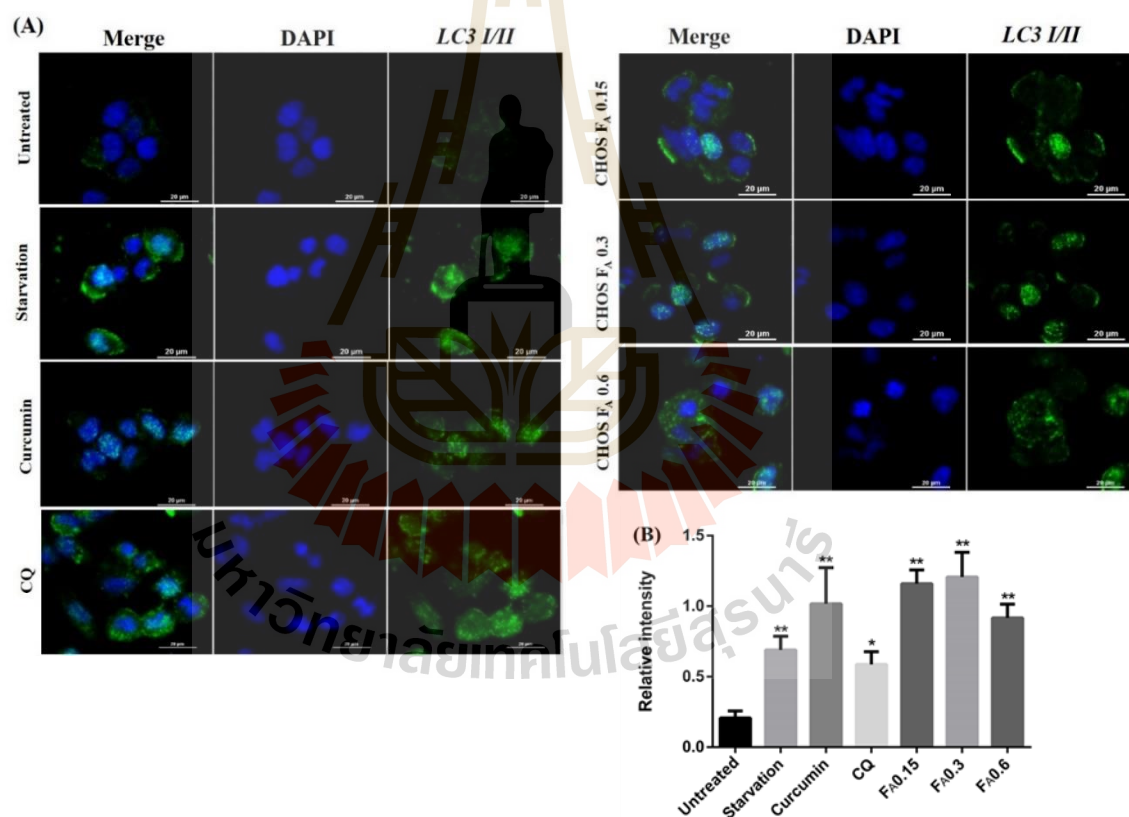


**Figure 5.8** Effect of CHOS on *LC3/III* protein expression. The cells were pre-treated with DMEM with 5% FBS (untreated), DMEM without FBS (Starvation), 20 μM Curcumin, 50 μM CQ and 1,000 μg/ml of various degrees of acetylated CHOS (F<sub>A</sub> 0.15, 0.3 and 0.6). The treated cells were incubated at 37 °C with 5% CO<sub>2</sub> for 6 h, except CQ treated cell were incubated for 3

h. Following this incubation period, the cells were stained with MDC at 50  $\mu\text{M}$ . Cells were analyzed by confocal microscopy as described in materials and methods. (A) Confocal images of *LC3/III* protein stained with Alexa 488 dye by immunofluorescence assay. (B) The fluorescence intensity of *LC3 III* normalized with DAPI. The data were represented as mean  $\pm$ SD (n=3). \*p<0.05, \*\*p<0.01 versus untreated.

To monitor autophagosome, the cells were stained by MDC that preferentially accumulates in autophagosome due to a combination of ion trapping and specific interactions with membrane lipids (Munafó and Colombo 2001). The result shows that all of the samples increased the accumulation of autophagosome (Figure 5.9).

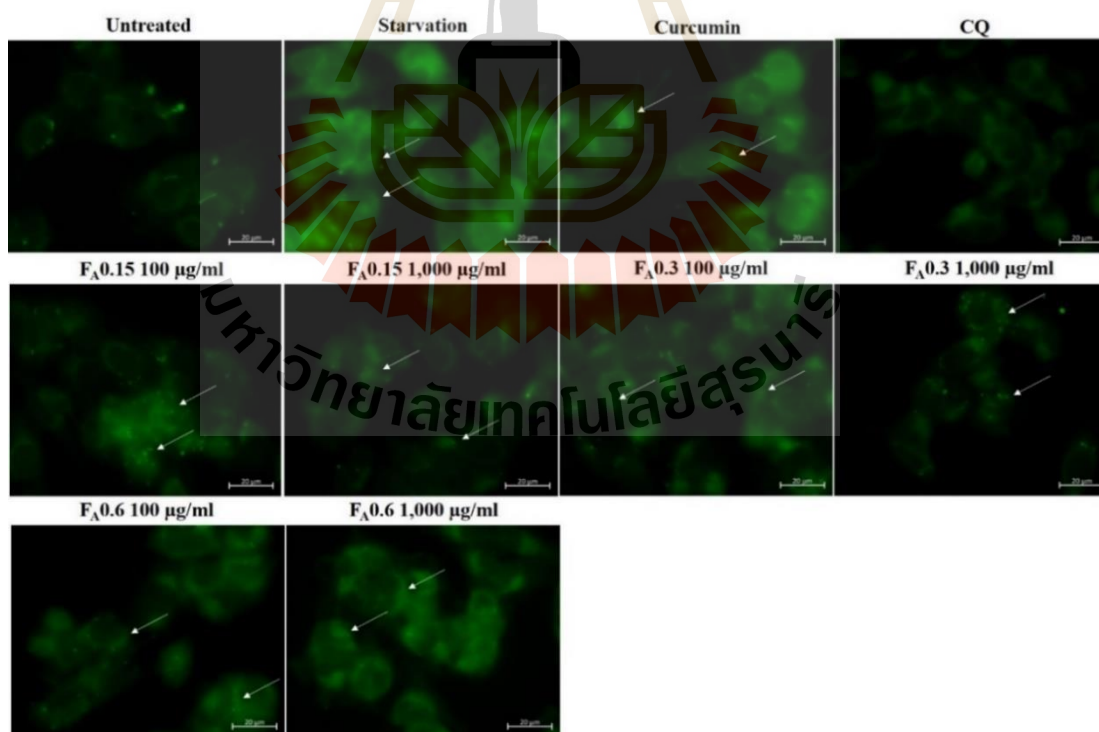


**Figure 5.9** MDC-labeled autophagosome. The cells were pre-treated with DMEM with 5% FBS (untreated), DMEM without FBS (Starvation), 20  $\mu\text{M}$  Curcumin, 50  $\mu\text{M}$  CQ and 1,000  $\mu\text{g/ml}$  of various degrees of acetylated

CHOS ( $F_A$  0.15, 0.3 and 0.6). The treated cells were incubated at 37 °C with 5%  $CO_2$  for 6 h, except CQ treated cell were incubated for 3 h. Following this incubation period, the cells were stained with MDC at 50  $\mu$ M. Cells were analyzed by fluorescence microscopy. The arrow indicated the accumulation of autophagosome.

The immunoblot analysis of *LC3 I/II* and *P62* or *SQSTM1* were used as marker for autophagic flux analysis (Jiang and Mizushima 2015). *LC3-I* is cytosolic protein, and *LC3-II* is conjugated with phosphatidylethanolamine (PE) and is presented in autophagosome membrane (Kabeya et al. 2004). The *P62* or sequestosome 1 (*SQSTM1*) is also important since it is a substrate for *LC3* which facilitates selective degradation during autophagy. The *P62* protein is itself degraded by autophagy and serves as a marker to study autophagic flux. When autophagy is inhibited, *P62* accumulates, while when the autophagy is induced, *P62* quantities decrease (Komatsu et al. 2007). In this study, the autophagic flux was monitored by immunoblotting of *LC3 I/II* and *P62*, CHOS with  $F_A$  0.6 shows the best effect for autophagy induction (Figure 5.10). The result shows that *LC3 I* upregulated and *P62* downregulated after incubation with 1,000  $\mu$ g/ml  $F_A$ 0.6 CHOS for 6 h. While,  $F_A$  0.15 and 0.3 CHOS upregulated only *LC3 I* (Figure 5.10B). For prolonged incubation at 24 h, the expression level of *LC3 I/II* protein increased in  $F_A$ 0.3, 0.15 CHOS, DMEM serum free (starvation), and 20  $\mu$ M Curcumin (Figure 5.10E). Whereas, the relative expression of *P62* increased when compared with untreated (Figure 5.10F). However, the expression level of *P62* protein at 24 h was decreased when compared to 6 h (Figure 5.10A,B).

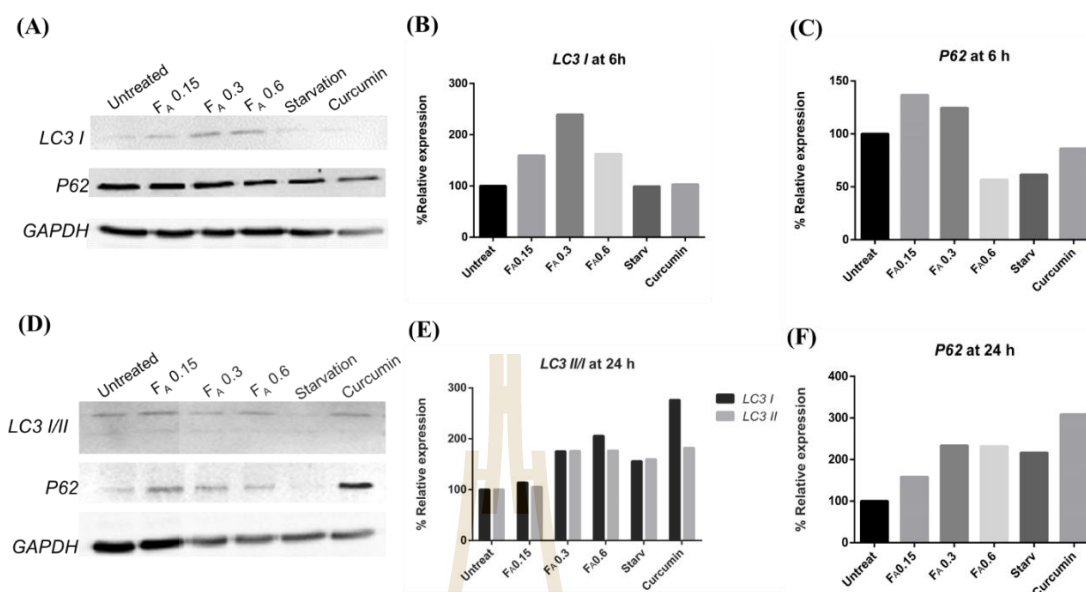


**Figure 5.10** Expression level of *LC3 I/II* and *P62* determined by western blotting.

GAPDH was used as the internal control. The cells were incubated with DMEM with 5% FBS (untreated), DMEM without FBS (starvation), 20  $\mu$ M curcumin, 1,000  $\mu$ g/ml of various degrees of acetylated CHOS ( $F_A$  0.15, 0.3 and 0.6) for 6 and 24 h. Western blots of *LC3 I/II* (B,E) and *P62* (C,F) were quantified by densitometry using Quantity one program.

## 5.5 Discussion and conclusion

CHOS was previously reported to possess many biological activities such as antibacterial, antioxidant, anti-diabetic, anti-inflammatory, and neuroprotective activities (Aam et al. 2010, Muanprasat and Chatsudthipong 2017). There have been many researches of CHOS on the neuroprotection and antioxidant. Huang et al, 2015 reported that CHOS attenuate  $\text{Cu}^{2+}$  induced cellular oxidative damage and cell apoptosis involving Nrf2 activation in SH-SY5Y cell (Huang et al. 2015). The protective effect of CHOS on primary culture of hippocampal neurons against glutamate-induced

neurotoxicity also reported (Zhou et al. 2008). Moreover, the neuroprotective effect of CHOS from  $\beta$ -amyloid peptide induced neurotoxicity, involving the suppression of ROS production and apoptosis in primary hippocampal neurons was also reported (Dai et al. 2013). However, most of the research on molecular mechanism of CHOS has been done with CHOS mixtures with various  $F_A$ ,  $M_w$ , and DP. Consequently, when using complex mixtures of CHOS in biological activity assays, it is difficult to know which molecule/molecules are causing the effects.

In this study, we investigated the effect of well-defined CHOS with various degrees of acetylation ( $F_A$  0.15, 0.3 and 0.6) on neurotoxicity, oxidative stress and apoptosis related gene changes induced by paraquat and autophagy modulation. The paraquat is a quaternary nitrogen herbicide capable of generating oxidative stress and producing brain damage after chronic exposure (Czerniczyniec et al. 2013).

We examine the protective effect of CHOS against paraquat. Our results show that CHOS pretreatment on SH-SY5Y attenuated the paraquat induced cellular oxidative damage and cell apoptosis. We also investigated the effect of CHOS on activation of apoptosis related gene. We observed that significant increase in ratio of the pro-apoptotic member and the anti-apoptotic (*BAX/BCL2*) gene appeared after challenge the SH-SY5Y to paraquat alone, and all CHOS pretreatment significantly decreased the *BAX/BCL2*. Interestingly, CHOS  $F_A$  0.6 shows the best effect to decrease the expression of *BAX* and upregulate *BCL2* expression.

Moreover, we also examined the modulatory effect of CHOS on the autophagy that has not been reported yet. The autophagy is major intracellular machinery for degrading aggregated proteins and damaged organelles. It has been reported that the autophagy involved in the occurrence of pathological changes in many

neurodegenerative diseases (Fang et al. 2018). Induction of autophagy by drugs is one of the promising therapeutic approaches for treatment of neurodegenerative diseases such as Alzheimer's disease (Steele et al. 2013), Parkinson's disease (Moors et al. 2017), and Huntington's diseases (Williams et al. 2008). These diseases all involve the accumulation of aggregated proteins and damaged organelles in the cytosol of neural cells (Sarkar et al. 2007). The other natural oligosaccharides such as glucosamine and trehalose were reported to be able to induce the autophagy (Shintani et al. 2010, Krüger et al. 2012).

Interestingly, we found that CHOS activated the autophagy by induce the gene and protein expression of *LC3 I/II* in human neuroblastoma cell. These results were confirmed by using MDC which is specific autophagosome marker to analyze at the molecular level the machinery involved in the autophagic process. SH-SY5Y treated with CHOS showed an increase in a number of autophagosomes. Additionally, the autophagic flux was monitored by immunoblotting of *LC3 I/II* and *P62*. CHOS with FA 0.6 shows the best effect by upregulated *LC3* and downregulated *P62*.

In summary, this study suggested that CHOS could effectively protect the human neuroblastoma cell against neurotoxic agent by regulating apoptosis and autophagy pathways. CHOS might be used as a potential neuroprotective agent in neurodegenerative disorder in the future.

## 5.6 References

- Aam, B. B., Heggset, E. B., Norberg, A. L., Sørli, M., Vårum, K. M. and Eijsink, V. G. H. (2010). Production of chito oligosaccharides and their potential applications in medicine. **Marine Drugs** 8(5): 1482-1517.

- Bahrke, S., Einarsson, J. M., Gislason, J., Haebel, S., Letzel, M. C., Peter-Katalinić, J. and Peter, M. G. (2002). Sequence analysis of chitoooligosaccharides by matrix-assisted laser desorption ionization postsorce decay mass spectrometry. **Biomacromolecules** 3(4): 696-704.
- Ciechanover, A. and Kwon, Y. T. (2015). Degradation of misfolded proteins in neurodegenerative diseases: therapeutic targets and strategies. **Experimental & Molecular Medicine** 47: e147.
- Czerniczyniec, A., Lores-Arnaiz, S. and Bustamante, J. (2013). Mitochondrial susceptibility in a model of paraquat neurotoxicity. **Free Radical Research** 47(8): 614-623.
- Dai, X., Chang, P., Zhu, Q., Liu, W., Sun, Y., Zhu, S. and Jiang, Z. (2013). Chitosan oligosaccharides protect rat primary hippocampal neurons from oligomeric  $\beta$ -amyloid 1-42-induced neurotoxicity. **Neuroscience Letters** 554(0): 64-69.
- De Duve, C. (1963). The lysosome. **Sci Am** 208: 64-72.
- Dodson, M., Darley-Usmar, V. and Zhang, J. (2013). Cellular metabolic and autophagic pathways: Traffic control by redox signaling. **Free Radical Biology and Medicine** 63: 207-221.
- Fang, G., Xinyao, L., Huaibin, C. and Weidong, L. (2018). Autophagy in neurodegenerative diseases: pathogenesis and therapy. **Brain Pathology** 28(1): 3-13.
- Heggset, E. B., Dybvik, A. I., Hoell, I. A., Norberg, A. L., Sørli, M., Eijsink, V. G. H. and Vårum, K. M. (2010). Degradation of chitosans with a family 46 chitosanase from *Streptomyces coelicolor* A3(2). **Biomacromolecules** 11(9): 2487-2497.
- Heggset, E. B., Hoell, I. A., Kristoffersen, M., Eijsink, V. G. H. and Vårum, K. M. (2009). Degradation of Chitosans with Chitinase G from *Streptomyces coelicolor* A3(2): production of chito-oligosaccharides and insight into subsite specificities. **Biomacromolecules** 10(4): 892-899.

- Horie, T., Kawamata, T., Matsunami, M. and Ohsumi, Y. (2017). Recycling of iron via autophagy is critical for the transition from glycolytic to respiratory growth. **Journal of Biological Chemistry** 292(20): 8533-8543.
- Huang, H.-C., Hong, L., Chang, P., Zhang, J., Lu, S.-Y., Zheng, B.-W. and Jiang, Z.-F. (2015). Chitooligosaccharides Attenuate Cu<sup>2+</sup>-Induced Cellular Oxidative Damage and Cell Apoptosis Involving Nrf2 Activation. **Neurotoxicity Research** 27(4): 411-420.
- Jaroonwichawan, T., Chaicharoenaudomrung, N., Namkaew, J. and Noisa, P. (2017). Curcumin attenuates paraquat-induced cell death in human neuroblastoma cells through modulating oxidative stress and autophagy. **Neuroscience Letters** 636: 40-47.
- Jiang, P. and Mizushima, N. (2015). LC3- and p62-based biochemical methods for the analysis of autophagy progression in mammalian cells. **Methods** 75: 13-18.
- Kabeya, Y., Mizushima, N., Yamamoto, A., Oshitani-Okamoto, S., Ohsumi, Y. and Yoshimori, T. (2004). LC3, GABARAP and GATE16 localize to autophagosomal membrane depending on form-II formation. **J Cell Sci** 117(Pt 13): 2805-2812.
- Kalyanaraman, B., Darley-Usmar, V., Davies, K. J. A., Dennery, P. A., Forman, H. J., Grisham, M. B., Mann, G. E., Moore, K., Roberts, L. J. and Ischiropoulos, H. (2012). Measuring reactive oxygen and nitrogen species with fluorescent probes: challenges and limitations. **Free radical biology & medicine** 52(1): 1-6.
- Komatsu, M., Waguri, S., Koike, M., Sou, Y.-s., Ueno, T., Hara, T., Mizushima, N., Iwata, J.-i., Ezaki, J., Murata, S., Hamazaki, J., Nishito, Y., Iemura, S.-i., Natsume, T., Yanagawa, T., Uwayama, J., Warabi, E., Yoshida, H., Ishii, T., Kobayashi, A., Yamamoto, M., Yue, Z., Uchiyama, Y., Kominami, E. and Tanaka, K. (2007). Homeostatic Levels of p62 Control Cytoplasmic Inclusion Body Formation in Autophagy-Deficient Mice. **Cell** 131(6): 1149-1163.
- Kroemer, G., Mariño, G. and Levine, B. (2010). Autophagy and the integrated stress response. **Molecular cell** 40(2): 280-293.

- Krüger, U., Wang, Y., Kumar, S. and Mandelkow, E.-M. (2012). Autophagic degradation of tau in primary neurons and its enhancement by trehalose. **Neurobiology of Aging** 33(10): 2291-2305.
- Levine, B. and Klionsky, D. J. (2004). Development by Self-Digestion: Molecular Mechanisms and Biological Functions of Autophagy. **Developmental Cell** 6(4): 463-477.
- Li, L., Chen, Y. and Gibson, S. B. (2013). Starvation-induced autophagy is regulated by mitochondrial reactive oxygen species leading to AMPK activation. **Cellular Signalling** 25(1): 50-65.
- Menzies, F. M., Fleming, A., Caricasole, A., Bento, C. F., Andrews, S. P., Ashkenazi, A., Füllgrabe, J., Jackson, A., Jimenez Sanchez, M., Karabiyik, C., Licitra, F., Lopez Ramirez, A., Pavel, M., Puri, C., Renna, M., Ricketts, T., Schlotawa, L., Vicinanza, M., Won, H., Zhu, Y., Skidmore, J. and Rubinsztein, D. C. (2017). Autophagy and Neurodegeneration: Pathogenic Mechanisms and Therapeutic Opportunities. **Neuron** 93(5): 1015-1034.
- Mizushima, N. and Komatsu, M. (2011). Autophagy: Renovation of Cells and Tissues. **Cell** 147(4): 728-741.
- Moors, T. E., Hoozemans, J. J., Ingrassia, A., Beccari, T., Parnetti, L., Chartier-Harlin, M. C. and van de Berg, W. D. (2017). Therapeutic potential of autophagy-enhancing agents in Parkinson's disease. **Mol Neurodegener** 12(1): 11.
- Muanprasat, C. and Chatsudthipong, V. (2017). Chitosan oligosaccharide: Biological activities and potential therapeutic applications. **Pharmacology & Therapeutics** 170(Supplement C): 80-97.
- Munafó, D. B. and Colombo, M. I. (2001). A novel assay to study autophagy: regulation of autophagosome vacuole size by amino acid deprivation. **Journal of Cell Science** 114(20): 3619.
- Pechsrichuang, P., Lorentzen, S. B., Aam, B. B., Tuveng, T. R., Hamre, A. G., Eijsink, V. G. H. and Yamabhai, M. (2018). Bioconversion of chitosan into chito-oligosaccharides

- (CHOS) using family 46 chitosanase from *Bacillus subtilis* (BsCsn46A). **Carbohydrate Polymers** 186: 420-428.
- Pechsrichuang, P., Yoohat, K. and Yamabhai, M. (2013). Production of recombinant *Bacillus subtilis* chitosanase, suitable for biosynthesis of chitosan-oligosaccharides. **Bioresource Technology** 127: 407-414.
- Redmann, M., Benavides, G. A., Berryhill, T. F., Wani, W. Y., Ouyang, X., Johnson, M. S., Ravi, S., Barnes, S., Darley-Usmar, V. M. and Zhang, J. (2017). Inhibition of autophagy with bafilomycin and chloroquine decreases mitochondrial quality and bioenergetic function in primary neurons. **Redox Biology** 11: 73-81.
- Sarkar, S., Perlstein, E. O., Imarisio, S., Pineau, S., Cordenier, A., Maglathlin, R. L., Webster, J. A., Lewis, T. A., O'Kane, C. J., Schreiber, S. L. and Rubinsztein, D. C. (2007). Small molecules enhance autophagy and reduce toxicity in Huntington's disease models. **Nature chemical biology** 3(6): 331-338.
- Schapira, A. H. and Gegg, M. (2011). Mitochondrial contribution to Parkinson's disease pathogenesis. **Parkinsons Dis** 2011: 159160.
- Shintani, T., Yamazaki, F., Katoh, T., Umekawa, M., Matahira, Y., Hori, S., Kakizuka, A., Totani, K., Yamamoto, K. and Ashida, H. (2010). Glucosamine induces autophagy via an mTOR-independent pathway. **Biochemical and Biophysical Research Communications** 391(4): 1775-1779.
- Songsiriritthigul, C., Pesatcha, P., Eijsink, V. G. H. and Yamabhai, M. (2009). Directed evolution of a *Bacillus* chitinase. **Biotechnology Journal** 4(4): 501-509.
- Sørbotten, A., Horn, S. J., Eijsink, V. G. H. and Vårum, K. M. (2005). Degradation of chitosans with chitinase B from *Serratia marcescens*. **FEBS Journal** 272(2): 538-549.
- Steele, J. W., Fan, E., Kelahmetoglu, Y., Tian, Y. and Bustos, V. (2013). Modulation of autophagy as a therapeutic target for alzheimer's disease. **Postdoc journal : a journal of postdoctoral research and postdoctoral affairs** 1(2): 21-34.

- Vårum, K. M., Antohonsen, M. W., Grasdalen, H. and Smidsrød, O. (1991). Determination of the degree of *N*-acetylation and the distribution of *N*-acetyl groups in partially *N*-deacetylated chitins (chitosans) by high-field n.m.r. spectroscopy. **Carbohydrate Research** 211(1): 17-23.
- Williams, A., Sarkar, S., Cuddon, P., Ttofi, E. K., Saiki, S., Siddiqi, F. H., Jahreiss, L., Fleming, A., Pask, D., Goldsmith, P., O'Kane, C. J., Floto, R. A. and Rubinsztein, D. C. (2008). Novel targets for Huntington disease in an mTOR-independent autophagy pathway. **Nature Chemical Biology** 4: 295.
- Zhou, S., Yang, Y., Gu, X. and Ding, F. (2008). Chitooligosaccharides protect cultured hippocampal neurons against glutamate-induced neurotoxicity. **Neuroscience Letters** 444(3): 270-274.

### Critical Note

After completing the experiments, while this manuscript was being prepared, we decided to test for mycoplasma contamination of the SH-SY5Y cells that we have been used in the experiments. Unfortunately, we found that these cells were contaminated by mycoplasma as shown by PCR detection in Fig 5.11. Therefore, we couldn't publish the results. However, we think that the results did suggest that CHOS can have protective effect on human neuroblastoma SH-SY5Y cells and other cells. In addition, CHOS with different degree of acetylation could have different effects. Therefore, we will repeat our experiments on SH-SY5Y and other cell lines such as human dermal fibroblast and THP-1 macrophage and publish our work on biological activities of CHOS on different cell lines in the future.



**Figure 5.11** Mycoplasma detection by PCR-based technique.

## CHAPTER VI

### CONCLUSIONS

1. *BsCsn46A* containing OmpA signal peptide was more efficient than those containing the native *Bacillus* signal peptide, for both expression and secretion, but cleavage of the signal peptide was not precise.
2. *BsCsn46A* can efficiently convert chitosans with different degrees of acetylation into mixtures of CHOS with varying chain lengths and compositions, depending on the substrate and the reaction conditions.
3. The initial specific activities of chitosan degradation were  $5.5 \times 10^3$  and  $8.4 \times 10^3 \text{ min}^{-1}$  for chitosans with  $F_A$  0.15 and  $F_A$  0.3, respectively. Thus, *BsCsn46A* seems to be one of the fastest chitosanases reported so far.
4. CHOS obtained from degradation of chitosan with various  $F_A$  (0.15, 0.3 and 0.6) was successfully characterized by size exclusion chromatography (SEC),  $^1\text{H}$  NMR, and mass spectrometry (MS) methods.
5. Well-defined CHOSs produced from *BsCsn46A* or *ChiA3* may protect the human neuroblastoma cell against neurotoxic agent by regulating apoptosis and autophagy pathways. Thus, CHOS might be used as a potential neuroprotective agent or anti-cellular damaging compounds in the future.

## BIOGRAPHY

Miss Phornsiri Pechsrichuang was born on August 24, 1984 in Surin Province, Thailand. She graduated with a Bachelor's Degree from Department of Biotechnology, Faculty of Technology, Khon Kaen University in 2007. She received her Master's degree in school of Biotechnology from Suranaree University of Technology in 2012. In 2013-2018, she had an opportunity to study Doctoral degree enrollment in School of Biotechnology, Institute of Agricultural technology, Suranaree University of Technology. She received SUT-PhD scholarship from Suranaree University of Technology supporting on her study and research experience at Faculty of Chemistry, Biotechnology, Biotechnology and Food Science, Norwegian University of Life Science (NMBU), Norway for 1 year. Her work and research interests in bioconversion of chitosan into chito-oligosaccharide (CHOSs) and biological activities of CHOS in medical application. She had presented research work in Asian Congress for Biotechnology (ACB2017), July 23-27,2017 at pullman Khon Kaen raja orchid hotel, Thailand (Poster presentation; Chito-oligosaccharide (CHOS) Modulates Autophagy and Prevents Apoptosis in Human Neuroblastoma SH-SY5Y Cells). The 5<sup>th</sup> School of Biotech International colloquium, September 22, 2016, Suranaree University of Technology, Thailand (Oral presentation; In-depth Characterization of Chitooligosaccharide (CHOS) produced from *Bacillus subtilis* Family GH46).

**Publications in International Scientific Journals:**

1. Pechsrichuang, P., Lorentzen, S. B., Aam, B. B., Tuveng, T. R., Hamre, A. G., Eijsink, V. G. H., & Yamabhai, M. (2018). Bioconversion of chitosan into chito-oligosaccharides (CHOS) using family 46 chitosanase from *Bacillus subtilis* (BsCsn46A). *Carbohydrate Polymers*, 186, 420-428.
2. Pechsrichuang, P., Songsiriritthigul, C., Haltrich, D., Roytrakul, S., Namvijitr, P., Bonaparte, N., & Yamabhai, M. (2016). OmpA signal peptide leads to heterogenous secretion of *B. subtilis* chitosanase enzyme from *E. coli* expression system. *SpringerPlus*, 5(1), 1200.
3. Sak-Ubol, S., Namvijitr, P., Pechsrichuang, P., Haltrich, D., Nguyen, T.-H., Mathiesen, G., Eijsink, V., Yamabhai, M. (2016). Secretory production of a beta-mannanase and a chitosanase using a *Lactobacillus plantarum* expression system. *Microbial Cell Factories*, 15(1), 81.
4. Pechsrichuang, P., Yoohat, K., & Yamabhai, M. (2013). Production of recombinant *Bacillus subtilis* chitosanase, suitable for biosynthesis of chitosan-oligosaccharides. *Bioresource Technology*, 127, 407-414.
5. Songsiriritthigul, C., Lapboonrueng, S., Pechsrichuang, P., Pesatcha, P., & Yamabhai, M. (2010). Expression and characterization of *Bacillus licheniformis* chitinase (ChiA), suitable for bioconversion of chitin waste. *Bioresource Technology*, 101(11), 4096-4103.